NOVEL ENVIRONMENTAL AND EXPLOSIVES DETECTION APPLICATIONS FOR MOLYBDENUM OXIDES

By

KEVIN NAKIA BARBER

Bachelor of Science in Chemical Engineering
University of Oklahoma
Norman, Oklahoma
1999

Master of Science in Chemical Engineering
Oklahoma State University
Stillwater, Oklahoma
2005

Submitted to the Faculty of the
Graduate College of the
Oklahoma State University
in partial fulfillment of
the requirements for
the Degree of
DOCTOR OF PHILOSOPHY
July, 2009

NOVEL ENVIRONMENTAL AND EXPLOSIVES DETECTION APPLICATIONS FOR MOLYBDENUM OXIDES

Dissertation Approved:

Dr. Allen W. Apblett

Dissertation Adviser

Dr. Nicholas Materer

Dr. Jeffery White

Dr. Legrande Slaughter

Dr. John Veenstra

Dr. A. Gordon Emslie

Dean of the Graduate College

ACKNOWLEDGMENTS

If I were to thank everyone individually who helped make this work possible in both large and small ways this acknowledgements section would be larger than the dissertation itself.

I especially thank Dr. Allen Apblett for all of his instruction, his patience, his advice, and especially his friendship over these last four years. He is a man I have learned a great deal from, have a great deal of respect for, and would do well to emulate. I also thank Dr. Nicholas Materer for all his help with these projects I have worked on, for his help with the XPS data, for his advice and (always constructive) criticism, and for his friendship. I thank my committee members: Dr. Legrande Slaughter who was my first instructor in this department when I took his Graduate Inorganic Chemistry course for my technical elective in engineering; Dr. Jeffery White who taught me heterogeneous catalysis; Dr. John Veenstra, with whom I also worked in my engineering studies.

I also thank the rest of the faculty and staff of the Chemistry Department, including, but definitely not limited to, Drs. Ohrtman and Iob with whom I have worked in the teaching labs. Drs. Berlin, Raff, and Bunce who were always willing to advise me and answer questions.

I thank Alan Piquette for all of his assistance with and training on the various instrumentation and equipment and his patience therein. I thank Dane Scott who was always to cheerfully willing lend a hand. I thank Cory Perkins for all of his help and his many hours of hard work assisting me with the statistically designed experiments associated with the aqueous synthesis of the sodium hydrogen molybdenum bronzes. I thank the rest of our research group for their assistance and friendship. I also thank Dr. Charlotte Ownsby for her help with the scanning and transmission electron microscopes, Dr. Shushing Tan for teaching me to operate the atomic force electron microscope, and Terry Colberg for his assistance in preparing samples.

I thank my family for all their love, help, and faith in me: My father and mother Charles and Juanita Barber who have helped me so much and taught me by example; my aunt Betty Maggard Elliot who has supported me in all things; my uncle Dale Maggard, who has passed on, who taught me to fix televisions; my grandmother, Mrs. Cammie Virden, who has also passed on, who taught me to read, write, add, and subtract, the ultimate foundations of this work, when I was still nearly a baby; my cousin Tammy Duvall Parks, who's more like a sister than a cousin, who has always supported me (and defended me when necessary).

I thank all of my friends including, but not limited to, Ronetta Kerntke and her family, Louis Rose, Mark Deaver, Joe Hurdle, Wei (George) Liu, Dr. Jerry Newman, and many others for all of their support, their friendship, and keeping me relatively sane over the years.

In due humility I must also thank God for the opportunities that I have been given, the good people who I've met which have been such a help to me, my health and natural abilities, my good fortune in general, and other blessings too numerous to mention here.

I owe a lot of people for their assistance in making me a scientist, and I have a lot of good examples to live up to. I intend to do my best to make you all proud and bring honor to my instructors and to my *alma mater*.

TABLE OF CONTENTS

Chapter **Page**

Chapter **Page**

Chapter **Page**

LIST OF TABLES

Table **Page**

Table **Page**

Table **Page**

LIST OF FIGURES

Figure **Page**

Figure **Page**

Figure **Page**

Figure **Page**

Figure **Page**

Figure **Page**

CHAPTER I

INTRODUCTION

AIM OF THIS STUDY

The ultimate purpose of this study was to develop novel applications for molybdenum oxides, molybdenum oxide bronzes, and related compounds in environmental and wastewater applications, sustainable or "green" industrial processes, and homeland security and transportation related explosive detection technologies. Specifically the topics to be discussed include the following.

Preparation, synthesis and characterization of both the proton- and sodium-forms of molybdenum oxide bronzes:

For the sake of this study, alternative, room temperature, solution phase syntheses were developed for the hydrogen and sodium molybdenum bronzes. These syntheses were explored in detail and an attempt was made to optimize these reactions in terms of yield and reducing capacity of the products obtained.

Examination of the efficacy of the molybdenum oxide bronzes for the electrochemical reduction and/or removal of toxic metal cations from aqueous systems:

Due to the electrochemically reducing nature of these molybdenum materials, as well as their ability to undergo ion exchange reaction and intercalation of cationic species, they lend themselves well to the application of metal cation removal from wastewater and groundwater streams. This study examines the use of hydrogen and sodium molybdenum bronzes as a reducing agent for the purpose of chemically reducing hexavalent chromium in groundwater and wastewater streams as a possible method for treatment and environmental remediation.

Development of a catalyst for disproportionation of aqueous sulfite to elemental sulfate and sulfur:

Many industrial processes produce sulfur dioxide or aqueous sulfite streams as a by-product which must be removed as an additional cost of the operation. In this investigation a method was developed in which an aqueous sulfite waste stream can be catalytically treated in order to produce commodities - sulfur and sulfate ultimately turning a liability waste product into an asset. This treatment would also work for remediation of sulfur dioxide after its capture using aqueous alkaline solutions or amine trapping.

Development of a green molybdate process for processing copper ore without the need for an ore roasting process thus eliminating the need to produce sulfur dioxide:

Smelting of metal ore is one of the more notorious producers of sulfur dioxide gas, a known contributor to acid rain. The sulfur dioxide is produced in the roasting step for sulfide ores. This study proposes and develops an alternative process for the processing of metals, which was applied to copper, but could be readily applied to a wide variety of metal ores. This process utilizes a metal-molybdate intermediate which allows the sulfur containing components to be removed in the solution phase, alleviating the need for roasting. The process results in no production of sulfur dioxide and decreases the heat requirement of the process. Furthermore, the molybdate process contains a second facet of sustainability as the molybdate species is easily recycled.

Development of a set of sensors for the detection of improvised peroxide and chlorate explosives and their synthetic precursors:

This study examines a set of sensors for the detection of improvised explosives and their precursors, as well as other harmful oxidizers. The reducing nature of the bronzes as well as their reactive colorimetric response in the presence of certain oxidizers give them potential for uses in chemical sensing technology. Included in this section is the development of a dipstick type test strip which is well suited for the transportation safety industry as well as other homeland security applications.

INTRODUCTION

Structure and Properties of Molybdenum Bronzes

Oxide bronzes are partially reduced non-stoichiometric transition metal oxide insertion compounds. The term bronze comes from the metallic properties of these materials, which include: electrical conductivity, metallic luster, and bright color. Typically, ternary, or three component transition metal oxide bronzes have the form $A_xM_yO_z$. Where M is the transition metal; A is typically H^+, a group I (alkali metal) cation, group II (alkaline earth) cation, ammonium ion, lanthanides (rare earth) cations [1, 2], or other metals, including barium, lead, copper, and silver. Formally, the oxidation state of the transition metal is usually non-integer, hence the "non-stoichiometric" designation.

The history of these non-stoichiometric bronzes is interesting in its own right. The first oxide bronze was discovered by Wohler in 1823 [3]. These compounds were in conflict with Berzelius' Law of Definite Proportions [4]. At that time they were presumed to be mixtures of stoichiometric compounds. This mixture assumption held favor until around 1935 when Hagg proved the existence of a series of sodium tungsten bronzes, Na_xWO_3, with a continuous sodium composition over the range $0.32 < x < 1.0$, using the then new X-ray diffraction methods [5]. The oxide bronzes of primary interest in this study include the hydrogen bronzes and the alkali metal bronzes.

A complete understanding of the structure, properties, and chemistry of the oxide bronzes is not possible without a similar understanding of the molybdenum oxides that make up an integral part of the oxide bronze structure. Molybdenum forms two stoichiometric oxides: molybdenum(VI) oxide, MoO_3, and molybdenum(IV) oxide, MoO_2. Additionally, there are several intermediate oxides of molybdenum in which the molybdenum center has a formal oxidation state with an intermediate value between +4 and +6. These intermediate oxides include: Mo_9O_{26}, Mo_8O_{23}, Mo_5O_{14}, $Mo_{17}O_{47}$, Mo_4O_{11}.

Molybdenum trioxide is both the typical starting material for these bronzes and is also their structural basis. Alpha-molybdenum trioxide has a corrugated layered structure. It is built up from chains of corner-shared distorted MoO_3 octahedra with Mo-O distances of 1.94 Å, 1.95 Å, 1.73 Å, 1.67 Å, 2.25 Å, and 2.33 Å. These chains are joined together by edge sharing to generate layers [6-10]. The individual layers are connected to each other via van der Waals interactions with an interlayer distance of 6.929 Å[10]. It is precisely these gaps that are so instrumental in the formation of the molybdenum bronze materials. The intercalated species (i.e. H^+, Na^+, etc) in the bronze reside in the gaps between the layers. The overall laminar α-MoO_3 structure is orthorhombic with unit cell parameters of a = 3.963 Å, b = 13.855 Å, c = 3.696 Å [11]. Figure 1-1 illustrates the local coordination of the molybdenum atom in the distorted octahedra. Figure 1-2 illustrates the structure of the chains of MoO_6 octahedra and the layered structure that they form.

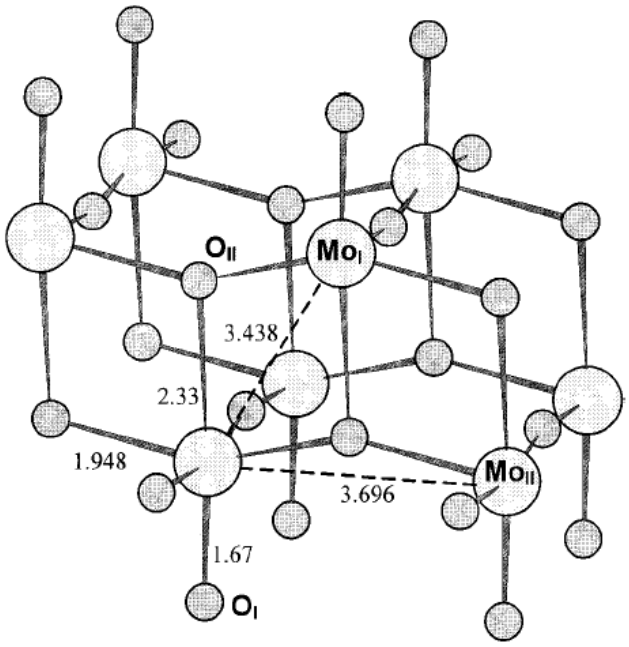

Figure 1-1: "Crystal Structure of Molybdenum Trioxide" (Adapted from Ref. [11])

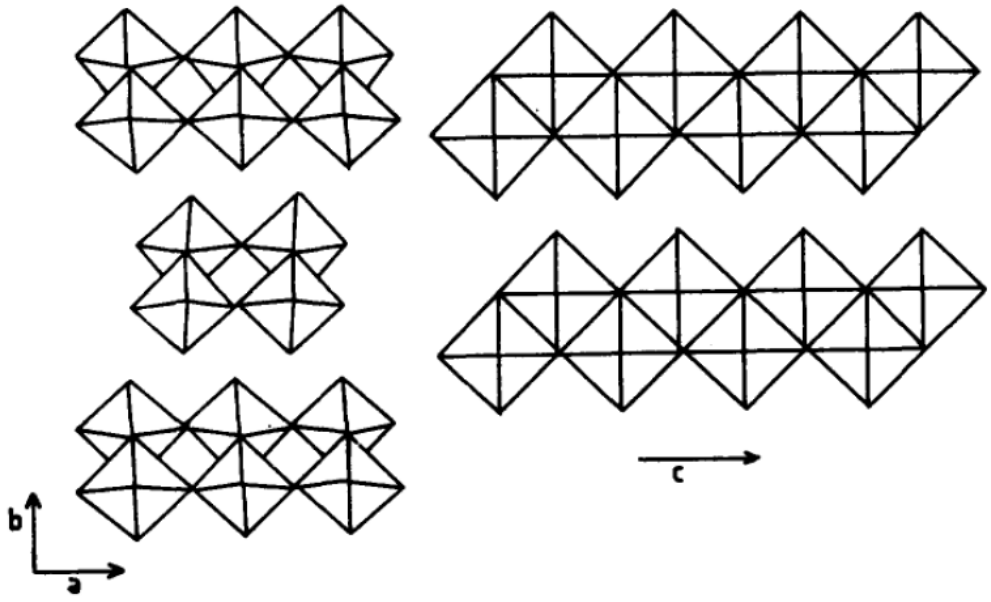

Figure 1-2: "Layered Structure (Left Side) Comprised of MoO_6 Chains (Right Side)" (Adapted from Ref. [12])

Beta-molybdenum trioxide is a meta-stable monoclinic form that is produced by heating a spray-dried solution of molybdic acid. The unit cell parameters are as follows: a = 7.122 Å, b = 5.374 Å, c = 5.565 Å [13]. Although α-molybdenum trioxide is commercially available, the β-molybdenum trioxide phase must be synthesized by passing a sodium molybdate solution through a cation exchange column filled with the hydrogen form of a cation exchange resin to obtain a solution of molybdic acid. The molybdic acid solution is then spray-dried using an inlet temperature of 180 ˚C and an outlet temperature of 80 ˚C. The resulting powder is dried at 300˚C for 1 h in oxygen to obtain the β-molybdenum trioxide product.

Hydrogen molybdenum bronzes are a special subset of the ternary molybdenum bronzes in which the A position is occupied by hydrogen. Typically they are represented as H_xMoO_3, with x variable over the range $0 < x \leq 2.0$. In actuality, the hydrogen is attached to an oxygen thus forming an acidic OH resulting in a more correctly represented form: $MoO_{3-x}(OH)_x$. Hydrogen molybdenum bronzes were first reported by Oskar Glemser and coworkers in the 1940's and 1950's [14-19]. Further studies determined the existence of four distinct phases of hydrogen molybdenum bronzes that differed in hydrogen content, color, and crystal structure along the $0 < x \leq 2.0$ range[20]. The compositions and colors of these phases are described as follows.

Type I Hydrogen Molybdenum Bronze

The Type I hydrogen molybdenum bronzes are blue in color and have an orthorhombic crystal structure. The composition of the Type I bronzes are homogeneous over the continuous range of $0.23 < x < 0.4$.

Type II Hydrogen Molybdenum Bronze

The Type II hydrogen bronze is also blue in color with a monoclinic crystal structure. The Type II bronze hydrogen composition is continuous over the range of $0.85 < x < 1.04$.

Type III Hydrogen Molybdenum Bronze

The Type III hydrogen bronze is red in color and is also monoclinic in structure. The hydrogen composition is continuous over the range $1.55 < x < 1.72$.

Type IV Hydrogen Molybdenum Bronze

The Type IV hydrogen bronze is green in color and monoclinic in structure. Unlike the other three phases, the Type IV bronze has a hydrogen composition of $x = 2.0$. This composition is constant.

Elastic and inelastic neutron diffraction studies suggest that the location of the proton in the molybdenum trioxide matrix varies with the type of bronze examined. In the case of the orthorhombic (Type I) hydrogen bronze, the proton is attached to the bridging oxygen atoms, while in the monoclinic hydrogen bronzes (Types II, III, and IV) the protons are attached to the terminal oxygen atoms [21]. The neutron diffraction data is consistent with NMR comparison of orthorhombic and monoclinic bronzes [22].

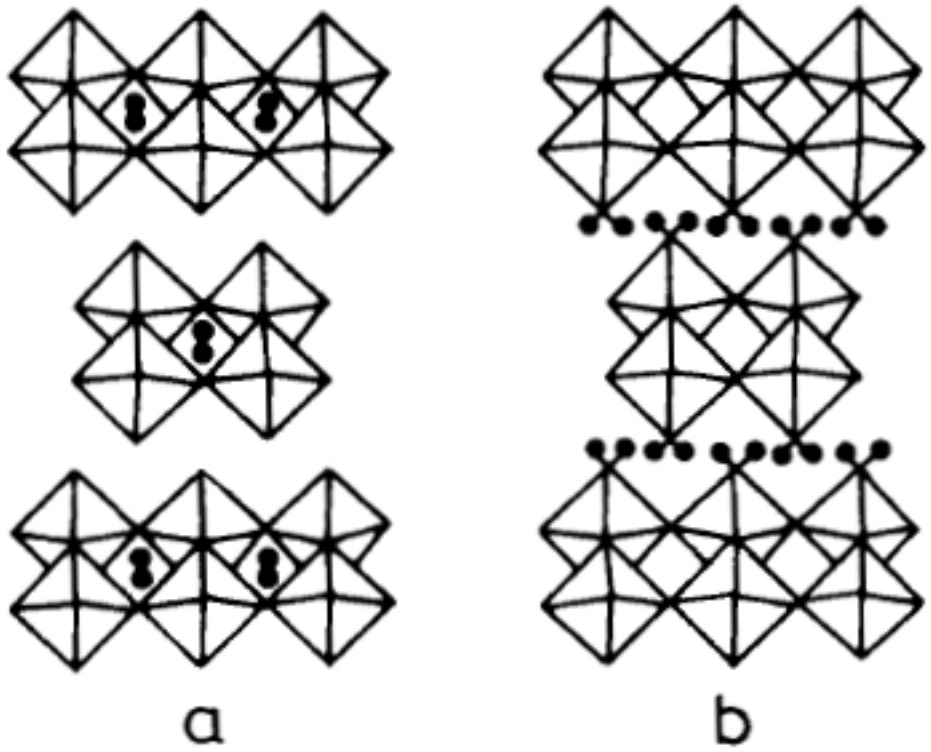

Figure 1-3: "Proton Sites in (a) Orthorhombic and (b) Monoclinic Hydrogen Molybdenum Bronzes" (Adapted from Ref. [23])

Alkali metal molybdenum bronze structures are somewhat similar to that of the hydrogen bronzes except that the alkali metal bronzes typically have monoclinic unit cells. Also, the molybdenum trioxide matrix layers are negatively charged with the alkali metals serving as the counterions in the interlayer region. (There are a few

exceptions observed for the lithium molybdenum bronzes). Figure 1-4 illustrates the structure of a prototypical alkali metal molybdenum bronze.

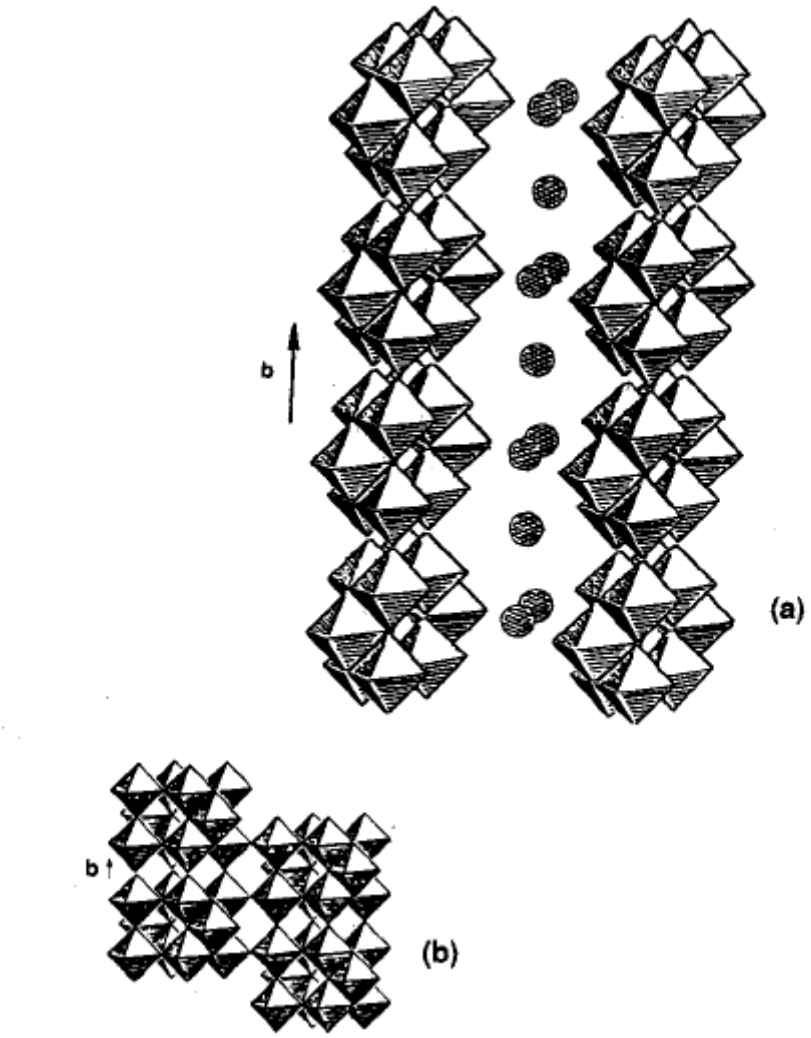

Figure 1-4: "Bonding Sites for Cations in Alkali Metal Bronzes" (Adapted from Ref. [24])

Like the hydrogen bronzes, the alkali metal bronzes are classified by their color, structure, and the alkali metal to molybdenum ratio. Examples of alkali metal molybdenum bronze series include: "blue bronzes" ($A_{0.3}MoO_3$; A = K, Rb and $Cs_{0.19}MoO_3$), "red bronzes" ($A_{0.33}MoO_3$; A = Li, K, Rb, Cs), and "purple bronzes"

($A_{0.9}Mo_6O_{17}$; A = Li, Na, K). Of less importance in this study but for the sake of completeness there also exists some three dimensional bronzes which are isostructural with the tungsten bronze series (ReO_3-structure) [24]; some rare earth two dimensional bronzes of the form $A_{0.08}MoO_3$ with A = La, Ce, Eu, Gd, Lu [25, 26]; and thallium versions of the previously mentioned alkali metal bronzes [27].

One method of determining the type of alkali metal bronze present is to examine the basal spacings between the MoO_3 layers as X-ray powder diffraction. The basal spacing for the orthorhombic blue hydrogen form of the bronze is 6.929 Å. Table 1-1 summarizes the basal spacings for the hydrogen form of the bronze, the hydrated alkali metal forms as well as other bronzes forms of interest. The data was obtained from bronzes derived from hydrated sodium bronze via ion exchange.

Table 1-1: Basal Spacings for Hydrated Alkali Metal Hydrogen Bronzes of Various Cation-Types" [28]

Intercalated Cation	Basal Spacing, d (Å)
H^+	6.929
Li^+	11.48
Na^+	11.41
K^+	10.72
Rb^+	9.51
Cs^+	9.83
NH_4^+	9.51
Mg^{2+}	13.80
Ca^{2+}	14.16
Sr^{2+}	14.18
Ba^{2+}	13.17
Ni^{2+}	16.68
Co^{2+}	16.76

Chemically, hydrogen molybdenum bronzes are reducing agents. The standard electrode potential for the formation of the Type I, blue orthorhombic bronze from MoO_3 under standard conditions (Equation 1-1) is 0.47V.

$$H^+ + e^- + (1/x)MoO_3 \rightarrow (1/x)\, H_xMoO_3 \qquad E^\circ = +0.47\ V\ [29] \qquad \text{(Equation 1-1)}$$

Assuming the average of the range:

$$H^+ + e^- + 3MoO_3 \rightarrow HMo_3O_9 \qquad E^\circ = +0.47\ V\ [29] \qquad \text{(Equation 1-2)}$$

This implies that the Type I hydrogen bronze is thermodynamically capable of reducing any species which has a standard reduction potential greater than + 0.47 V. The reducing capacity of the hydrogen molybdenum bronze corresponds to the amount of hydrogen in the bronze in a one to one relationship [30] such that the orthorhombic blue hydrogen molybdenum bronze, $H_{0.28}MoO_3$ has a reducing power of 0.28 +/- 0.01 reducing equivalents per molybdenum.

Galvanostatic reduction of a pressed powder MoO_3 working electrode carried out in a 0.1 M solution of H_2SO_4 with a cathodic current of 200 μA showed a series of potential steps at for various hydrogen loadings (Figure 1-5) [28].

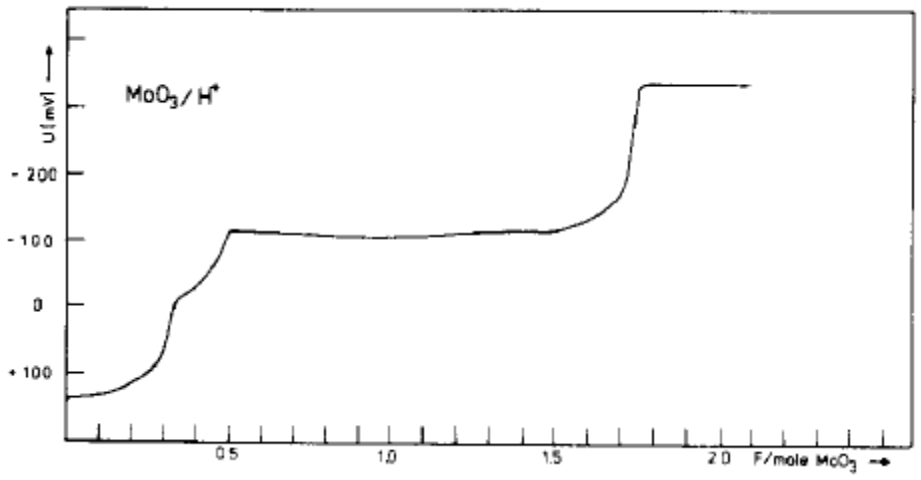

Figure 1-5: "Galvanostatic Trace of Cathodic Reduction of Pressed Powder MoO_3 Working Electrode in a 0.1 N H_2SO_4 Solution vs. SCE. Cathodic Current 200 μA." (Adapted From Ref. [28])

These potential steps were observed at e^-/Mo ratios of ~0.35, ~0.50, and ~1.75. These steps do not correspond exactly to the phase transitions in the bronze series, however the previously mentioned series were not synthesized under standard conditions. It is important to note that the e^-/Mo ratio is the same as the H/Mo ratio, or x value for the hydrogen molybdenum bronze. The determination of the e^-/Mo (H/Mo) was carried out using X-ray powder diffraction by examination of the basal spacings between the MoO_3 layers.

Hydrogen molybdenum bronzes participate in a wide variety of redox reactions. Since the lowest standard electrode potential for the hydrogen bronzes is +0.47 V they are thermodynamically capable of reducing any species with more positive reduction potentials. The bronzes can reduce many metal cations to a lower oxidation state or to the zero valent metal. For example hydrogen bronze is expected to be capable of

reducing Ag^{+} to Ag metal (E° = 0.799) or $Cr^{VI}_{2}O_{7}^{2-}$ to Cr^{3+} under acidic conditions (E° = +1.33 V). This property makes hydrogen molybdenum bronzes attractive for applications such as the removal of heavy metal cation from groundwater and wastewater.

Molybdenum bronzes are also thermodynamically capable of reducing many non-metallic and organic oxidizers such as hydrogen peroxide, organic peroxides, chlorates, and nitrate anions, that are used in conventional and improvised explosives. Use of alkali metal bronzes for detection and neutralization of these types of materials will be discussed in detail in Chapter III.

Hydrogen bronzes are strong Bronsted acids with pKa's in the superacidic range. They can undergo acid/base reactions with metal hydroxides to produce metal-substituted bronzes (e.g. Equation 1-3)

$$HMo_2O_6 + NaOH + 2\ H_2O \rightarrow NaMo_2O_6 \cdot 2H_2O \qquad \text{(Equation 1-3)}$$

The hydrogen molybdenum bronzes also react with Bronsted bases such as NH_3, organic amines, heterocyclic bases, and pyridine to form intercalation compounds of the protonated bases [28, 31] as shown in Equation 1-4. One example of this is the intercalation product with pyridine, $(C_5H_5NH)_{0.3}H_{0.2}MoO_3$.

$$nL + H_xMoO_3 \rightarrow (LH)_nH_{x-n}MoO_3 \qquad \text{(Equation 1-4)}$$

Alkali metal bronzes are also reducing agents that can undergo similar redox chemistry as the hydrogen bronzes. The fundamental difference in the redox chemistry of the two sets of bronzes is that the hydrogen form is acidic while the alkali metal forms are not. Accordingly, the alkali metal forms are better suited to redox chemistry in neutral and basic media. Galvanostatic data obtained for cathodic reduction of pressed MoO_3 electrodes to form the sodium, potassium, and cesium forms of the alkali metal bronzes is presented in Figures 1-6 to 1-8.

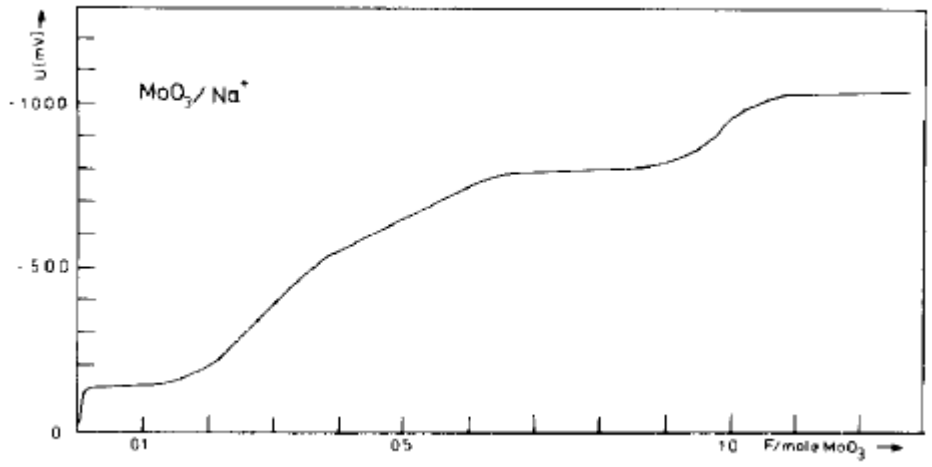

Figure 1-6: "Galvanostatic Trace of Cathodic Reduction of Pressed Powder MoO_3 Working Electrode in a 0.1 M Na_2SO_4 Solution vs. SCE. Cathodic Current 260 μA." (Adapted from Ref. [28])

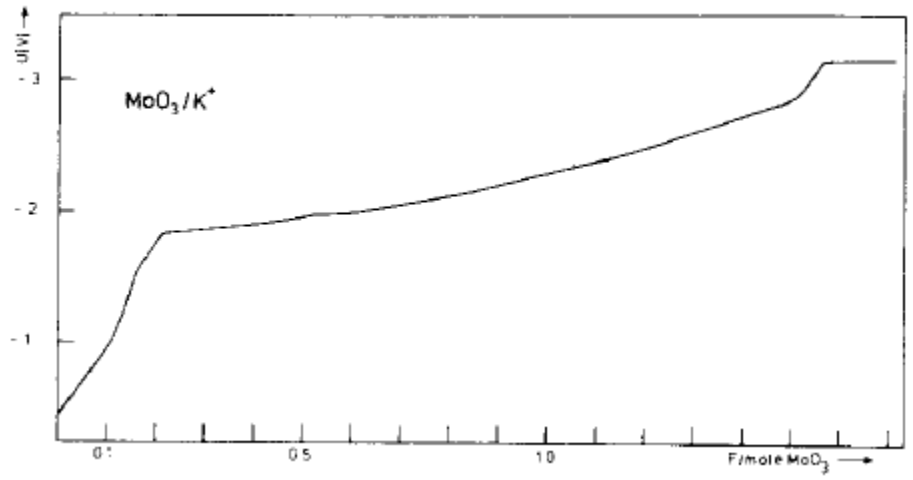

Figure 1-7: "Galvanostatic Trace of Cathodic Reduction of Pressed Powder MoO_3 Working Electrode in a 0.1 M KPF_6/DME Solution vs. SCE. Cathodic Current 200 μA." (Adapted fron Ref. [28])

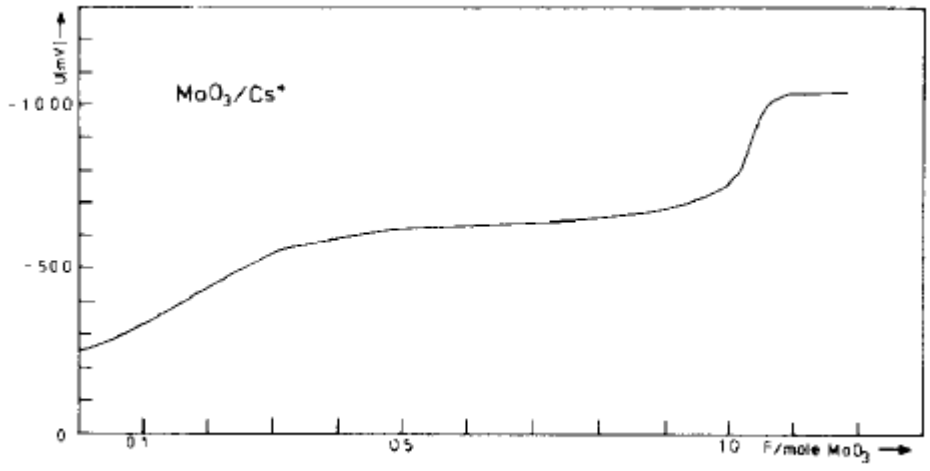

Figure 1-8: "Galvanostatic Trace of Cathodic Reduction of Pressed Powder MoO_3 Working Electrode in a 0.1 N Cs_2SO_4 Solution vs. SCE. Cathodic Current 500 μA." (Adapted from Ref. [28])

All of the molybdenum bronzes also undergo ion exchange, hydration, dehydration, acid-base, and redox reactions. The scheme shown in Figure 1-9 summarizes these reactions.

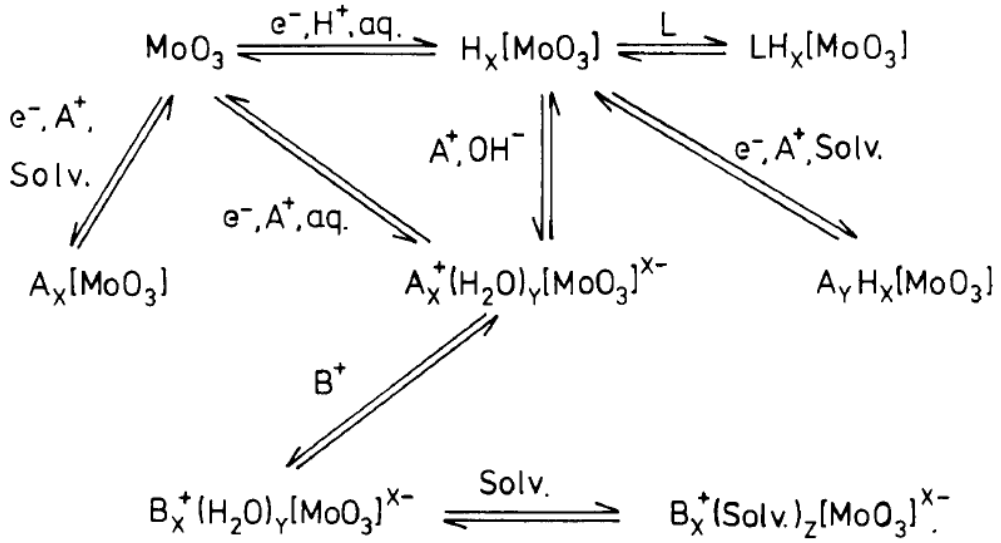

Figure 1-9: "Common Reactions of Molybdenum Oxide Bronzes" (Adapted from Ref. [28])

There has been some controversy in the literature regarding the actual nature of sodium molybdenum bronze. One research group [28] obtained a sodium bronze product that was thought to be $[Na(H_2O)_2]_x[MoO_3]$ (x = 0.45-0.50) by reduction of MoO_3 with a concentrated (1 M) solution of sodium dithionite. They attributed the variation over the range from 0.45 to 0.50 to be due to "protolysis of the alkali phase" during washing with water in which the sodium was replaced with protons to give a product of $[Na(H_2O)_2]_{0.5-n}H_n[MoO_3]$, where n = 0.00-0.05. Another group [32] obtained bronzes with a sodium to molybdenum ratio over the range of 0.10 to 0.25. They suggested that the formula was $Na_xH_{0.5-x}MoO_3$, based on the assumption that the molybdenum must be reduced a formal oxidation state of 5.5, corresponding to the $H_{0.5}MoO_3$ member of the hydrogen molybdenum bronze series. However the argument has been made [33] that this assertion might be invalid, since others have [30] claimed that the hydrogen bronze actually had a hydrogen to molybdenum ratio in the range of 0.23 to 0.40.

One group in particular [33] prepared a sodium molybdenum bronze product using an extremely inefficient process of using 60 g of sodium molybdate dihydrate as a buffer for the aqueous dithionite reduction of 2 g of molybdenum trioxide. They claimed that their product had a sodium to molybdenum ratio of 0.25 to 1 based on data obtained from inductively coupled plasma spectroscopy analysis and claimed that the product contained no protons. Their evidence for this assertion was that the bronze was synthesized in a pH neutral buffer and upon comparing the thermogravimetric weight loss between their dried product and a sample of their product that they protonated by soaking it in hydrochloric acid for 1.5 hours.

Electronic Band Structure of the Molybdenum Bronzes:

The electronic band structure of the molybdenum bronzes can be outlined as follows. Assuming that the bonding pattern in the bronzes is determined by the local octahedral geometry of the molybdenum trioxide matrix, the band structure is made up from the overlap of the molybdenum 4d, 5s, and 5p orbitals with the sp hybrid orbitals of the six oxygen atoms to yield six bonding and six antibonding σ molecular orbitals per formula unit. Furthermore, the three t_{2g} orbitals on the molybdenum can overlap with three of the remaining six p-orbitals on the oxygens to form three π bonding and three π antibonding orbitals. The remaining three oxygen p-orbitals do not have the requisite symmetry to overlap with any of the metal orbitals and therefore remain as three non-bonding p-type orbitals. Since the molybdenum trioxide matrix can essentially be

considered an infinite lattice the molecular orbitals broaden into bands resulting in the band structure illustrated in Figure 1-10. [34]

Considering that MoO_3 contains 24N electrons per mole (N being defined here as Avogadro's number) these 24N electrons can be allocated to the 6N σ-bonding, the 3N π-bonding, and 3N non-bonding bands. This leaves the π* and σ* bands empty. The resulting band gap is ~ 3.00 eV for MoO_3 and is slightly lower in the case of oxygen deficient MoO_3. Since the HOMO band is the completely filled non bonding p-orbitals on the oxygen, reduction of the MoO_3 requires that the additional electrons be placed in the π*-band (MoO_3 LUMO band) producing a metallic conductor.

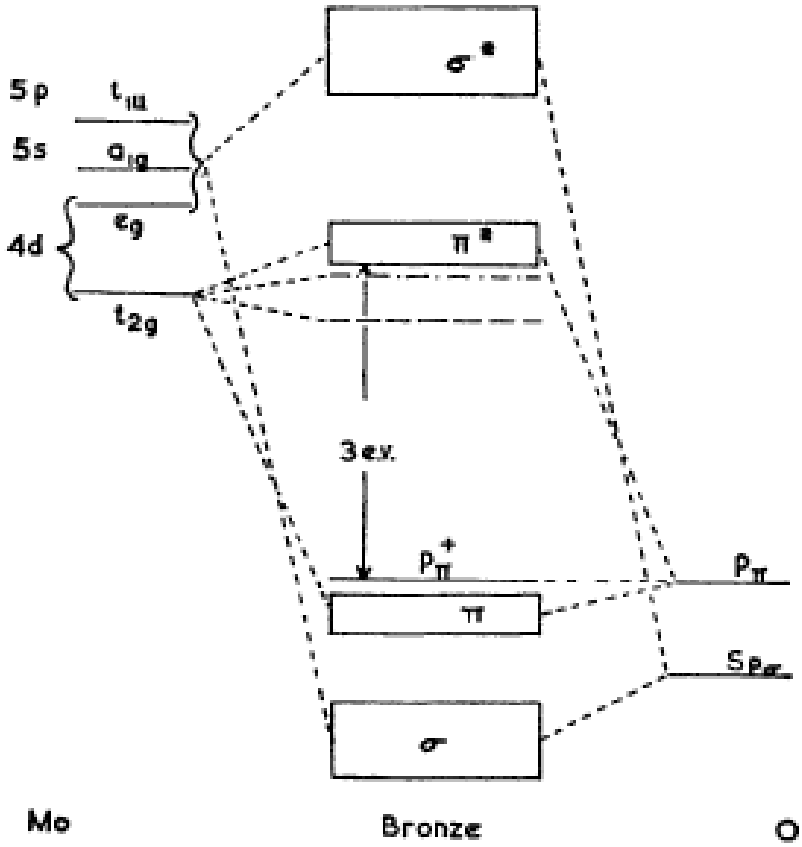

Figure 1-10: "Electronic Band Structure of Molybdenum Oxide Bronzes" (Adapted from Ref. [34])

Synthesis of Hydrogen Molybdenum Bronzes:

Reduction of MoO_3 by Hydrogen Spillover:

Hydrogen spillover synthesis of hydrogen bronzes is typically affected either by reduction of hydrogen (or deuterium) gas over a platinum surface [35-37]. Alternatively, in the solution phase the reaction of hydrochloric acid with zinc metal can be used to reduce an aqueous slurry of molybdenum trioxide. In either case the reductively active hydrogen is first disassociatively chemisorbed on the surface of the metal prior to reacting with the molybdenum trioxide.

Platinum Spillover

The platinum method involves platinization of the molybdenum trioxide by combining hexachloroplatinic acid with molybdenum trioxide and then reducing the hexachloroplatinic acid *in situ* to platinum metal in a hydrogen gas stream (Equation 1-5). After reduction of the platinum the hydrogen adsorbs on the surface of the platinum (Equation 1-6) and the resulting active atomic hydrogen is used to reduce the molybdenum trioxide to the bronze (Equation 1-7). This reduction can easily be carried out under mild conditions and under low hydrogen pressure.

$$H_2PtCl_6(g) + 2\ H_2(g) \rightarrow Pt^0(s) + 6\ HCl(g) \qquad \text{(Equation 1-5)}$$

$$H_2(g) + Pt^0(s) \rightarrow 2\ H^*(surface) \qquad \text{(Equation 1-6)}$$

$$MoO_3(s) + x\ H^*(surface) \rightarrow H_xMoO_3(s) \qquad \text{(Equation 1-7)}$$

The ultimate hydrogen molybdenum bronze product obtained by the platinum catalyzed reaction contains some solid platinum impurities in the product.

Dissolving Metal Reduction [17-19, 30, 38]

The dissolving metal reduction, also known as the zinc/hydrochloric acid reduction method, is much simpler and cheaper than the platinum method and takes place in an aqueous phase slurry. In this process a slurry of molybdenum trioxide and zinc granules are placed in a reaction vessel with a small amount of water. Hydrochloric acid is then slowly dropped into the slurry where it reacts with the metal to provide surface atomic hydrogen on the zinc. This surface hydrogen undergoes two reactions: some of it serves to reduce the molybdenum trioxide to the hydrogen bronze, and some of it combines with other atomic hydrogen atoms to form H_2 gas that bubbles out of the slurry. It is important to note that it is the surface atomic hydrogen that provides the reduction and not the dihydrogen by-product. The overall reaction for the formation of the bronze is given in Equation 1-8.

$$x\ HCl + x/2\ Zn + MoO_3 \rightarrow H_xMoO_3 + x/2\ ZnCl_2 \qquad \text{(Equation 1-8)}$$

Provided that sufficient hydrochloric acid is added to dissolve all of the zinc metal present the ultimate products of the reaction are the hydrogen molybdenum bronze, and a solution of hydrochloric acid and $ZnCl_2$, from which the desired bronze product is easily removed and purified via filtration and washing. This method can be used to synthesize any of the four types of bronzes. The higher hydrogen content bronzes are synthesized by adding more zinc metal and hydrochloric acid to the reaction vessel or performing multiple reductions [30, 38].

Chemical Reduction of MoO_3:

Hydrogen molybdenum bronzes (and other transition metal bronzes) can be synthesized by chemical reduction in an acidic media. Any number of reducing agents may be used and include sodium dithionite [39, 40], alcohols, and glycols [41, 42]. It is suggested that any reducing agent with $E^\circ < 0.34$ V should be sufficient to reduce molybdenum trioxide for synthesis of the bronze.

$$MoO_3 + x\ H^+ + x\ e^- \rightarrow H_xMoO_3 \qquad \text{(Equation 1-9)}$$

The electrochemical reduction method is extremely dependent on pH and concentration of cations, such as Na^+, K^+, etc., in the system. By varying these, it is possible to synthesize the hydrogen form of the bronze, the alkali metal form or a mixed alkali metal/proton bronze.

Hydrothermal Comproportionation: [43]

Hydrogen molybdenum bronzes can also be produced hydrothermally by comproportionation. Comproportionation is a redox reaction in which two reactants containing the same atom in differing oxidation states react to form a product with an intermediate oxidation state. In this reaction molybdenum metal reacts with molybdenum trioxide in the presence of water to form the hydrogen bronze (Equation 1-10).

$$x/(6-x)\ Mo^{0} + MoO_3 + (3x)/(6-x)\ H_2O \rightarrow 6/(6-x)\ H_xMoO_3 \quad \text{(Equation 1-10)}$$

Ion-Exchange [28, 44, 45]:

Hydrogen bronzes can be produced by ion exchange of hydrated alkali metal bronzes with protons from an acidic solution(Equation 1-11).

$$A_x^{+}(H_2O)_y[MoO_3\}^{x-} + x\ H^{+} \rightarrow H_xMoO_3 \qquad \text{(Equation 1-11)}$$

In many cases, the resulting hydrogen bronze retains a structure very similar to the alkali metal bronze from which it was derived.

Other Methods:

Hydrogen molybdenum bronzes have been produced by cathodic reduction of MoO_3 electrodes in acidic solution [28, 46]. In this process, a cathode is formed from pressed MoO_3 powder. The resulting electrode is placed into an acidic solution and current is passed through the solution, resulting in the formation of the hydrogen molybdenum bronze at the cathode.

Synthesis of Alkali Metal Bronzes:

Hydrothermal Synthesis:

Blue ($K_{0.30}MoO_3$) and red ($K_{0.33}MoO_3$) potassium molybdenum bronzes have been produced by multiple hydrothermal methods. One of these methods starts with single phase hydrogen molybdenum bronzes of H/Mo values of 0.25, 0.28, and 0.31[47]. In a typical synthesis, 0.009 moles of hydrogen bronze was placed in a 60 ml Teflon coated autoclave reactor with 30 ml of 0.9 M KCl and stirred magnetically to suspend the bronze. The reactor was then placed in a forced air convection oven at ~431 K for 30 hours. The resulting powder was filtered, dried, ground with a mortar and pestle, and washed multiple times with distilled water and centrifuged. The resulting products were examined by X-ray diffraction. They were found to depend on the H/Mo ratio of the hydrogen bronze starting material. H/Mo values of 0.25 and 0.28 resulted in the formation of blue potassium bronze phase while the product formed from the hydrogen

bronze with a H/Mo value of 0.31 resulted in formation of a red potassium bronze phase as determined by X-ray diffraction (Figure 1-11) [47]. A cutoff H/Mo value of ~0.30 was found to exist above which the red bronze is produced and below which the blue bronze is produced [48]. It is important to note that the products obtained in this reaction contained a large amount of molybdenum trioxide, which was found to be formed due to oxidation of the material by air in the autoclave, since products from reaction vessels prepared under nitrogen did not contain molybdenum trioxide.

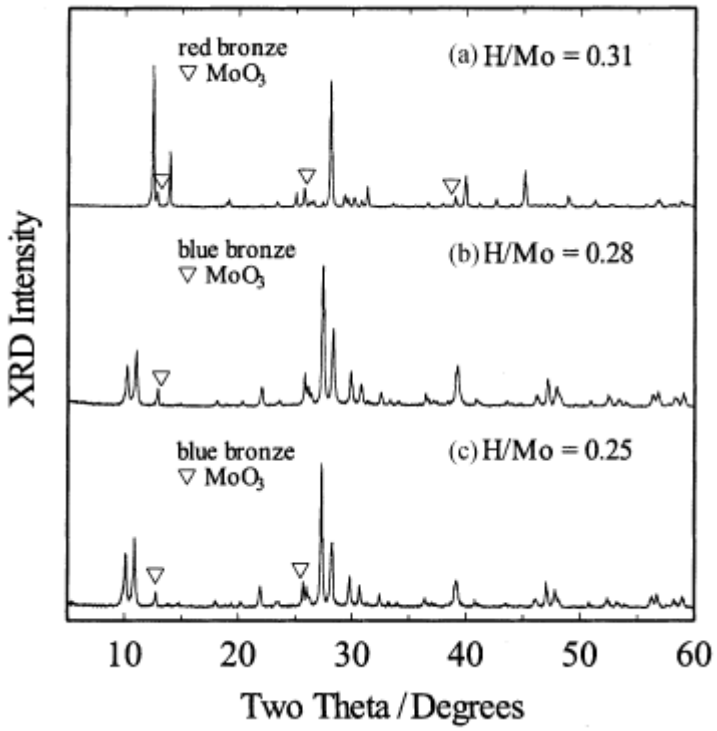

Figure 1-11: "X-Ray Diffraction Patterns of Potassium Bronze Products Obtained from Hydrogen Bronze Starting Materials with H/Mo Values of (a) 0.31, (b) 0.28, and (c) 0.25." (Adapted from Ref. [47])

The blue bronze is thought to be formed by an initial topotactic insertion of hydrated potassium cations into the hydrogen molybdenum bronze to form a hydrated mixed potassium/hydrogen bronze. The hydrated mixed bronze intermediate then

undergoes a structural rearrangement resulting in the formation of a non-hydrated blue bronze $K_{0.28}MoO_3$. This seems to be supported by X-ray diffraction data obtained at various points along the reaction coordinate [47] as well as solution calorimetry data [49].

The X-ray diffraction data shows the formation of an unknown intermediate phase that has a peak similar to the (020) reflection peak of hydrated potassium bronze, and is present at 18 hours into the reaction but is not detectable after 30 hours. Figure 1-12 illustrates the presence and disappearance of this intermediate. The flowchart in Figure 1-13 graphically illustrated the proposed scheme as well as the calorimetric heat flows associated with the reaction.

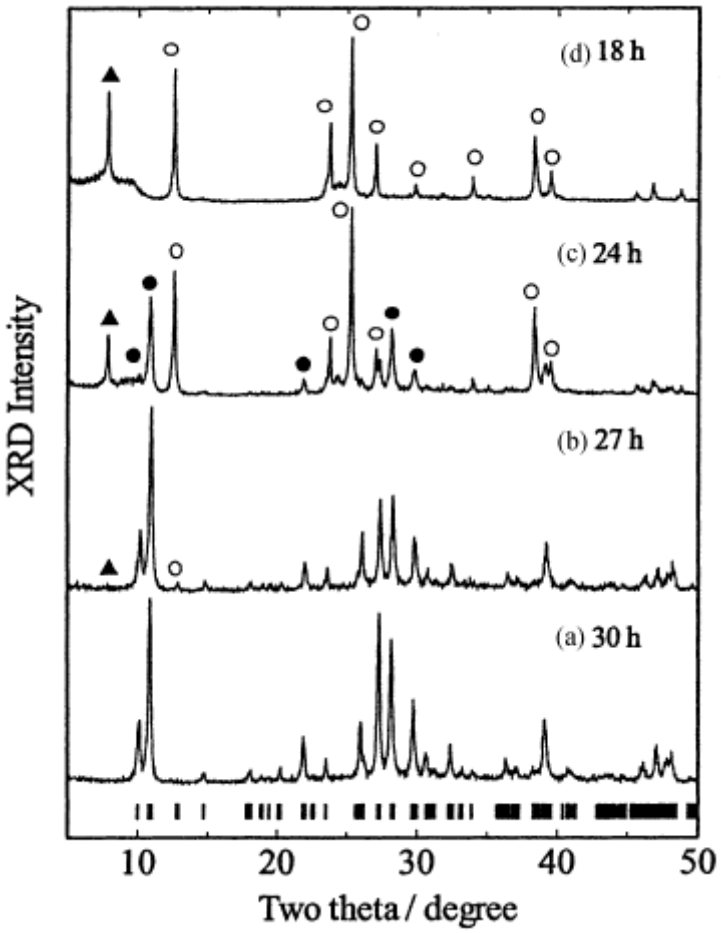

Figure 1-12: "X-Ray Diffraction Patterns of the Reaction Product at Various Points Along the Reaction Coordinate" (a) 30 hours, (b) 27 hours, (c) 24 hours, and (d) 18 hours. The black triangle denotes the unknown intermediate, the white circle denotes the starting hydrogen bronze material, the black circle denotes the blue potassium bronze product." (Adapted from Ref. [47])

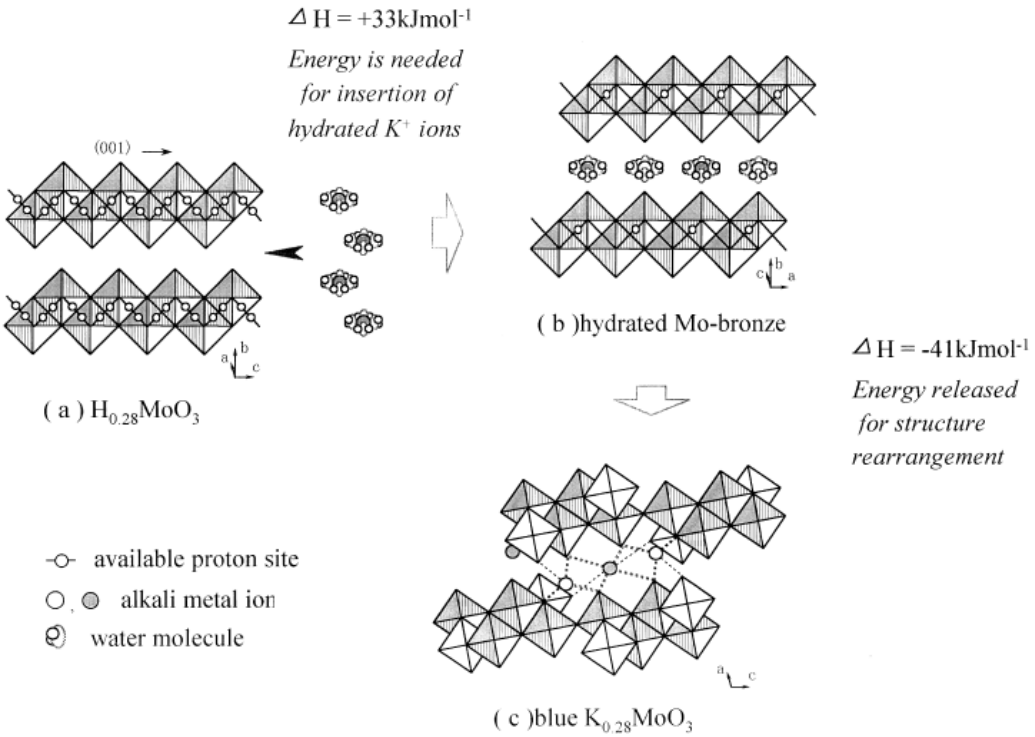

Figure 1-13: "A Proposed Reaction Scheme, Structural Rearrangement and Heat Flows Associated with the Formation of the Blue Potassium Bronze, $K_{0.28}MoO_3$." (Adapted from Ref. [49])

The following SEM micrographs in Figure 1-14 shows the starting material $H_{0.28}MoO_3$ at t = 0, the intermediate hydrated compound at t = 18 hours and 24 hours, and the blue potassium bronze product at t = 30 hours, respectively.

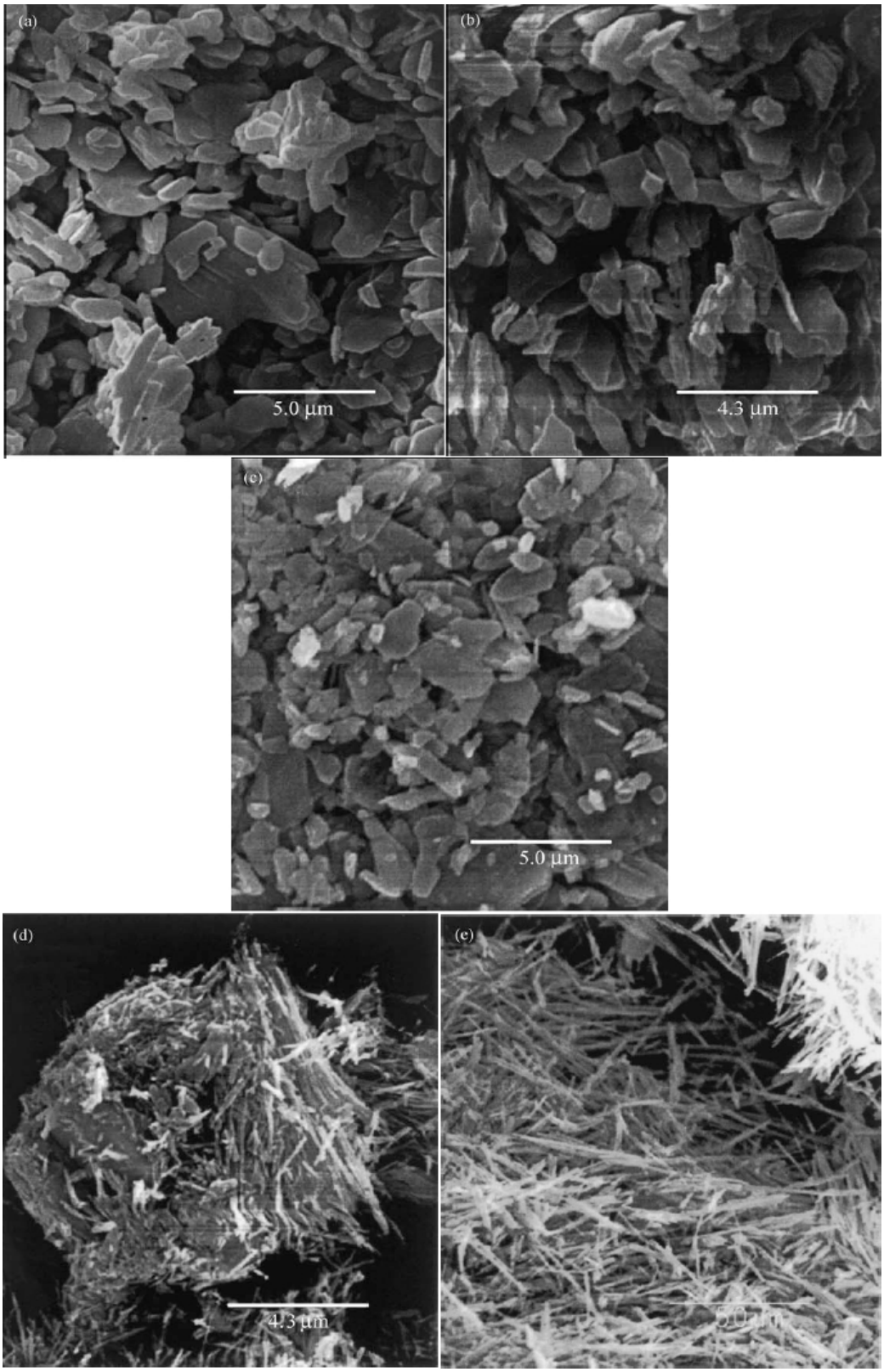

Figure 1-14: "SEM micrographs (a) $H_{0.28}MoO_3$ starting material, (b) product at t = 18 hours, (c) hydrated bronze intermediate, (d) product at t = 24 hours, (e) $K_{0.28}MoO_3$ end product." (Adapted from Ref. [47])

Based on the foregoing data it is suggested that the air-free hydrothermal reaction of the $H_{0.28}MoO_3$ bronze with aqueous KCl results in a net one to one replacement of the hydrogen with potassium to form the anhydrous blue potassium bronze, however there is a poorly defined hydrated, intermediate bronze containing both hydrogen and potassium, suggesting a reaction mechanism of the form summarized in Equation 1-12.

$H_{0.28}MoO_3 + 0.28\ K^+ \rightarrow$ hydrated intermediate $\rightarrow K_{0.28}MoO_3 + 0.28\ H^+$ (Equation 1-12)

The hydrothermal formation of the single phase red bronze, $K_{0.33}MoO_3$ was carried out by heating of $H_{0.36}MoO_3$ under similar conditions as that for the synthesis of the blue bronze. The identity of the product was determined by comparison of the X-ray pattern of the product with that of a pattern calculated from literature (Figure 1-15).

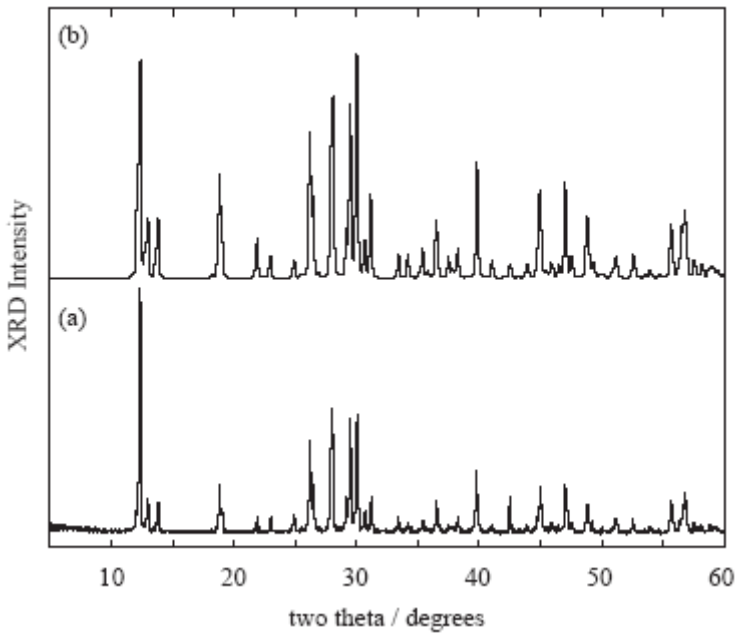

Figure 1-15: "Comparison of the X-Ray Diffraction Pattern of the Red Potassium Bronze Product (a) with a Pattern Calculated from Literature Data (b)." (Adapted from Ref. [48])

The proposed mechanism of the formation of the red potassium bronze is different than that of the blue potassium bronze. It is suggested by the literature [48] that the hydrogen bronze initially forms a hydrated mixed potassium hydrogen bronze, similar to that in the case of the blue bronze. However it is suggested that this phase decomposes to a mixture of molybdenum trioxide and molybdenum dioxide from which presumably the red bronze eventually forms, by some type of molybdenum comproportionation reaction in which the Mo(VI) and Mo(IV) react to form centers with an intermediate oxidation state of 5.67. There is some rather weak evidence supporting this in X-ray diffraction data obtained along various points along the reaction coordinate showing what the literature suggested was the formation and disappearance of molybdenum trioxide and molybdenum dioxide, see Figure 1-16. Additionally, the literature suggested that the larger crystallite dimensions of the $K_{0.33}MoO_3$ product compared to the $H_{0.36}MoO_3$ starting material, see Figure 1-17, was attributable to the product growing out of the hydrothermal solution from the molybdenum trioxide/dioxide mixture by a dissolution/deposition process. It is much more likely that the molybdenum trioxide disproportionates into a water soluble compound which goes on to react and form the product.

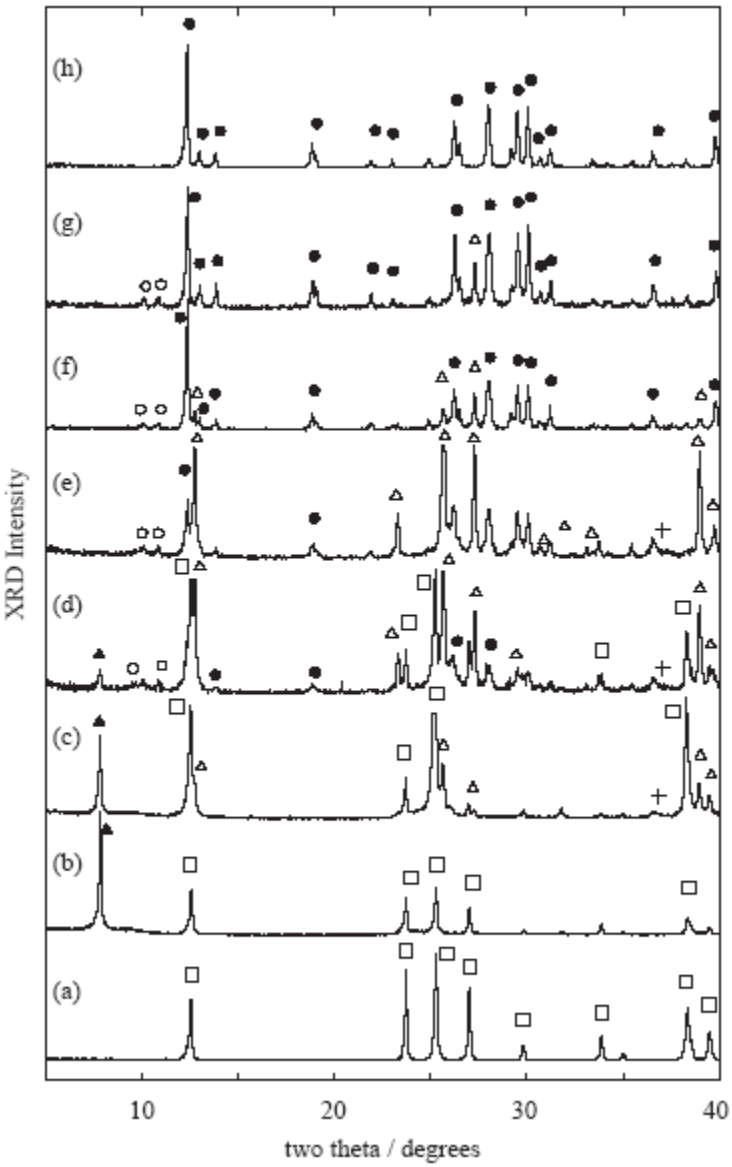

Figure 1-16: "X-Ray Diffraction Pattern as a Function of Reaction Coordinate for the Hydrothermal Synthesis of the Red Potassium Bronze, $K_{0.33}MoO_3$." (a) 0 hours, (b) 5 hours, (c) 13 hours, (d) 15 hours, (e) 15.5 hours, (f) 16 hours, (g) 17 hours, (h) 18 hours. The white square denotes the hydrogen bronze starting material, the black triangle denotes the hydrated intermediate, the white triangle denotes molybdenum trioxide, the cross denotes molybdenum dioxide, the white circle denotes a blue potassium bronze species, and the black circle denotes the red potassium bronze species, $K_{0.33}MoO_3$." (Adapted from Ref. [48])

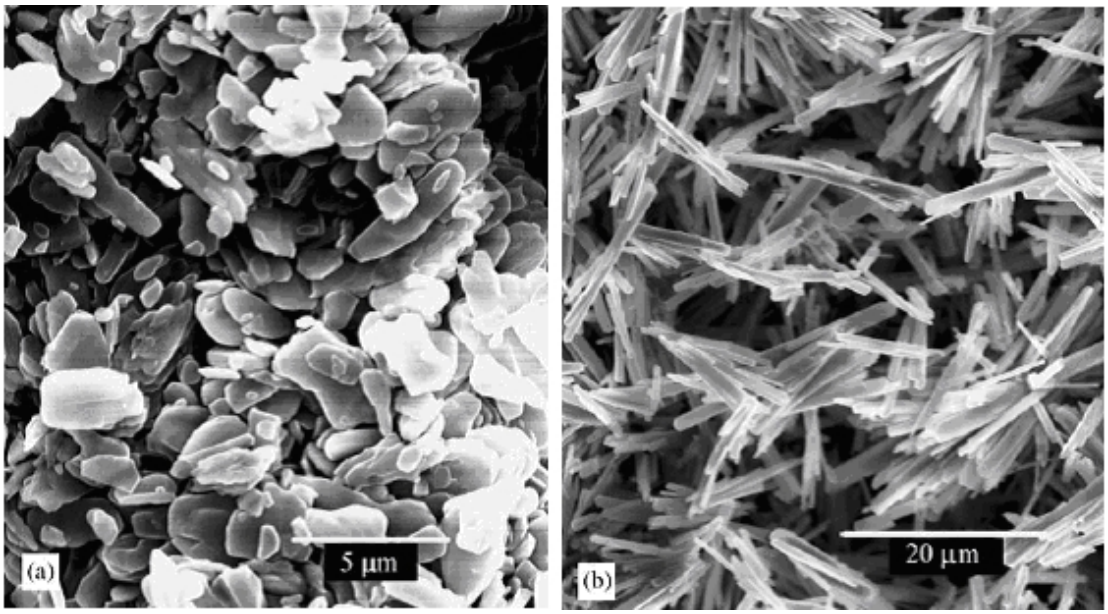

Figure 1-17: "SEM Micrograph of (a) the $H_{0.36}MoO_3$ Starting Material and (b) the $K_{0.33}MoO_3$ Red Potassium Bronze Product." (Adapted from Ref. [48])

Electrolytic Reduction of Molybdate-Molybdenum Trioxide Melts

Single crystals of the sodium and potassium forms of the molybdenum bronzes have been produced by electrolytic reduction of molten mixtures of molybdenum trioxide and the molybdate salt of the desired alkali metal bronze. For example Wold et al [50], produced single crystals of sodium and potassium molybdenum bronzes from melts of sodium molybdate-molybdenum trioxide and potassium molybdate-molybdenum trioxide, respectively, at a temperature of around 550 °C. Similar reactions carried out at 675°C yielded molybdenum dioxide, MoO_2. The reaction was carried out using the apparatus in Figure 1-18.

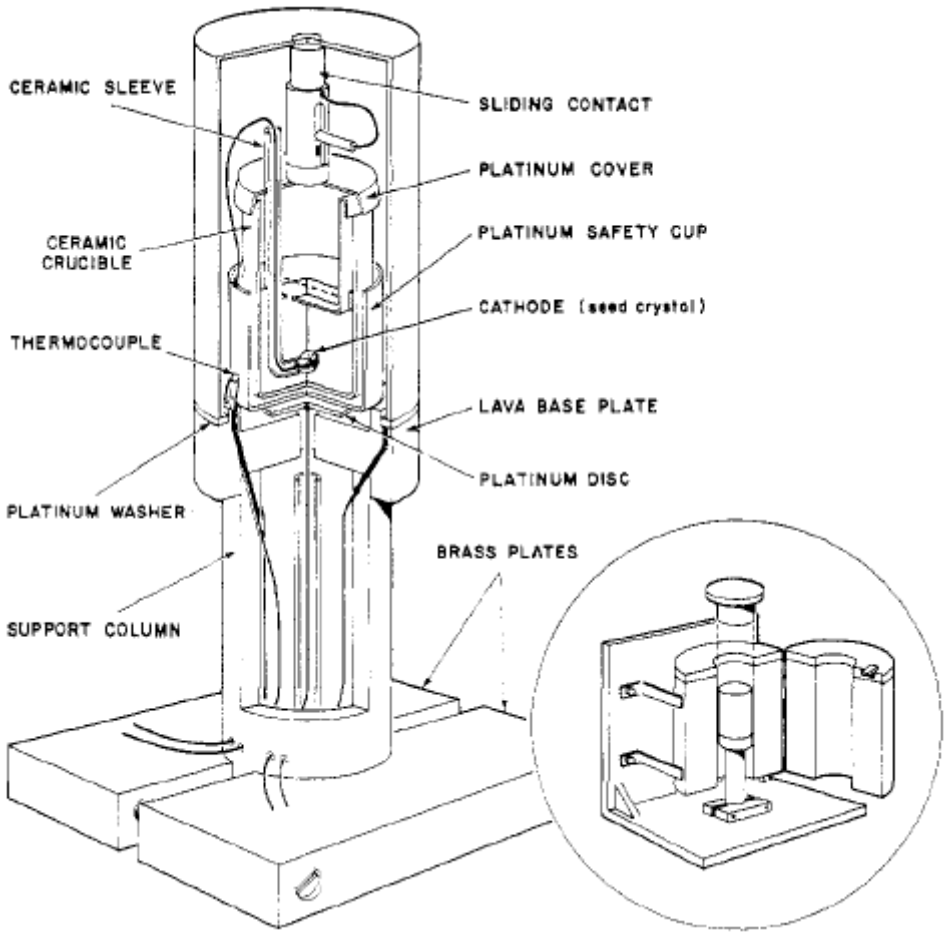

Figure 1-18: "Apparatus for Synthesis of Alkali Metal Bronzes via Electrolytic Reduction of Molten Molybdate/Molybdenum Trioxide" (Adapted from Ref. [50])

Other investigators have used similar methods to produce alkali metal bronzes [51-58]. For example, Bouchard *et al* [51] preferentially synthesized crystals of either the red potassium bronze or the blue potassium bronze by electrolysis of a melt of 3.15 MoO_3:1 K_2MoO_4. The product obtained depended on the temperature of the melt. Blue crystals were obtained at T = 550 °C, and red crystals were obtained at T = 570 °C. Mumme and Watts [52], used a similar method to synthesize $Cs_{0.25}MoO_3$ from a melt of $CsMoO_3$ and MoO_3 at 530 °C.

Temperature Gradient Flux Technique:

The temperature gradient flux method [57-61] involves charging a glass tube with a pelletized mixture consisting of the molybdate of the desired alkali metal, molybdenum trioxide, and molybdenum dioxide. The mixture ratios are defined by the stoichiometry shown in Equation 1-13.

$$n\ A_2MoO_4 + (1-2n)\ MoO_3 + n\ MoO_2 \rightarrow 2\ A_nMoO_3 \quad \text{(Equation 1-13)}$$

The sealed reaction tube is then placed in a two zone furnace in which the "cold zone" is approximately 50 °C colder than the "hot zone", thus setting up a temperature gradient in the furnace. The reaction tube is placed along this gradient, with the charged end in the hot zone and the other end in the cold zone. The respective temperatures in the oven are adjusted such that the reagents melt in the charged side. Single crystal bronzes grow in the melt while other bronze products grow along the gradient. Note that this method may also be used to grow large single crystals of MoO_2 and Mo_4O_{11}.

Chemical Reduction

Synthesis of the alkali metal bronzes may be carried out by reducing a suspension of molybdenum trioxide in a neutral pH aqueous solution of the desired alkali metal cation. Typically sodium dithionite, $Na_2S_2O_4$, is used as the reducing agent when the sodium form of the bronze is desired, thus providing both the reducing power and the

source of Na^+ ion. This generates a hydrated bronze product according to the reduction half reaction in Equation 1-14.

$$x\ A^+ + x\ e^- + y\ H_2O + MoO_3 \rightarrow A^+(H_2O)_y[MoO_3]^{x-} \quad \text{(Equation 1-14)}$$

In the case of the sodium bronze the analytical value for the Na/Mo ratio was ~ 0.45 – 0.50.

Cathodic Reduction of MoO_3 Electrode in Alkali Metal Cation Solution [28]

Production of the alkali metal bronzes by cathodic reduction is very similar to the synthesis of the hydrogen bronzes by the same method, however in the case of the alkali metal bronzes, an alkali metal cation solution is used in lieu of the acid. Typically the sulfate salt is used. One important consideration is the pH of the solution since if it is too low formation of a mixed alkali metal/hydrogen bronze is likely.

High Temperature-High Pressure Synthesis

Two phases of sodium molybdenum bronze were produced under high temperature and high pressure conditions [59]. Sodium molybdate dihydrate was annealed in a diamond anvil cell at a pressure of 5.7 to 6 MPa and a temperature of 1100 to 1273 K for 45-55 s. The resulting annealed product was dissolved in deionized water, heated to near boiling, filtered and recrystalized. The solid precipitate was then heated in

a muffle furnace at 600 K for 24 hours and dried in a vacuum dessiccator. The resulting product contained two phases of the sodium bronze, Na_xMoO_3. The first phase was a brown-red cubic phase with $0.33 < x < 0.92$ and a micron scale crystallite size (Figure 1-19). The second phase was a fluffy gray nanocrystaline phase with $0.03 < x < 0.08$ (Figure 1-20). The following micrographs illustrate each of the products.

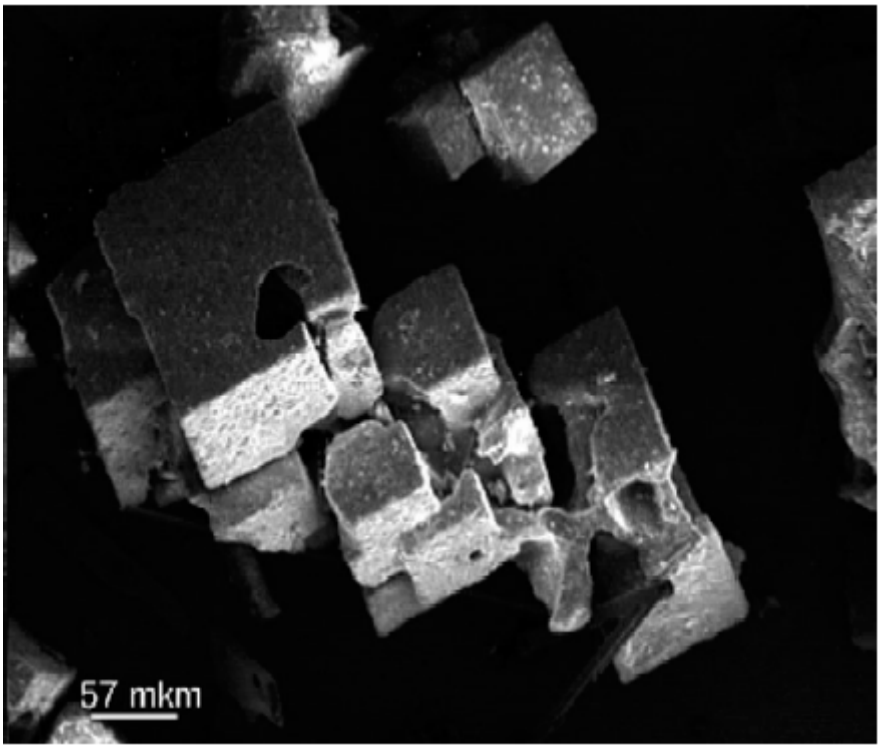

Figure 1-19: "SEM Micrograph of $Na_{0.90}MoO_3$ Micron Scale Crystals" (Adapted from Ref. [59])

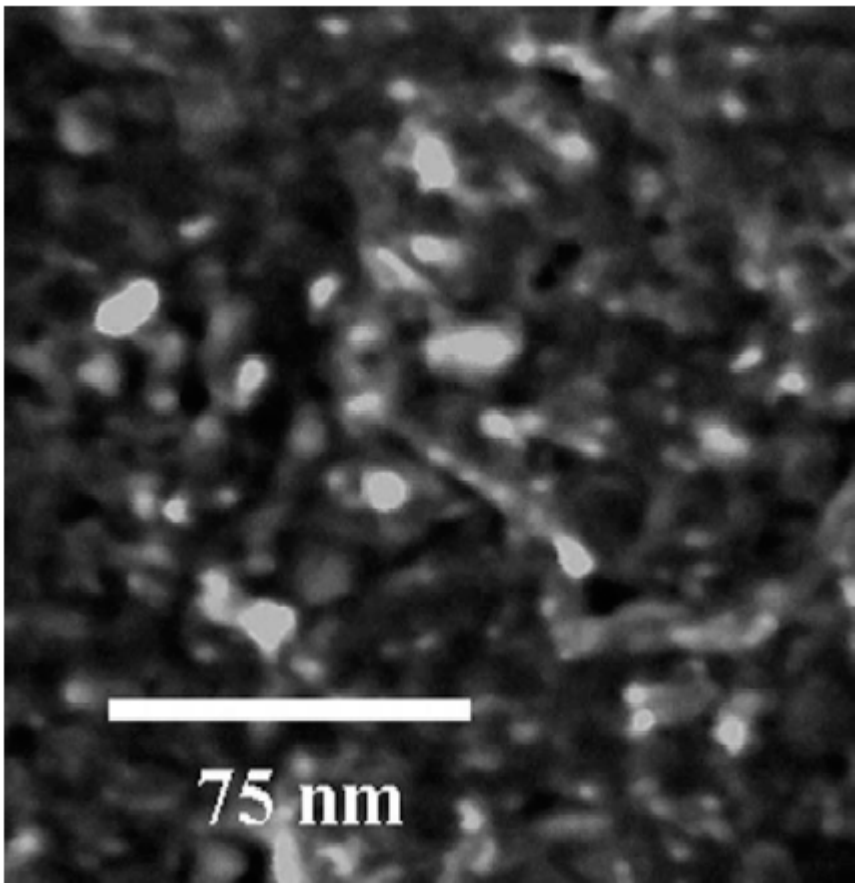

Figure 1-20: "TEM Micrograph of $Na_{0.03\text{-}0.08}MoO_3$ Nanoparticles" (Adapted from Ref. [59])

Applications of the Molybdenum Bronzes

Reduction and Removal of Heavy Metal Cations from Groundwater

The hydrogen molybdenum bronzes have been shown to efficiently remove some heavy metals, including radioactive elements, by reduction, from aqueous systems [42]. For example, bronze materials have been shown to be effective in removing uranyl ion, UO_2^{2+}, thorium(IV), lead(II), and neodymium(III). The uptake capacities for these

cations are summarized in Table 1-2. It was found that the products were metal molybdate salts and, presumably, redox processes do not play a part in these reactions.

Table 1-2: "Hydrogen Molybdenum Bronze Uptake Capacities for Various Metal Cations from Aqueous Solutions"

Metal Absorbed	Uptake capacity (mol metal/mol bronze)
Uranium(II)	~1.5
Thorium(IV)	1.1
Lead(II)	`1.5
Neodymium(II)	1.24

It is suggested that hydrogen molybdenum bronze materials could be used in permeable reactive barriers for the purpose of removing heavy metal cations from groundwater. Permeable reactive barriers can be thought of as an underground wall consisting of a material which is both permeable to groundwater flow and chemically reactive with the target contaminant. In operation the barrier is places in the path of an underground contaminant plume. The plume then flows through the barrier and the contaminant is reacted away.

Colorimetric Reagents

It is evident from the fact that the molybdenum bronze materials are intensely colored in the reduced state and yellow in the oxidized state, that these materials could be used as a colorimetric reagent for the detection of various species in water such as free chlorine, free bromine, iodine, and oxyanions of halogens such as hypochlorite, chlorite, chlorate, and perchlorate.

Electrochromic Devices

The yellow to blue color change associated with the reductive formation of the molybdenum bronze species from the molybdenum trioxide and the reverse color response upon oxidization of the bronze to the oxide, lends itself well to the use in electrochromic devices such as displays and “smart windows”. Electrochromic devices are optical materials which change their light transmittance (or absorbance) properties in response to an electrical stimulus. One application of electrochromic devices is “smart windows” which are windows which change from transparent to translucent when a voltage is applied. Additionally, similar technology is used to create electronic displays.

The choice of transition metal oxides, such as molybdenum trioxide and tungsten trioxide, and their bronzes for these devices is a good one for a number of reasons [60]. First, since they are large-band-gap semiconductors, their thin films are essentially transparent. Secondly, their non-stoichiometric bronzes are intensely colored. Thirdly, the transitions between the oxide and bronze phases are redox reactions that can be initiated in either direction by a voltage bias. Fourthly, it is easy to form thin-films of the oxides using a number of deposition methods including evaporative methods [60], radio-frequency (RF) sputtering, chemical vapor deposition (CVD), and electrodeposition [61]. Finally, the readily-formed hydrates of these oxide films are strong proton conductors allowing electron and proton injection resulting in a strong visible adsorption band. For

these reasons, several groups have been specifically interested in using molybdenum bronzes for these types of applications [61, 62].

Co-Catalytic Hydrogen Molybdenum Bronze-Platinum Oxidation of Organics

Hydrogen bronzes have been shown to improve the catalytic oxidation of small organic molecules by platinum metal [66-68]. For example, in the platinum-polyaniline-hydrogen molybdenum bronze catalytic system [63] the presence of the bronze increases the oxidation rate of formaldehyde, methanol, and formic acid in acidic (H_2SO_4) solution. The proposed mechanism for the action of the bronze is that it accelerates the oxidation and subsequent removal of the adsorbed intermediates on the surface of the platinum by taking up hydrogen upon reduction of the adsorbed intermediate and subsequently releasing the excess electrons and protons upon re-dissolution in the acidic solution in the form of the polymolybdate [64], as shown in the following scheme.

$$Pt\text{-}[CH_zO]_{ads} + wPt\text{-}[H_yMoO_3]_{ads} + H_2O \rightarrow CO_2 + Pt + wPt\text{-}[H_xMoO_3]_{ads}$$

$$wPt\text{-}[H_xMoO_3]_{ads} \rightarrow wPt\text{-}[H_yMoO_3]_{ads} + w(x\text{-}y)\, e^- + w(x\text{-}y)\, H^+$$

Scheme 1-1: "Role of hydrogen bronze as promoter in platinum catalyzed oxidation of polyaniline"

Other Applications:

Numerous other applications include the use of molybdenum bronze containing materials in the detection and chemical neutralization of explosives, including nitro

aromatics; improvised explosives, such as triacetone triperoxide; and improvised explosive precursors, such as hydrogen and organic peroxides and perchlorates. Additionally, the hydrogen form of the bronze is a two dimensional proton conductor and lends itself well to fuel cell and battery applications.

CONCLUSION

The structure and properties of the molybdenum oxide bronzes, various methods for their synthesis, and their numerous possible applications have been discussed in detail in this chapter in order to acquaint the reader with the these materials. These bronzes are partially reduced non-stoichiometric transition metal oxide insertion compounds have a rich chemistry and a myriad of applications made possible by their dual nature as a wide band gap semiconductor in their oxidized state and as a metallic conductor in their reduced state, with such starkly different properties such as electrical conductivity, metallic luster, and bright color which lend them well to applications as sensors.

Their layered structure and their ability to both reduce oxidants and intercalate cations lend them very well to applications as a both a reducing agent and an absorbent. Furthermore, their cyclic redox nature lends them well to catalytic applications.

CHAPTER II

SYNTHESIS AND CHARACTERIZATION OF MOLYBDENUM OXIDE BRONZES

INTRODUCTION

Molybdenum oxide bronzes can be synthesized by a wide variety of methods as discussed in the previous chapter. Of particular interest are lower temperature aqueous phase synthetic methods for obtaining the alkali metal bronzes, such as sodium bronze.

The objective of this study was to examine and develop low-temperature, solution phase chemistry to enable high yield synthesis of the hydrogen and sodium forms of the bronzes. This study examined the synthesis and characterization of hydrogen molybdenum bronzes via the zinc-hydrochloric acid method as a starting point, to determine its formula and reducing properties, as well as to develop a reproducible synthetic method for a hydrogen bronze with known properties. This was especially important considering the many phases of hydrogen bronzes that exist as described in Chapter I.

Synthesis of hydrogen and sodium bronzes by dithionite reduction was examined and the effects of pH, dithionite ratio, and buffer ratio on yield and composition of the product was examined systematically. Ultimately resulting in the development of an ethanolic process that consistently produced the sodium form of the bronze at an 80+% yield. The formula and reducing characteristics of this bronze was then determined. Also characterization methodologies were developed for the purpose of determining the number of reducing equivalents in the products obtained.

EXPERIMENTAL

All reagents were commercial products, ACS Grade or better and were used without further purification.

Synthesis of Proton Bronze by Dissolving Metal Reduction

The proton bronze was synthesized by *in situ* reduction of MoO_3 with nascent hydrogen produced by the reaction of zinc metal and hydrochloric acid as described in Equations 2-1 and 2-2. It is important to note that while H_2 gas is produced in this reaction, it is not the active reducing agent, but an unreacted byproduct of the reaction. The reducing agent was atomic hydrogen.

$$H^{+}_{(aq)} + Zn^{0}_{(s)} \rightarrow H_{(atomic)} \qquad \text{(Equation 2-1)}$$

$$xH_{(atomic)} + MoO_3 \rightarrow H_xMoO_3 \qquad \text{(Equation 2-2)}$$

As previously mentioned, there are several different phases of the bronze possible depending upon the extent of the reduction. For this reason it is possible to synthesize the lower air-stable bronzes as well as the higher bronzes. However the higher bronzes will immediately oxidize in the presence of oxygen to form the air-stable bronzes. In this study the zinc and hydrochloric acid were added in sufficient excess quantities to ensure, first, that the reducing equivalents were sufficient to reduce the MoO_3 into the highest air-stable form. (this was done by deliberately reacting the MoO_3 to a higher, more reduced, form and allowing it to oxidize "down" to the highest air stable form) and secondly that the zinc metal was completely dissolved by the acid such that no zinc metal remained at the end of the reaction.

Initially 30.0 g (0.208 moles) of molybdenum trioxide were placed in a 250 ml three-neck flask containing 56.80 g of zinc metal and a magnetic stirbar. A sufficient amount of water (5-10 ml) was added to form a slurry and allow magnetic stirring. The flask was then placed in a room temperature water bath to provide a heat sink for the exothermic reaction of the hydrochloric acid with the zinc. A dropping funnel containing 200 ml of concentrated hydrochloric acid was fitted into the center neck; one of the other necks was plugged with a glass stopper and a bleed-off valve was present in the third neck leading to a paraffin bubbler.

The hydrochloric acid was added to the reaction via the dropping funnel at a rate of approximately one drop per second. Evidence of the reaction was immediate with the yellow MoO_3 slurry turning purple in color and hydrogen gas being evolved and removed through the bubbler. It was important to add the acid slowly as this reaction is both exothermic and evolves hydrogen gas, which is explosive.

The reaction mixture was allowed to react overnight in order to ensure complete reaction of the zinc metal in the system. The initially formed product was greenish-gold in color but it slowly transformed to a red violet color and finally to a dark blue color. It was found that attempts to filter the more reduced bronzes usually led to clogging of the sintered glass frit, so the reaction mixture was allowed to oxidize for at least 12 hours in water by exposure to air after the initial removal of the filtrate. Once the blue color was obtained, the solid was further washed with water (3 times 300 ml) and was then dried in vacuo. The yield of the hydrogen bronze product was 28.77 g (95.58%). There is some loss of product due to the slight solubility of the bronze in the hydrochloric acid solution. There may also have been some loss of nanoparticulate product as evidenced by a blue coloration in the wash water.

Synthesis of Proton Bronze by Reduction of Molybdenum Trioxide with Sodium Dithionite

The hydrogen molybdenum bronze was synthesized by the reduction with sodium dithionite in a non-buffered aqueous system. The reaction is summarized in Equations 2-

3 through 2-5.

Reduction: $2\ MoO_3 + H^+ + 2\ e^- \rightarrow 2\ H_{0.5}MoO_3$ (Equation 2-3)

Oxidation: $S_2O_4^{2-} + 4\ H_2O \rightarrow 2\ SO_4^{2-} + 8\ H^+ + 6\ e^-$ (Equation 2-4)

$6\ MoO_3 + S_2O_4^{2-} + 4\ H_2O \rightarrow 2\ H_{0.5}MoO_3 + 2\ SO_4^{2-} + 5\ H^+$ (Equation 2-5)

Ten grams (0.0695 moles) of molybdenum trioxide were suspended in 125 ml of deionized water and continuously stirred to form a slurry. A separate sodium dithionite solution was prepared by dissolving 0.278 moles of $Na_2S_2O_4$ in 125 ml of deionized water. The dithionite solution was added to the MoO_3 slurry to initiate the reaction. The reaction was evidenced by a change in color of the reaction slurry from yellow to purple. The reaction was allowed to proceed for three days to ensure complete reaction. The as-prepared product was subsequently vacuum filtered through a fine glass frit filter, washed with water until the filtrate ran clear and vacuum dried. The pH of the filtrate was 2.5. The overall mass of the recovered product was 8.84 g.

Synthesis of the Sodium Molybdenum Bronze via Dithionite Reduction in Aqueous Media

In general, the bronze products were prepared by reacting a solution of sodium dithionite and sodium bicarbonate with a slurry of molybdenum trioxide suspended in an aqueous solution of sodium bicarbonate. Initially, the solution of sodium bicarbonate was prepared and split into two equal volumes. In the first solution, molybdenum

trioxide was suspended by magnetic stirring in a round bottom flask. Sodium dithionite was dissolved into the second volume of sodium bicarbonate solution. The dithionite containing solution was then placed into a dropping funnel and added to the molybdenum trioxide slurry at a rate of 1 to 2 drops per second. Upon addition of the dithionite solution the reaction immediately took place as evidenced by a color change from yellow to dark blue-black. However the reaction was allowed to proceed overnight to ensure that the reaction had reached completion. The solid reaction product was then removed from the reaction mixture by vacuum filtration and rinsed 5 times with 200 ml of water. The resulting product was vacuum dried and collected.

For each of these reactions, there were three factors that were varied at three different levels. These factors were: the total volume of the solvent, the dithionite to molybdenum trioxide ratio, and the sodium bicarbonate to dithionite ratio. The levels examined for the volume were 150, 300, and 450 ml. The sodium dithionite to molybdenum trioxide ratio levels were 0.107 to 1, 0.214 to 1, and 0.320 to 1. The sodium bicarbonate to sodium dithionite ratios examined were 0 to 1, 4.7 to 1, and 9.4 to 1.

For each of these experiments the mass of the solid product, the final pH of the reaction filtrate, and the percent sodium composition of the product were examined as a function of these factors.

Synthesis of the Sodium Molybdenum Bronze via Dithionite Reduction in Ethanolic Media

Two ethanolic solutions were examined initially: 35% H_2O-65% ethanol, and 50% H_2O-50% ethanol. Both solutions were successful for carrying out the reaction between sodium dithionite and molybdenum trioxide. However slightly better dissolution of the dithionite was possible with the 35%/65% mixture.

The sodium bronze was prepared by dissolving 1.779 g of the 85.4% purity dithionite in 2000 ml of the H_2O:ethanol with magnetic stirring. When the dithionite was dissolved, 10.007g of MoO_3 was added to the stirred solution via a wide spout funnel. Upon addition of the MoO_3 the slurry slowly turned from yellow to purple over several hours. The reaction was allowed to proceed for two days in order to ensure complete reaction. The resulting product was then vacuum filtered and washed with an ethanolic solution of identical composition as the reaction media and vacuum dried at room temperature. The mass of the product was 8.64 g for the 35:65 solvent mixture. The mass of product recovered for the 50:50 solvent mixture was 8.54 g.

Assay of the Purity of the Sodium Dithionite via Iodometric Titration

For these experiments the sodium dithionite used was technical grade 85+%. As the dithionite purity tends to decrease over time due to decomposition to sodium sulfate it was necessary to assay the dithionite prior to use. The assay method chosen was an

iodometric method and is described in detail. In the overall process a sample of sodium dithionite, $Na_2S_2O_4$, was fixed with excess formaldehyde to form the stable sodium formaldehyde sulfoxylate as shown in Equation 2-6.

$$Na_2S_2O_4 + 2CH_2O + H_2O \rightarrow NaHSO_2 \cdot CH_2O + NaHSO_3 \cdot CH_2O \qquad \text{(Equation 2-6)}$$

The sodium formaldehyde sulfoxylate compound was then oxidized by "solublized I_2" (triiodide, I_3^-) to form sodium bisulfate, $NaHSO_4$ and hydrogen iodide, HI, as shown in Equation 2-7.

$$NaHSO_2 \cdot CH_2O + 2\ I_2 + 2\ H_2O \rightarrow NaHSO_4 + CH_2O + 4HI \qquad \text{(Equation 2-7)}$$

Once the amount of triiodide required to titrate the solution was determined, the amount of dithionite present was calculated.

Three solutions were prepared for this method, including a standard iodine solution, a formaldehyde fixing solution and an acetic acid solution.

Preparation of the Standard Iodine Solution:

The standard iodine solution was prepared on a 2000 ml scale by dissolving 36 to 40 g of potassium iodide, KI, in 600 ml of deionized water. Then 25.6 to 26 g of elemental iodine, I_2, was ground with a mortar and pestle and dissolved in the potassium

iodide solution. Upon dissolution of the iodine, the entire solution was filtered through a glass funnel plugged with glass wool in order to remove any insoluble material from the solution. The glass funnel and glass wool was then rinsed with deionized water into the filtered solution until all of the red solution was removed. Finally the volume of the filtered solution was brought up to 2000 ml total volume with deionized water.

The prepared iodine solution was then standardized with sodium thiosulfate using the following procedure. First, 50 ml of 0.1013 N sodium thiosulfate standard solution was pipetted into a 125 ml Erlenmeyer flask, placed on the stir-plate of a Schott Digital Buret and magnetically stirred. The thiosulfate was then titrated with the iodine solution to a point near the expected endpoint. Then 1-2 ml of 1% starch indicator solution was added to the titrated solution and the solution was titrated to the endpoint as evidenced by the starch indicator.

Preparation of the Formaldehyde Solution:

The formaldehyde fixing solution was prepared by dissolving 350 ml of 37.0 wt % formaldehyde in 500 ml of water resulting in 850 ml of fixing solution. The pH of the formaldehyde solution was adjusted within the range of 8 to 9 by addition of sodium carbonate. Eighty five milliliters of this solution will fix up to 8 g of dithionite.

The adjustment of the pH is extremely important to the successful outcome of this measurement, because if the pH is too high the triiodide will react with oxygen in the

solution as well as the dithionite resulting in a large overestimation of the dithionite content. It is important to note that the literature suggested 3 g of sodium carbonate per 850 ml volume of formaldehyde solution, however this resulted in a pH of 11.1, and a greatly erroneous measure of the dithionite content in excess of 110%. It was determined that 0.335 g of sodium carbonate results in a pH of 8.1 to 8.3 for an 850 ml volume of the fixing solution.

Preparation of the Acetic Acid Solution:

A 20 wt % acetic acid solution was prepared by diluting glacial acetic acid with water in a 1:4 glacial acetic acid:water w/w ratio.

Fixation of Dithionite:

The dithionite was fixed by the following procedure. First, 75 ml of the formaldehyde solution was transferred to a 500 ml volumetric flask using a long-stem funnel in order to avoid splashing of the solution onto the neck of the flask. A second dry long-stem funnel was used to transfer up to 8 g of sodium dithionite into the flask. Then 10 ml of the formaldehyde solution poured through the second funnel in order to rinse any remaining dithionite into the volumetric flask. Both funnels were rinsed into the volumetric flask with deionized water, and then the volume of the solution was adjusted to 500 ml.

Titration of the Dithionite Solution:

The titration of the dithionite solution was carried out by first pipetting 10 ml of the fixed dithionite solution into a 250 ml beaker and then adding 90 ml of deionized water and 5 ml of 20% acetic acid solution. The beaker was magnetically stirred on the stir-plate of the digital buret and titrated to near the endpoint with the standardized iodine solution. Once the endpoint was approached, 1-2 ml of 1% starch indicator was added to the beaker and the solution was titrated to the endpoint.

Determination of the Molar Reducing Equivalents of the Bronze Products

Determination of the number of reducing equivalents was carried out by two independent methods: The reduction of chromate to chromium(III) and the reduction of iodine solution (triiodide).

Determination of the reducing equivalents via chromate reduction was carried out by reacting a known amount of the bronze products with an excess of potassium dichromate solution. The initial and final concentrations were determined by UV-Visible absorption using a Cary 50 UV-visible spectrophotometer. A known solution of 9.970 mM concentration in chromium(VI) ion was initially prepared by dissolving 0.2939 g of potassium dichromate in 200.140 g of water. The absorbance of this solution was then determined at 440 nm in a 1 cm path length cuvette. The resulting absorbance was determined to be 2.2773. By application of Beer's Law, the extinction coefficient was

determined to be 228.4 $cm^{-1}M^{-1}$ at 440 nm. Known amounts of the bronzes were placed into scintillating vials and reacted with ~20 g of the dichromate solution for ~29 h. The solutions were then filtered using a 0.45 micron polypropylene syringe filter.

The reaction of the bronze with the chromium(VI) of the dichromate solution is a three-electron process. That is, for every mole of chromium(VI) reduced to chromium(III), three molar reducing equivalents were required. Therefore, by knowing the initial and final concentrations of the chromium(VI) in the solution and assuming that all of the reducing equivalents come from the bronze, and that the bronze was completely oxidized, it was possible to determine the number of molar reducing equivalents in the bronze.

Triplicate reactions were run for both the hydrogen molybdenum bronze and the sodium molybdenum bronzes in order to determine the error in the experiment. The experiments are summarized in Table 2-1.

Table 2-1: "Data from Determination of Bronze Molar Reducing Equivalents by Reduction of Dichromate"

Type of Bronze	mg of Bronze	g of Dichromate solution	Initial [Cr^{6+}]	Final [Cr^{6+}]	Reducing Equivalents per mole Bronze
Hydrogen	44.7	20.0319	9.970 mM	7.461 mM	0.487
Hydrogen	45.7	20.0020	9.970 mM	7.789 mM	0.414
Hydrogen	41.2	20.0006	9.970 mM	7.753 mM	0.466
Sodium	76.3	20.0138	9.970 mM	8.186 mM	0.226
Sodium	75.3	20.0010	9.970 mM	8.224 mM	0.224
Sodium	71.6	20.0184	9.970 mM	8.189 mM	0.239
Control	0	20.0037	9.970 mM	9.924 mM	--

The reducing capacity of the hydrogen bronze was determined to be 0.456 ± 0.038 equivalents per mole. Likewise, the reducing equivalents for the sodium bronze was determined to be 0.230 ± 0.008 equivalents per mole.

Reducing equivalent determination via triiodide reduction was carried out in a similar way as in the chromate method. Scintillation vials were charged with ~100 mg of hydrogen molybdenum bronze or ~200 mg of sodium molybdenum bronze. Then 20.00 g of iodine solution ($[I_2]$ = 0.05000 ± 0.00025 M) was added to each vial and agitated for 48 h. The contents were then filtered through 0.45 micron PTFE syringe filters using a 10 ml syringe.

An extinction coefficient was determined for the iodine solution to be 365.46 cm^{-1} M^{-1} at 490.0 nm by measuring the absorbance of the 0.05000 M standard iodine solution in a 0.1 cm path length quartz cuvette. As an alternate method a calibration curve of concentration vs. absorbance was created using iodine concentrations of 0.01249,

0.02499, 0.03753, and 0.05000 M resulting in the following relationship in Equation 2-8 and Figure 2-1. Inherent in the calibration curve was the 0.1 cm pathlength and 490 nm wavelength.

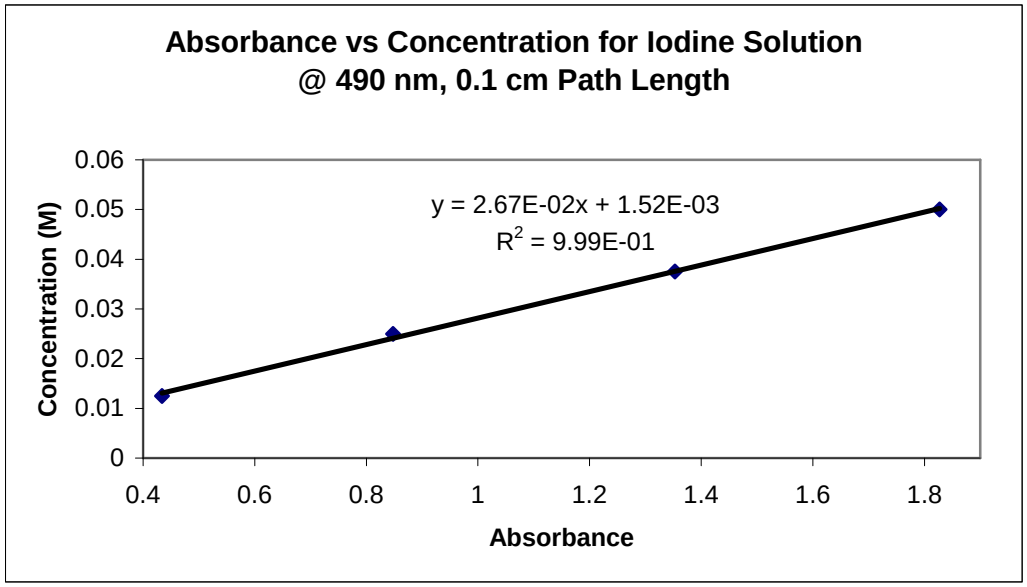

Figure 2-1: "Calibration Curve of Concentration vs. Absorbance for Iodine Solution"

Conc. (M) = 0.0267(Absorbance) + 0.00152 M; R^2 = 0.9985 (Equation 2-8)

Triplicate reactions were run for both the hydrogen molybdenum bronze and the sodium molybdenum bronzes in order to determine the error in the experiment. The concentrations were calculated using the calibration curve and adjusted for the control concentration. The experiments are summarized in Table 2-2.

Table 2-2: "Data from Determination of Bronze Molar Reducing Equivalents by Reduction of Iodine"

Type of Bronze	Amount of Bronze (mg)	Amount of Iodine Solution (g)	Initial $[I_2]$, (M)	Final $[I_2]$, (M)	Reducing Equivalents per mole Bronze (Control Adjusted)
Hydrogen (Zn/HCl)	101.3	20.0182	0.05000	0.03916	0.582
Hydrogen (Zn/HCl)	101.7	20.0052	0.05000	0.03945	0.562
Hydrogen (Zn/HCl)	101.3	20.0114	0.05000	0.03884	0.599
Sodium (Ethanolic)	198.9	20.0250	0.05000	0.04231	0.228
Sodium (Ethanolic)	201.4	20.0012	0.05000	0.04182	0.241
Sodium (Ethanolic)	203.8	20.0209	0.05000	0.04124	0.256
Control	0	20.0104	0.05000	0.04934	--

The resulting data suggested average values for the molar reducing equivalents of 0.581 ± 0.019 Eq for the hydrogen molybdenum bronze product, and 0.242 ± 0.014 Eq for the sodium bronze.

Other methods were examined for this purpose including reduction of permanganate in basic media, and reduction of silver nitrate. These methods were unsuccessful for this purpose. The permanganate underestimated the number of reducing equivalents significantly. This difficulty was likely due to formation of a mixture of manganese species. The silver nitrate method overestimated the number of reducing equivalents significantly, however this was because the silver cation reacted with the molybdenum bronze to form a silver molybdate species.

Determination of the Sodium Content of the Bronze Products

The sodium content of the bronzes were determined by inductively coupled plasma spectroscopy (ICP). The samples were prepared be dissolving them in a hydrogen peroxide/ammonium hydroxide solution. The sodium concentration of the resulting solution was determined via ICP and corrected for the trace of sodium that was present in the solvent mixture. Sources of sodium in the control were expected to come from the glass vial, and from impurities in the ammonium hydroxide. A standard of known sodium concentration was also included.

RESULTS AND DISCUSSION

Hydrogen Molybdenum Bronze Products:

The yield and number of molar reducing equivalents were determined for each of the hydrogen molybdenum bronze products synthesized (Table 2-1). The loss of product associated with the zinc/hydrochloric method results from the fact that hydrogen bronze product is somewhat soluble in hydrochloric acid. This was evidenced by a dark color in the filtrate that, when exposed to air changed color from a brownish gold to a reddish purple to an ultimately blue color, much like the solid bronze. The product loss associated with the dithionite reduction method resulted from the competitive reaction of the reduced molybdenum centers with sodium cations present in the solution to form the

sodium molybdenum bronze product. This sodium bronze product had a solubility of approximately 50 millimoles per liter (Refer to Chapter III) in water after 5 days.

Table 2-3: "Comparison of the Product Yields for the Two Synthetic Methods for the Hydrogen Molybdenum Bronzes"

Synthetic Method	**Yield**
Zinc/Hydrochloric Acid	95.6%
Dithionite Reduction (washed)	75.0%

The XRD pattern of the hydrogen molybdenum bronze from the dissolving metal reduction in Figure 2-2 did not exactly match the literature values in the XRD library. However this was to be expected as the hydrogen to molybdenum ratio was determined to be 0.58 to 1. However, in order to ensure that the XRD spectra did not originate from a something besides a hydrogen bronze, the product was heated in a muffle furnace in air for several hours in order to completely oxidize the product. The XRD spectrum in Figure 2-3 of the pyrolyzed product corresponded to molybdenum trioxide with no other peaks present. This suggested that the product was a hydrogen molybdenum bronze.

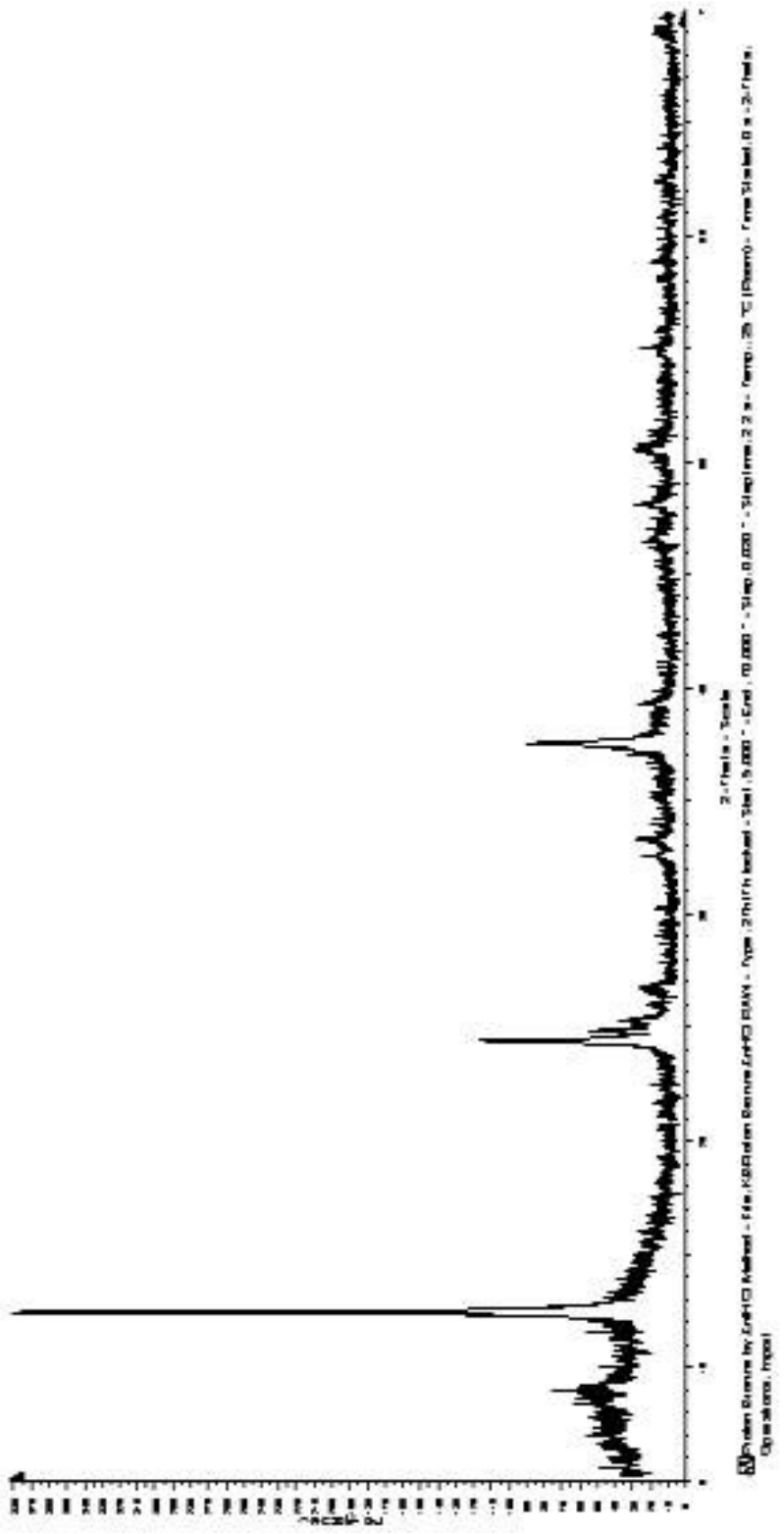

Figure 2-2: "XRD Spectrum of Hydrogen Molybdenum Bronze Synthesized by Zinc/Hydrochloric Acid Method"

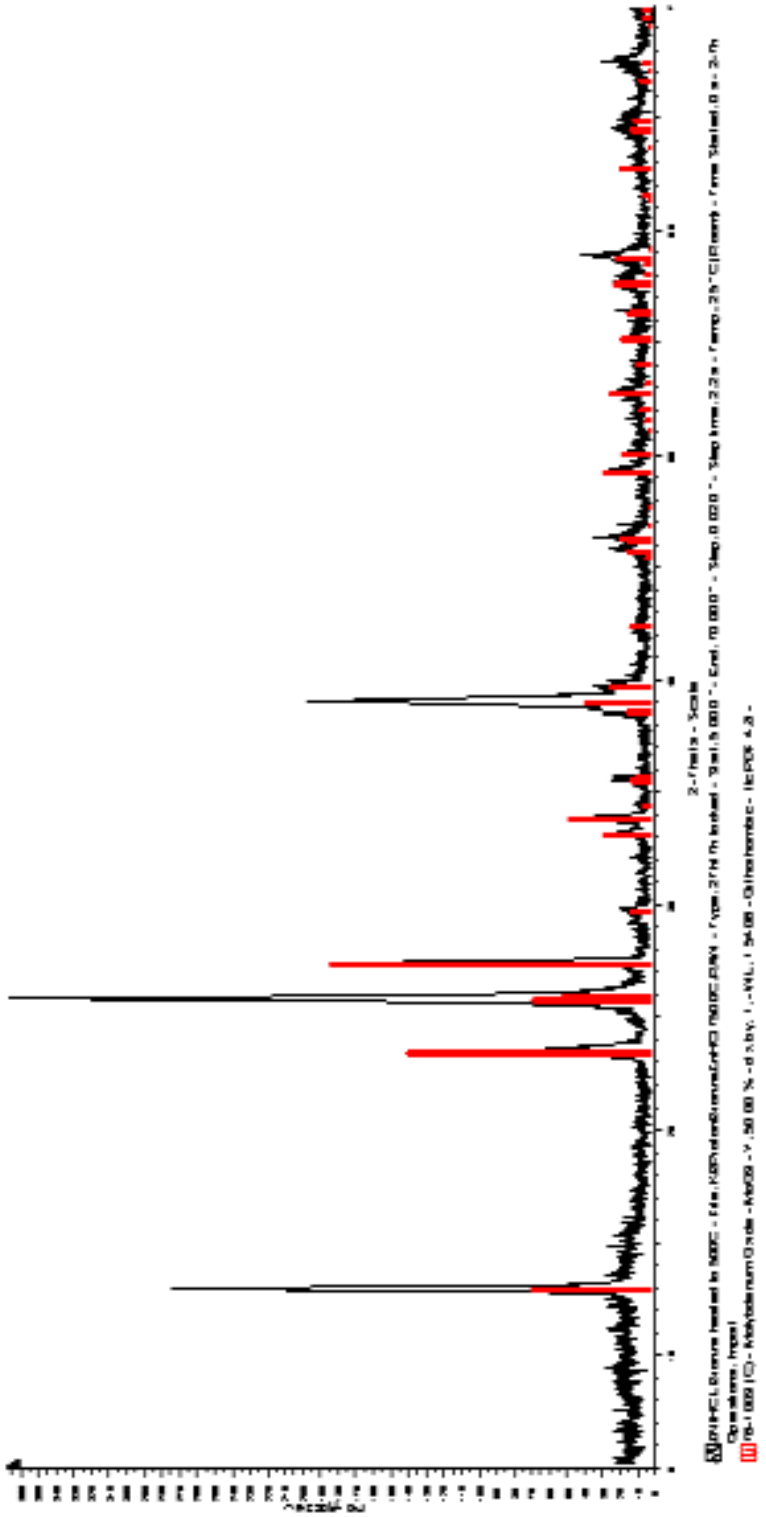

Figure 2-3: "XRD Spectrum of Pyrolysis at 500 ºC Product of Hydrogen Molybdenum Bronze Synthesized by Zinc/Hydrochloric Acid Method"

One interesting outcome of this experiment was the value obtained for the molar reducing equivalents of 0.58. The phases of hydrogen bronzes observed by Glemser[15, 18, 19] and revised by Bertill [30] were found to have the approximate hydrogen to molybdenum ranges as described in Table 2-4.

Table 2-4: "H/Mo Ranges for the Various Phases of Hydrogen Molybdenum Bronzes"

Phase	Description	Range
I	Blue, Orthorhombic	0.23 – 0.40
II	Blue, Monoclinic	0.85 – 1.04
III	Bordeaux Red, Monoclinic	1.55 – 1.72
IV	Green Monoclinic	2.0
Ref. [65]	Blue Monoclinic	0.25 – 0.60

The product obtained in this experiment lay outside the range of either of these phases. It is likely that the product was a member of a newly discovered fifth phase of hydrogen bronze with a hydrogen to molybdenum ratio varying from 0.25 to 0.60 [65].

Synthesis of Proton Bronze by Reduction of Molybdenum Trioxide with Sodium Dithionite

Although the stoichiometry of the reaction would suggest a 1:0.167 MoO_3:$S_2O_4^{2-}$ ratio, trial and error experimentation determined that a 1:0.25 MoO_3:$S_2O_4^{2-}$ ratio was required to ensure that no molybdenum trioxide was present in the product as determined by powder X-ray diffraction. The XRD spectrum in Figure 2-4 was obtained for the

1:0.167 MoO_3:$S_2O_4^{2-}$ ratio product which contains some molybdenum trioxide. Figure 2-5 illustrates the XRD spectrum for the 1:0.25 MoO_3:$S_2O_4^{2-}$ ratio product.

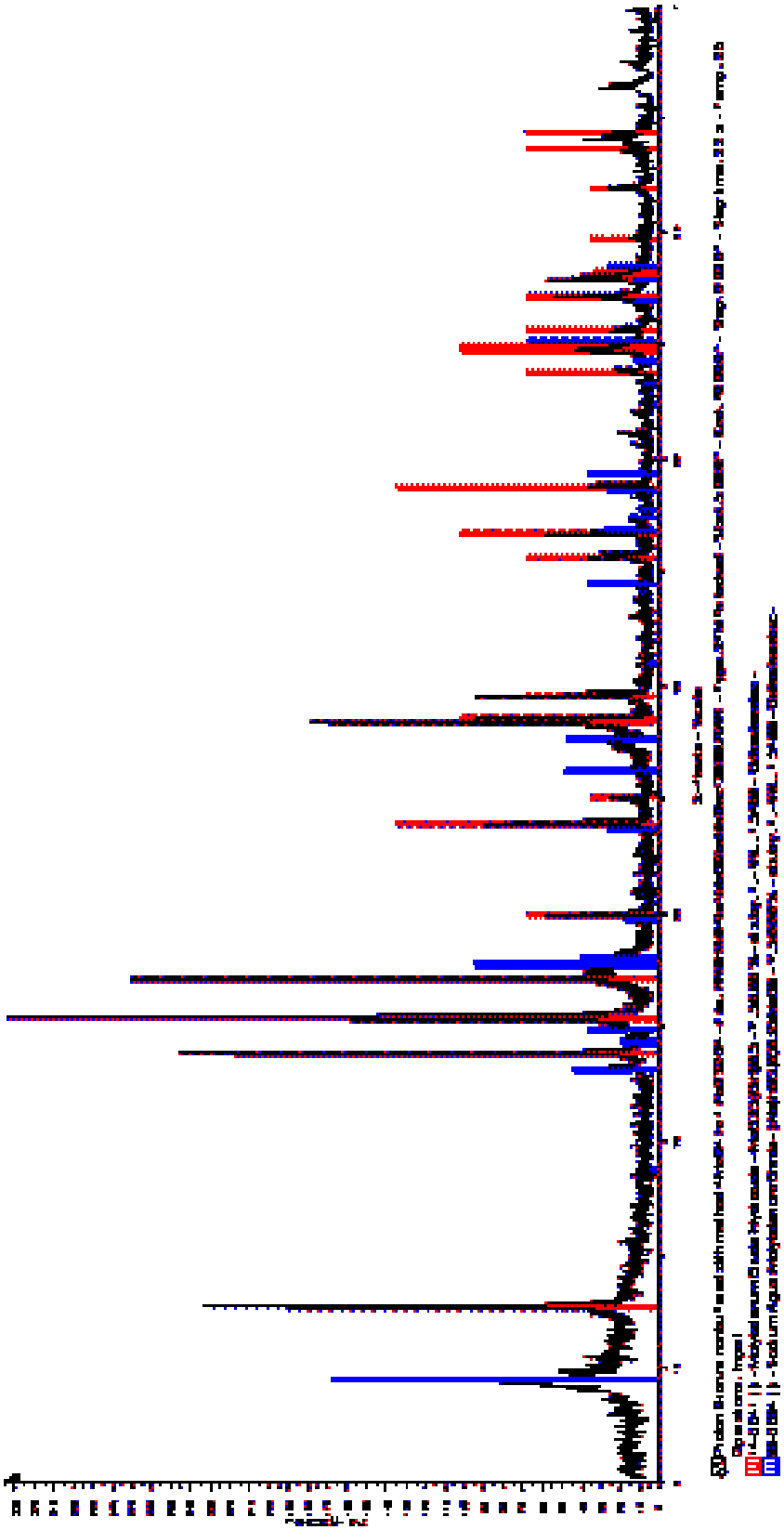

Figure 2-4: "XRD Spectrum for the 6:1 MoO_3:$S_2O_4^{2-}$ Product"

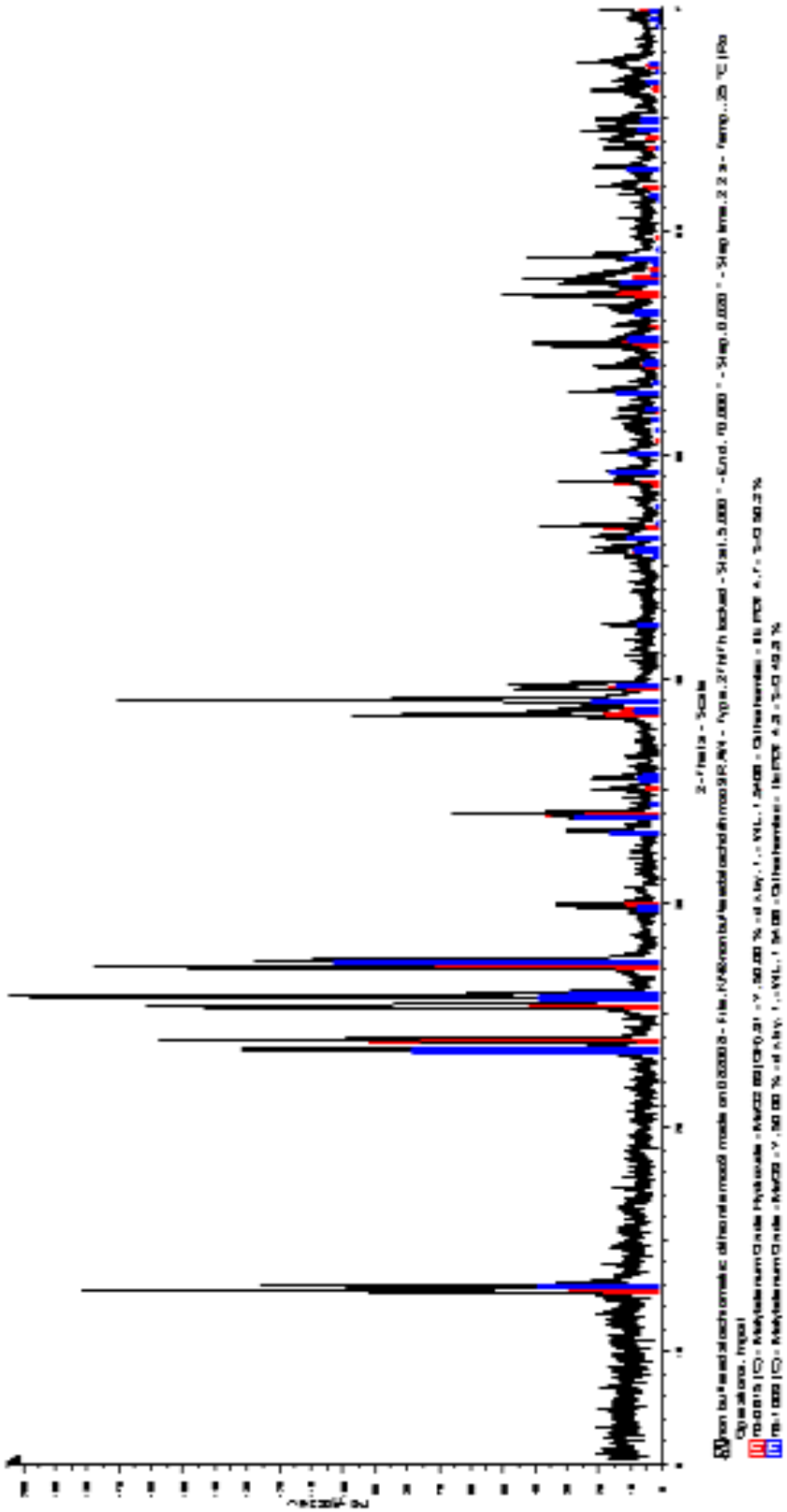

Figure 2-5: "XRD Spectrum for the 4:1 MoO_3:$S_2O_4^{2-}$ as Prepared Product"

The XRD analysis of the as prepared product suggested the presence of sodium bronze in the product. The sole source of the sodium in the system was the sodium dithionite. Suggesting that there is an exact optimum value for the dithionite to molybdenum trioxide ratio however it was more practical from a synthetic point of view to slightly exceed this maximum and err on the side of production of sodium bronze since the sodium bronze was found to be much more soluble in water compared with the hydrogen bronze, and thus, it was possible to remove the sodium bronze from the sample by stirring the product with water for several days. However molybdenum trioxide is nearly insoluble and not easily removed from a mixture of hydrogen bronze and molybdenum trioxide. Powder X-ray diffraction analysis of the washed product indicated that only the proton form of the bronze was remaining. Approximately 85.2% of the mass of the mixed bronze product was recovered which suggested that 7.53 g of the product from the reaction was the hydrogen bronze. This corresponded to an actual yield of around 78%.

Aqueous Sodium Molybdenum Bronze Products:

For the aqueous synthesis of the molybdenum bronze products the reaction volume had little or no effect upon the average composition of the solid product as illustrated in Figures 2-6 to 2-8. The effects of the dithionite to molybdenum trioxide ratio, and the sodium bicarbonate to sodium dithionite ratio were uniform as a function of

volume. For this reason the foregoing data was explained in terms of the 300 ml set of experiments.

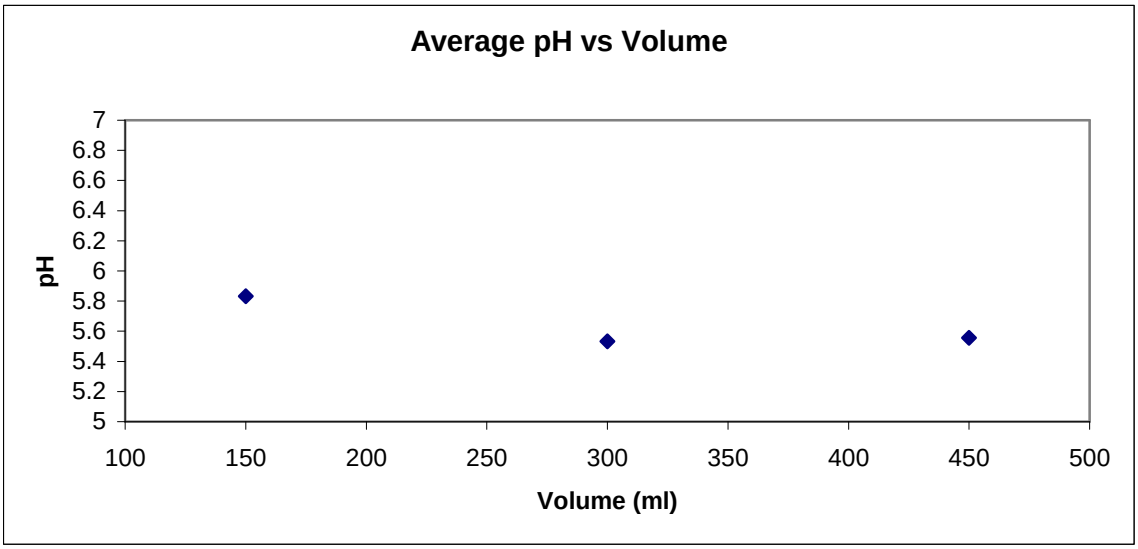

Figure 2-6: "Average Final pH of Filtrate vs. Reaction Volume"

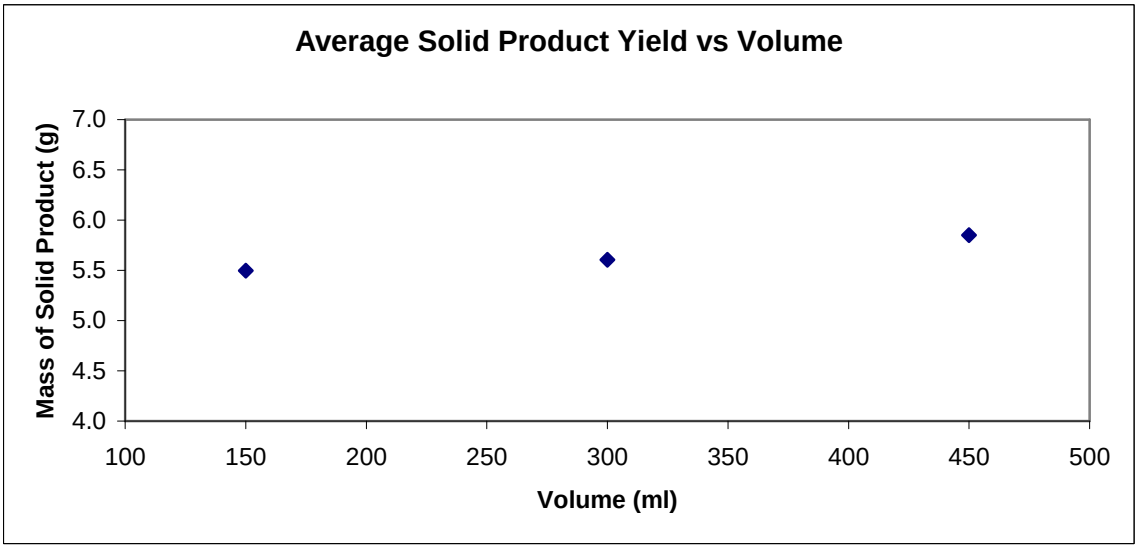

Figure 2-7: "Average Solid Product Yield vs. Reaction Volume"

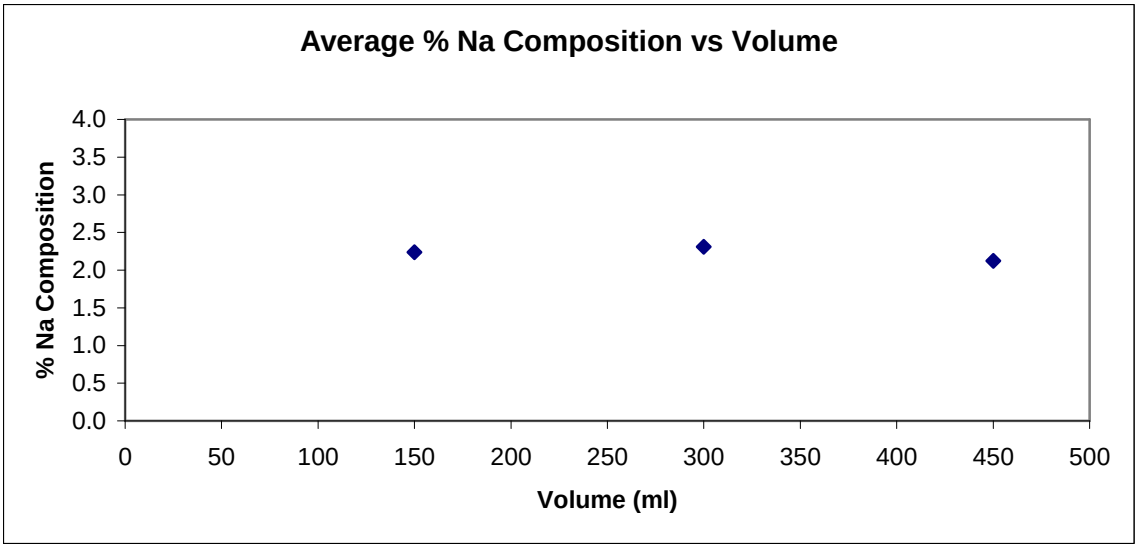

Figure 2-8: "Average Percent Sodium Composition in the Solid Product vs. Reaction Volume"

The data for the 300 ml set of experiments are presented in Table 2-5, as well in the form of surface plots in Figures 2-9 through 2-11.

Table 2-5: "Effects of Dithionite:Molybdenum Trioxide Ratio and Sodium Bicarbonate:Dithionite Ratios on pH, Solid Product Mass, and Sodium Composition of Sodium Molybdenum Bronze Product, 300 ml Set"

$Na_2S_2O_4$:MoO_3	$NaHCO_3$:$Na_2S_2O_4$	pH After	m prod	%Na by Mass
0.11	0	2.6	9.24	0.13
0.11	4.65	4.8	2.53	2.88
0.11	9.37	5.9	2.94	3.59
0.21	0	3	8.28	0.20
0.21	4.68	5.9	3.56	3.68
0.21	9.37	8.3	4.23	3.75
0.32	0	2.9	9.48	0.56
0.32	4.687	7.8	6.26	3.79
0.32	9.37	8.6	3.92	3.51

The effects of the sodium dithionite to molybdenum trioxide ratio and the sodium bicarbonate to sodium dithionite ratios on final pH of the reaction mixture, the mass of

recovered solid product, and the percent sodium composition of the solid product are graphically illustrated in the three-dimensional surface plots in Figures 2-9 to 2-11.

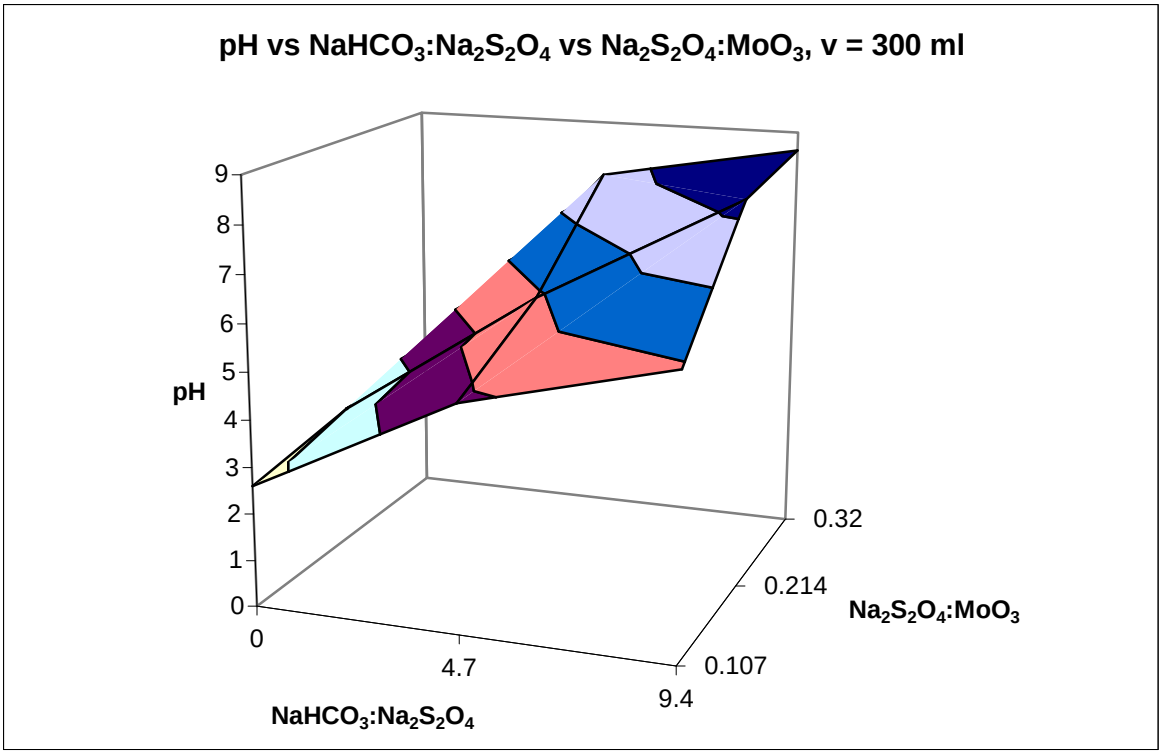

Figure 2-9: "Surface Plot of Final pH vs. Sodium Dithionite:Molybdenum Trioxide vs. Sodium Bicarbonate:Sodium Dithionite"

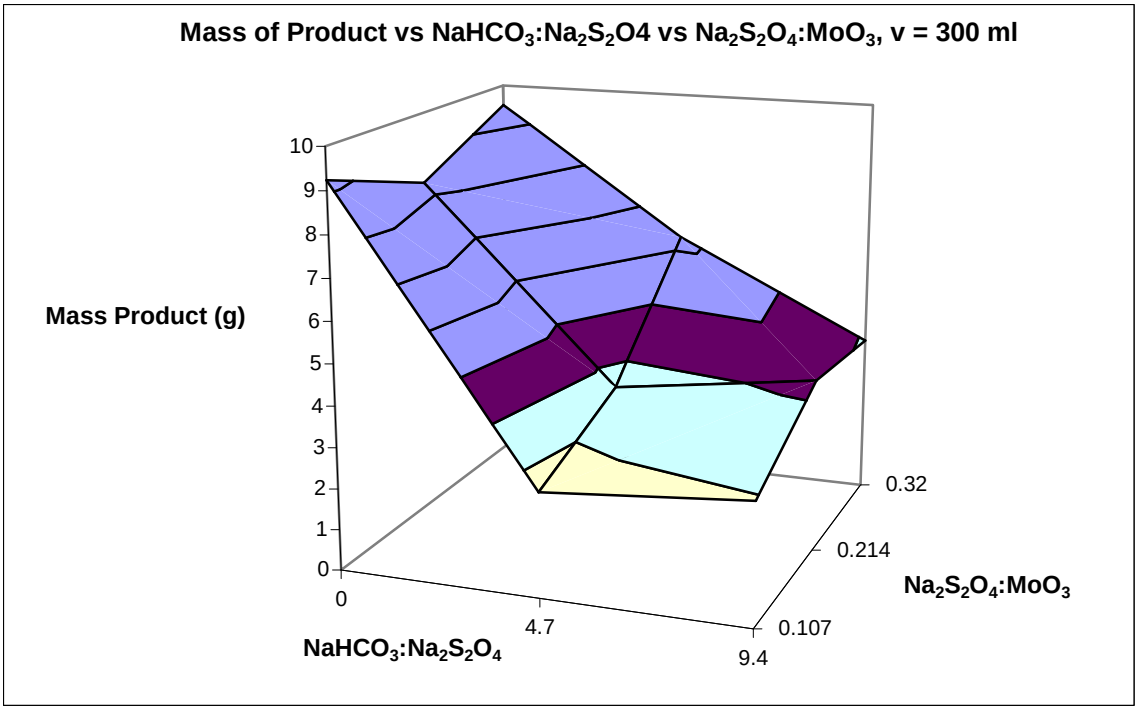

Figure 2-10: "Surface Plot of Recovered Solid Product Mass vs. Sodium Dithionite:Molybdenum Trioxide vs. Sodium Bicarbonate:Sodium Dithionite"

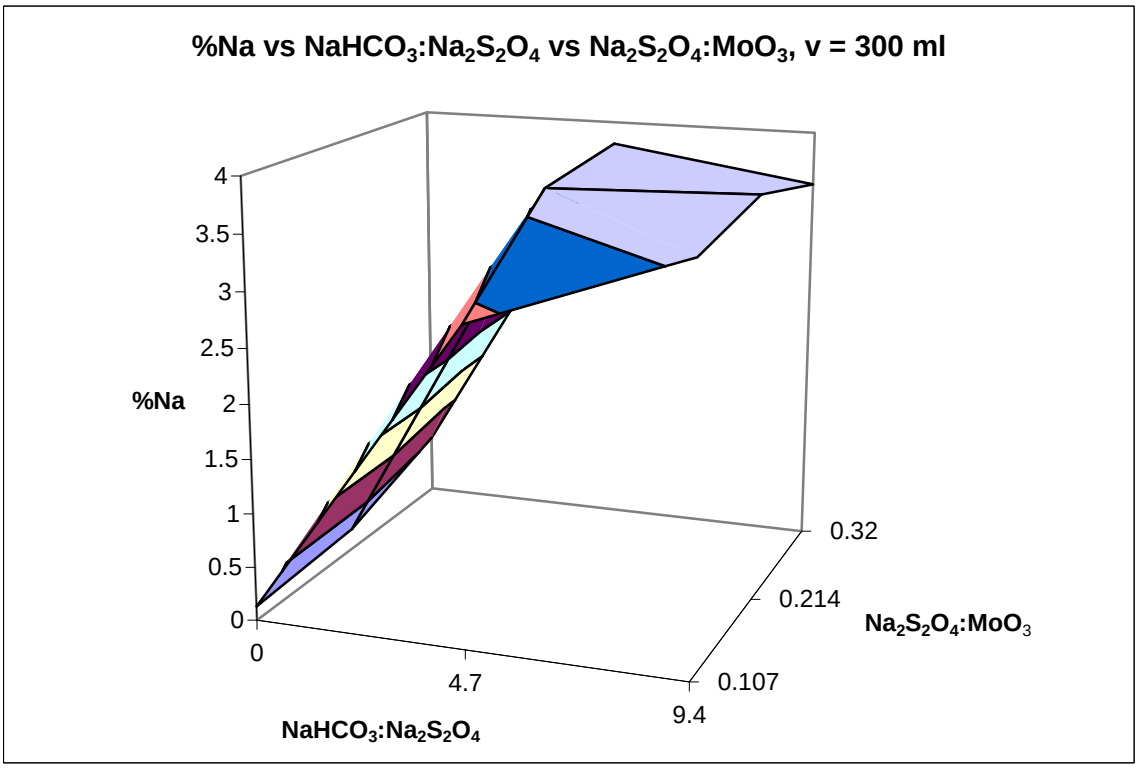

Figure 2-11: "Surface Plot of Percent Sodium Composition of the Solid Product vs. Sodium Dithionite:Molybdenum Trioxide vs. Sodium Bicarbonate:Sodium Dithionite"

As the bicarbonate:dithionite ratio was increased relative to the dithionite:molybdenum trioxide ratio (and relative to the absolute amount of dithionite in the system as the molybdenum trioxide loading was held constant) the final pH increased, see Figure 2-9. This was intuitive, as the purpose of the sodium bicarbonate in the system was to remove excess protons and provide a source of sodium cations. It was also observed that the pH increased when the dithionite:molybdenum trioxide ratio increased relative to the bicarbonate:dithionite ratio.

The mass of the recovered solid product tended to decrease with increasing bicarbonate:dithionite ratio, see Figure 2-10. The effect of the dithionite:molybdenum trioxide was not as clear, though it appeared to increase the mass recovery at higher values of bicarbonate:dithionite.

The effect of increasing the bicarbonate:dithionite ratio tended to sharply increase the sodium composition of the solid, as shown in Figure 2-11, for a constant dithionite:molybdenum trioxide ratio. Likewise, increasing the dithionite:molybdenum trioxide ratio increased the sodium composition of the solid as well, but the effect was smaller in magnitude than that caused by an increase in bicarbonate.

When no bicarbonate was used, there was a small amount of sodium present in the form of sodium bronze, and the major product was the hydrogen form of the bronze. For the bicarbonate-free reactions the amount of sodium bronze observed (from the

sodium content of the product) increased from 0.133 wt% to 0.559 wt % when the dithionite to molybdenum ratio was increased three-fold.

When taken as a whole this data suggested that increasing the sodium to molybdenum trioxide ratio tended to increase the sodium composition of the product. Furthermore, the effect of the sodium addition toward this end was increased when the sodium was added in the form of the bicarbonate buffer. This is likely to be a consequence of the removal of protons from the system, as evidenced by the increased pH, resulting in a higher sodium to proton ratio in the reaction mixture and in the product.

Another important observation was the fact that the mass of solid recovered decreased as the percent sodium composition increased as illustrated in Figure 2-12. This suggested that the sodium bronze product, which was the desired product in this synthesis, was too soluble in the reaction mixture to obtain a good yield under the best of conditions for its formation. It is important to note that the product could not be easily recovered from the filtrate because the other by products of the reaction, such as sulfate and bicarbonate, were also soluble in the water.

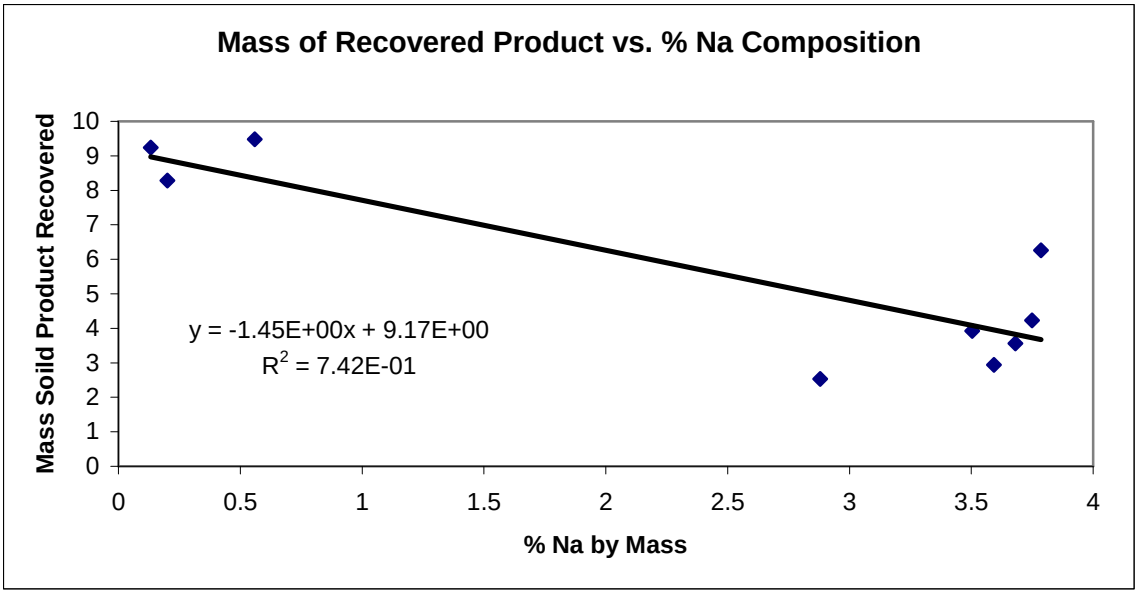

Figure 2-12: "Mass of Solid Product Recovered vs. Percent Sodium Composition"

In order to obtain the sodium molybdenum product in a better yield, it was necessary to examine other solvent systems in which the reaction would take place but the sodium product would be sufficiently insoluble to improve the yield. It was to this end that the ethanolic dithionite reduction synthesis was developed.

Ethanolic Sodium Molybdenum Bronze Products

In order to determine the actual yield and chemical formula of the sodium bronze produced it was necessary to determine the amount of sodium present in the bronze as well as the degree of hydration. The former was determined by ICP. The latter had to be calculated by using the sodium composition data and the ceramic yield data in Table 2-6. The molar reducing equivalents for the sodium bronzes were determined by oxidization with chromate and iodometry and are summarized in Table 2-7.

Table 2-6: Percent Sodium and Ceramic Yield Data for the Ethanolic Sodium Bronze Product

Percent Sodium by Mass:	3.72 %
Ceramic Yield (500 ºC):	94.35 %

Table 2-7: "Comparison of the Product yields, Sodium Content, and Molar Reducing Equivalents of Product Obtained by Ethanolic Synthesis of the Sodium Molybdenum Bronze"

Yield	**Na/Mo Ratio (ICP)**	**Molar Reducing Equivalents Dichromate Oxidation**	**Molar Reducing Equivalents Iodometry**
81.31 %	0.26	0.230 ± 0.008	0.242 ± 0.014

The XRD spectrum of the ethanolic sodium bronze is illustrated in Figure 2-13, and corresponded to library data for sodium aqua molybdenum oxide.

It was initially assumed that the product had the general formula, $Na_xMoO_3 \cdot yH_2O$. The ceramic yield calculation assumes that the products of the pyrolysis of the bronze consisted of sodium oxide, molybdenum trioxide and water as illustrated in Equation 2-9.

$$Na_xMoO_3 \cdot yH_2O \rightarrow (x/2)\ Na_2O + MoO_3 + y\ H_2O \qquad \text{(Equation 2-9)}$$

Thus from the data, sodium oxide and molybdenum trioxide accounted for 94.35 percent of the original mass of the bronze. Furthermore from the ICP analysis it is determined that 3.72 percent of the total mass of the bronze is sodium. Taking a basis of 100 grams of sodium bronze it was possible to determine the relative amounts of sodium,

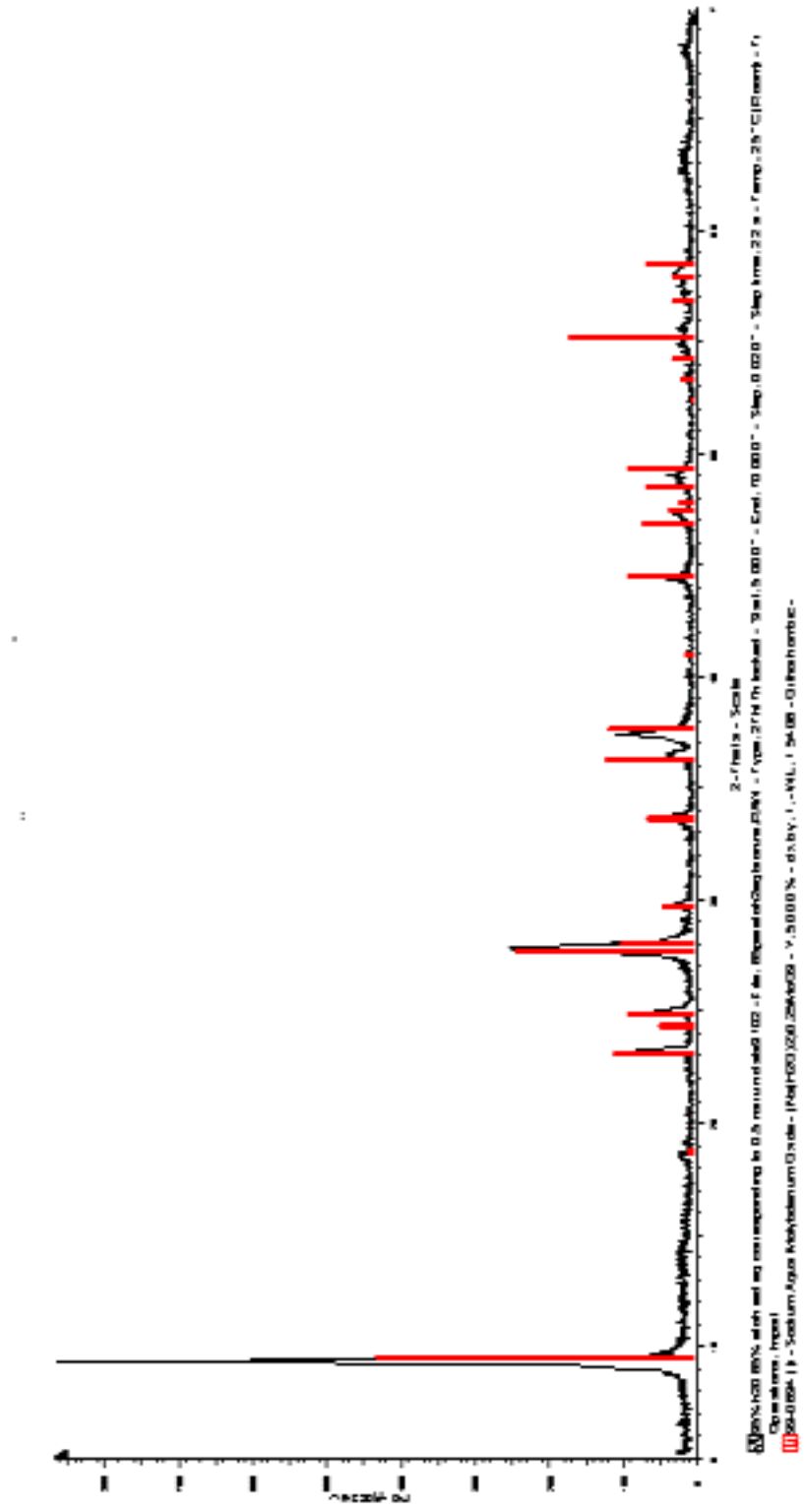

Figure 2-13: "XRD Spectra of Sodium Molybdenum Bronze Prepared by Ethanolic Method"

molybdenum and water, and thus determine the empirical formula:

$Na_{0.26}MoO_3 \cdot 0.62H_2O$, which suggested a formula weight of 161.08 g/mole (per molybdenum basis). However, it was expected that the degree of hydration would be two molecules of water per sodium ion, as suggested by the literature. Assuming this, the formula can be rewritten as $[Na \cdot 2H_2O]_{0.26}MoO_3 \cdot 0.10H_2O$. The extra water is most likely present as hydroxyl groups attached to the molybdenum ions. This raises the question of whether it is the hydrogen ions or the sodium ions that are associated with Mo(V) ions. Notably the reaction of iodine with the bronze produced hydrogen iodide, suggesting that the former is the case. Thus the product can be described as a hydrogen bronze that contains sodium molybdenum(VI) oxide centers, i.e.

$[Na \cdot 2H_2O \cdot Mo^{VI}]_{0.26}[MoO_3]_{0.50}[Mo^{V}(OH)O_2]_{0.24}$.

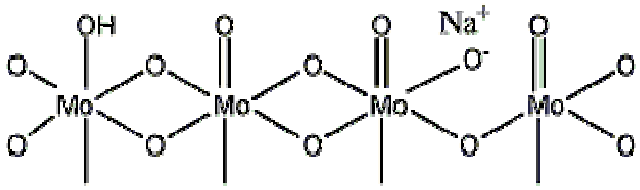

Figure 2-14: "Diagram of Sodium Hydrogen Bronze Structure"

CONCLUSIONS

The zinc hydrochloric acid synthesis of the hydrogen produced an air stable bronze with a formula $H_{0.58}MoO_3$, as determined by iodometry. The powder X-ray spectrum for this bronze was determined and did not match any of the spectra for hydrogen bronzes in the ICDD library of X-ray diffraction data. However it was

suggested by the literature that this hydrogen bronze was most likely a member of a newer phase as suggested by Eda.

The dithionite reduction synthesis of the hydrogen bronze still contained the molybdenum trioxide starting material when ran at the presumed stoichiometric ratio of 6 to 1 molybdenum trioxide to dithionite, however when the dithionite was increased such that the molybdenum trioxide to dithionite ratio was 4 to 1, the resulting product was a mixture of hydrogen bronze and sodium bronze. The sodium bronze can be washed out to leave a pure hydrogen bronze phase, which according to the XRD spectra was $H_{0.5}MoO_3$. Additionally, this suggested that the sodium and hydrogen bronzes present were a discrete mixture of the two bronzes instead of a homogeneous product with mutually intercalated hydrogen and sodium atoms. However, synthesis of the sodium bronze by dithionite reduction, resulted in very low yields due to the relatively high aqueous solubility of the sodium bronze.

The ethanolic synthesis of the sodium bronze resulted in a much higher yield of the sodium bronze and resulted in a hydrated sodium bronze product with an empirical formula around $[Na\cdot 2H_2O]_{0.26}MoO_3\cdot 0.10H_2O$. Additionally the molar reducing equivalent value of ~0.24 suggested that the protonic sites are reducing sites (as was the case with the hydrogen bronzes) and likewise the sodium sites were not reductive in nature. Due to the closeness of our reducing equivalent value, within one standard deviation (σ = 0.0140), to 0.25 suggested that an actual formula of

$[Na \cdot 2H_2O \cdot Mo^{VI}]_{0.26}[Mo^{VI}O_3]_{0.50}[Mo^{V}(OH)O_2]_{0.24}$ was reasonable, thus settling the controversy regarding the formula of the sodium molybdenum bronze.

ACKNOWLEDGEMENTS

I would especially like to thank Mr. Cory Perkins, our NSF REU (National Science Foundation Research Opportunities for Undergraduates) student for all of his fine and diligent work with the aqueous dithionite synthesis of the sodium bronze experiments and all of the hours he spent in the lab.

.

CHAPTER III

NANOPARTICULATE PHASE CHARACTERISTICS, COLORIMETRY, AND EXPLOSIVE SENSING APPLICATIONS OF SODIUM MOLYBDENUM BRONZE

INTRODUCTION

In addition to the solid bulk phases of the sodium molybdenum bronzes that have been addressed thus far, it is also possible to prepare nanoparticulate suspensions of these materials. The first objective of this study was to determine the characteristics of these sodium molybdenum nanoparticles materials including their sodium and molybdenum composition, particle size, and molar reducing equivalents, since it is often the case with nano-phase materials have chemical properties that differ from the bulk material.

The second objective of this study was to examine the efficacy of the sodium bronze solution as a colorimetric reagent for the analysis of oxidizing species aqueous solution. Determination of the chlorine concentration was chosen as an example because there are a number of inexpensive testing methods available to test the results against.

The U.S. Environmental Protection Agency sets a concentration limit of 4 ppm for chlorine and chloroamine in drinking water [66]. Currently chlorine concentrations are determined using colorimetric test kits such as swimming pool test kits employing othotolidine [67] which turns yellow in the presence of chlorine as well as color wheel test kits and digital colorimeters such as are available from HACH Company [68] which utilize N,N-diethyl-p-phenylene which turns pink in the presence of chlorine.

The third objective of this study was to examine the effectiveness of sodium molybdenum bronze as a detection reagent for improvised peroxide explosives and their precursors. A peroxide explosive contains one or more R-O-O-R group, where R is typically an organic group, these peroxides are often cyclic. Examples of these compounds include triacetone triperoxide (TATP), hexamethylene triperoxidediamine (HMTD), diacetone diperoxide (DADP), and tetramethylene diperoxidecarbamide (TMDD) [69]. These compounds are easily prepared using common commercially available chemicals and easily obtained instructions from the internet.

These organic peroxide compounds can be detected and neutralized by hydrogen bronze reagents. For instance TATP reacts with hydrogen molybdenum bronze to form acetone and molybdenum trioxide as described by Equation 3-1.

$$6\ Mo_2O_5(OH) + (Me_2COO)_3 \rightarrow\ 12\ MoO_3 + 3\ H_2O + Me_2C{=}O \qquad \text{(Equation 3-1)}$$

In the process of this reaction the blue hydrogen molybdenum bronze is oxidized to the yellow molybdenum trioxide. The color change associated with this reaction can be used to indicate the presence of the explosive in a suspect sample or as an indicator that more reagent is needed in the case that the bronze is being used to neutralize the compound. It is suspected that the sodium form of the bronze would have similar chemistry and would therefore be a good candidate for explosive sensing applications.

EXPERIMENTAL

The sodium bronze solution was prepared from the sodium bronze product synthesized by the ethanolic process. The iodine solution had a concentration of 0.1000 +/- 0.0005 N per I, (0.05000 M as I_2) and was purchased from Fisher. The trichloro-s-triazinetrizone was used in the form of a swimming pool tablet consisting of 93.5 wt % trichloro-s-triazinetrizone, 1.5 wt % copper sulfate pentahydrate, and 5.0 wt % inert ingredients, sold under the trade name of "HTH^{TM} dual action chlorinating tablets" sold by Arch Chemicals Inc. P.O. Box 723547 Atlanta, Ga. The concentration of chlorine in the solution was estimated using "HTH^{TM} 6-way test strips" also from Arch Chemicals.

Preparation of Sodium Bronze Solution

A sodium bronze solution was prepared by placing 1.020 g of the ethanolic product in 50.05 g water and agitating the mixture for 5 days. The resulting dark blue solution was centrifuged and filtered through a polypropylene 0.45 micron syringe filter.

Determination of the Concentration of the Sodium Bronze Solution

The concentration of the bronze solutions was determined by two independent methods. The molybdenum concentration was initially determined to be 49.56 mM using X-ray fluorescence spectroscopy. A calibration curve was constructed by analyzing four molybdenum standards (Table 3-1) and determining the area under the curve for the molybdenum peak in the range from 17.16 – 17.72 keV, using a live time of 600 seconds. The data yielded the calibration curve shown in Figure 3-1. Linear regression was performed and the relationship between the concentration and the integrated peak intensity in the region of interest were related by Equation 3-1.

$$\text{ppm Molybdenum} = 0.001143(\text{Peak Intensity}) - 415.9,\ R^2 = 0.9985 \qquad \text{(Equation 3-1)}$$

The concentration of the bronze solution was adjusted to fall within the calibration range by diluting 3.0134 g of the original solution to a final solution mass of 30.0251g. The diluted solution was analyzed on the X-ray fluorometer and the peak intensity was determined to be 781299 counts corresponding to a concentration of 477.16 ppm in molybdenum. Taking into account the dilution the initial molybdenum concentration was calculated to be 4754.4 ppm or 49.56 mM.

Table 3-1: "X-Ray Fluorescence Calibration Data for Molybdenum"

Mo Concentration (ppm)	Integrated Intensity (counts)
1000	1232974
799.1	1065874
598.8	899134
401.6	707291

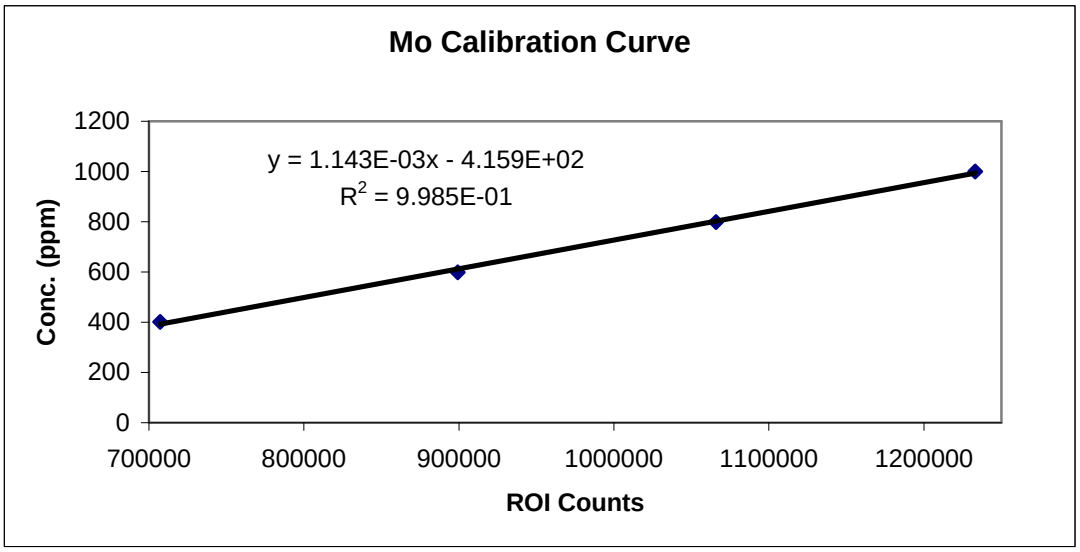

Figure 3-1: "Calibration Curve for Mo Concentration vs. Integration Count"

The second method employed inductively coupled plasma spectroscopy which was used to determine both the molybdenum concentration and the sodium concentration. The resulting concentration for molybdenum was 51.59 mM and the sodium concentration was determined to be 19.97 mM. The value obtained via the inductively coupled plasma data for molybdenum was 4.10% higher than that for the X-ray fluorescence data.

These concentrations were further examined based upon the ceramic yield by first evaporating 19.3414 g of the sodium bronze solution (density was assumed to be 1 g/cc) in an oven at 80 ºC to dryness in a pre-weighed beaker. The resulting solid was heated to

500 ºC for at least three hours to obtain a ceramic residue of 0.1568 g. The oxygen content in the residue was calculated.

Determination of Reducing Capacity of Solutions

Determination of the reducing capacity of the solution was determined by reacting the bronze solution with an excess of iodine solution. The residual iodine concentration was determined by UV-Visible absorbance spectroscopy using a Cary 50 Bio UV-visible spectrophotometer, and the number of reducing equivalents per mole of solution phase molybdenum was determined from the difference in the iodine.

In the case of the sodium molybdenum bronze solution, approximately 5 g of sodium bronze was placed in a 20 ml scintillating vial with approximately 5 g of 0.05000 M iodine standard solution. The reaction vessels were then agitated for ~24 h, filtered through a 0.45 micron PTFE syringe filter using a 10 ml syringe. The filtered solutions were then measured using UV-visible absorbance spectroscopy and the final iodine concentrations determined from calibration calibration curve shown in Figure 3-2. The dilution of the iodine solution by the sodium bronze solution was accounted for in the calculation of the amount of the iodine consumed. The experiment was performed in triplicate in order to determine an average value and standard deviation for the molar reducing equivalents per liter for the solution phase bronzes. The data for this experiment is summarized in Table 3-2.

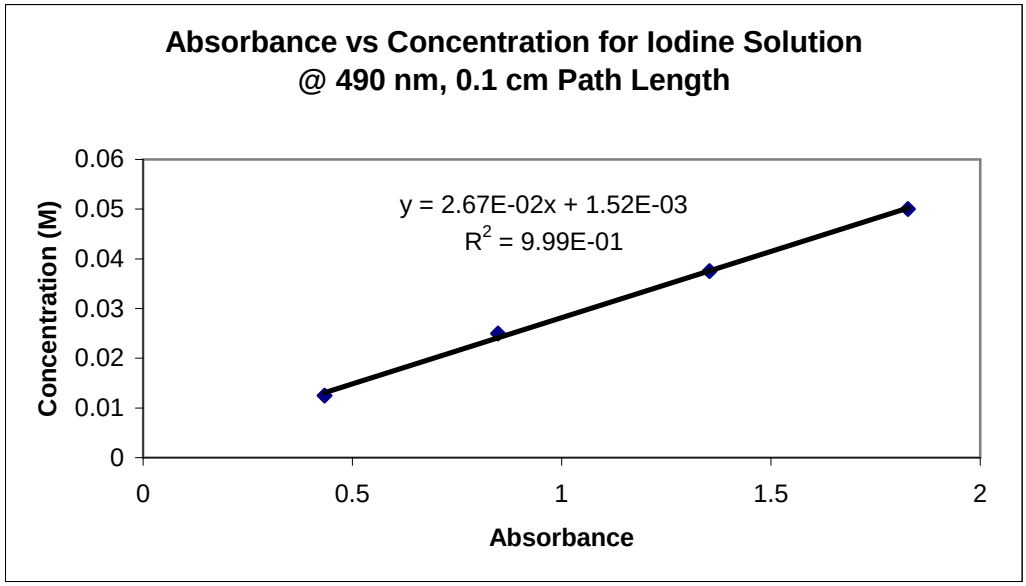

Figure 3-2: "Calibration Curve, Absorbance vs. I_2 Concentration at 490 nm, 0.1 cm Pathlength."

Table 3-2: "Data for Determination of Molar Reducing Equivalents in Sodium Bronze Suspension"

g Sodium Bronze Suspension	g Iodine Solution	mMoles Iodine Initial	mMoles Iodine Final	mMoles Sodium Bronze	mEq/mole Sodium Bronze	mEq/L Solution
5.0605	5.0333	0.02517	0.02291	0.2759	0.09958	5.137
4.9976	4.9998	0.02500	0.02297	0.2725	0.08379	4.323
5.0491	5.0251	0.02513	0.02311	0.2753	0.08215	4.238

The average value for the number of mEq per mole of bronze was determined to be 0.08851 ± 0.00962 Eq/mol sodium bronze. The average value for the number of mEq per liter of solution was 4.6 ± 0.5 mEq/L.

Particle Size Analysis

Particle size analysis was performed on a Malvern HPPS dynamic light scattering particle size analyzer. The average hydrodynamic diameter of the solution was

determined to be 0.572 nm as illustrated by the particle size distribution shown in Figure 3-3.

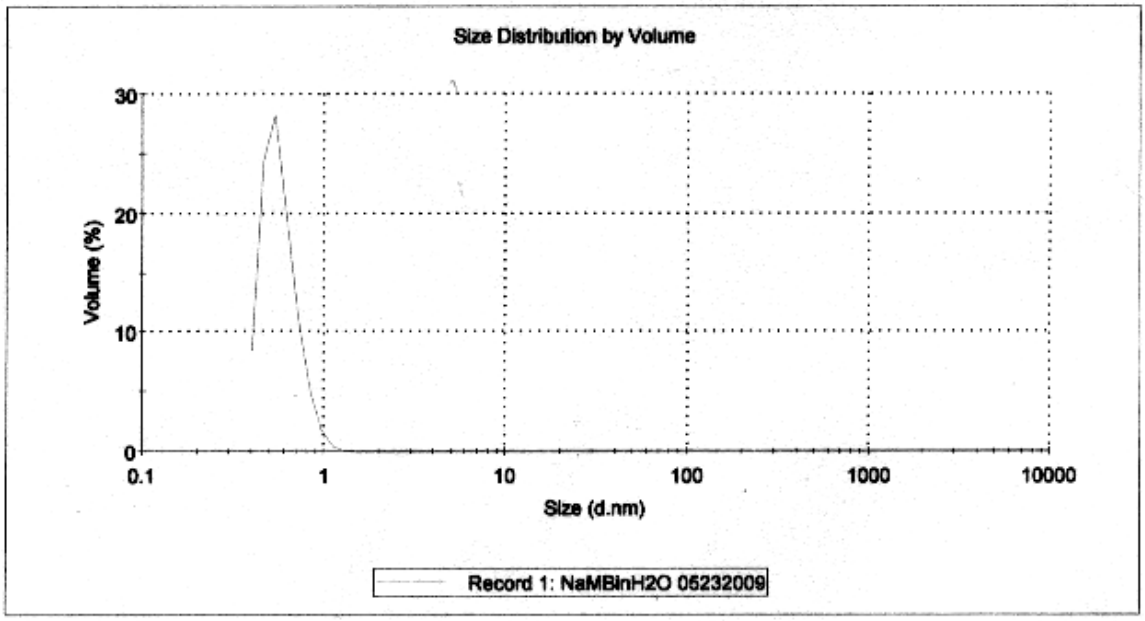

Figure 3-3: "Particle Size Distribution of Sodium Molybdenum Bronze Suspension"

Reaction of the Sodium Bronze Solution with the Chlorine (Trichloro-s-triazinetrizone) Solution

The HTH^{TM} dual action chlorinating tablet was pulverized into a powder and used to prepare a solution with chlorine concentration of approximately 4 ppm of as verified by the HTH^{TM} 6-way test strips. A control solution was then prepared by adding 10.0002 g of water to a 20 ml scintillation vial. An experimental solution was prepared by adding 10.0028 g of the 4 ppm chlorine solution to an identical vial. Then 0.5107 g and 0.5109 g of the sodium bronze solution was added to the control sample and the experimental sample respectively. Both solutions were allowed to react for an hour and were then analyzed using UV-visible absorbance spectroscopy.

Reaction of Sodium Bronze Test Strips with Hydrogen Peroxide

Test strips were prepared by concentrating a sodium bronze solution and applying it to a blank test strip using a pipette. The test strip was allowed to air dry for ~ 6 hours and was immersed into a 1 wt% hydrogen peroxide solution for 20 minutes. Consecutive digital photographs were taken of the test strip every minute until the reaction of the sodium bronze test strip with the hydrogen peroxide reached completion as evidenced in the color of the test strip changing from blue to colorless.

Reaction of Sodium Bronze Solution with Sodium Chlorate

Approximately 5 ml of sodium bronze solution was treated with one drop of Triton-X 100 surfactant (as a wetting agent), and dropped onto a small pile of sodium chlorate and observed in contact with the chlorate for 20 minutes.

Electronic Detection of Peroxide Vapor Using Sodium Bronze-Vycar Material

A sodium molybdenum bronze paste was prepared by mixing 1.60 g of Vycar^{TM} aqueous binding agent with 3.26 g on bulk sodium bronze. The paste was then packed onto a glass slide between two immobilized gold-coated electrodes purchased from Radio Shack. The separation between the two electrodes was approximately 3 mm. The apparatus is illustrated in Figure 3-4.

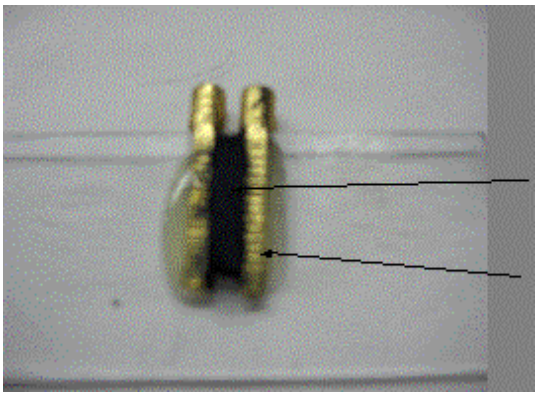

Figure 3-4: "Electronic Sodium Bronze Peroxide Vapor Detector"

The apparatus was then hooked up to a voltmeter and placed into a gas stream containing ~ 35 ppm hydrogen peroxide at a flow rate of ~ 20 standard cubic centimeters per minute and the resistance across the electrodes were measured.

RESULTS AND DISCUSSION

The average value for the reducing equivalents for the sodium bronze solution was determined to be 0.0885 Eq/mol of molybdenum in solution, compared to 0.242 Eq/mol of molybdenum for the bulk product. Additionally, the sodium to molybdenum ratio for the solution was found to be 0.3872 Na/Mo, while that of the bulk material was determined to be 0.26 Na/Mo. From this data it was deduced that the solubilized form of the bronze is a different species than that of the bulk material with an approximate molybdenum normalized empirical formula of $Na_{0.39}H_{0.09}MoO_3$. Thus, disproportionation of the original sodium hydrogen bronze occurred to product a more soluble sodium rich bronze less reduced bronze.

Based on the sodium and the reducing equivalent data it was possible to determine the percent molar composition of the solubilized species as summarized in Table 3-3.

Table 3-3: "Mole Percent Composition of the Solubilized Species and Bulk Sodium Hydrogen Bronze"

Element	Solubilized Composition (mole percent)	Bulk Composition, Anhydrous Basis (mole percent)
Mo	22.32	22.22
Na	8.71	5.77
H	2.01	5.33
O	66.96	66.67

The compositional differences between the solubilized material taken together with the small particle size imply two important things. First, as the composition of the solubilized material is not the same as the bulk material one can assume that these structures are not merely very small particles of the bulk material, or their composition would be similar. Secondly, if these structures are not nanoparticles, then they must be relatively large molecules with a hydrodynamic diameter on the order of 0.572 nm. This seems to imply that this solubilized material is a polyoxoanion of molybdenum of the general form: $[Mo_xO_yH_z]^{w-}$ $[Na(H_2O)_2]^{w+}$.

The reducing nature of this solution is consistent with a poly-oxo-hydroxide anion containing at least one acidic hydroxide group, which would require approximately ten molybdenum centers as a minimum based on the hydrogen to molybdenum ratio of ~ 0.1. Due to some inherent uncertainty in the measurements a better value could not be

determined. One proposed formula that is consistent with the data, within the limits of uncertainty is $[Mo_{10}O_{29}(OH)]^{4-} + 4\ [Na(H_2O)_2]^{+}$.

Determination of Chlorine Concentration

Comparison of the UV-visible spectrum of the experimental solution with the control solution in Figure 3-5 indicated that the absorbance intensity associated with the solution containing the chlorine was approximately half of that of the control suggesting that the sodium bronze was oxidized by the chlorine in the solution. The concentration of the sodium bronze solution in the control solution and the experimental solution was determined by Beer's Law to be 2.181 mM and 1.052 mM respectively on a molybdenum basis, corresponding to a difference between the control concentration and the experimental concentration of 1.129 mM.

Using this change, the concentration of the chlorine in the aqueous solution was determined to be 0.09993 mEq/L. This result is in agreement with the concentration determined using the test strips (0.08 to 0.14 mEq/L). Therefore, the sodium hydrogen bronze solution functions as an excellent colorimetric reagent for the detection of chlorine concentrations. It could also be utilized to prepare test strips for this purpose.

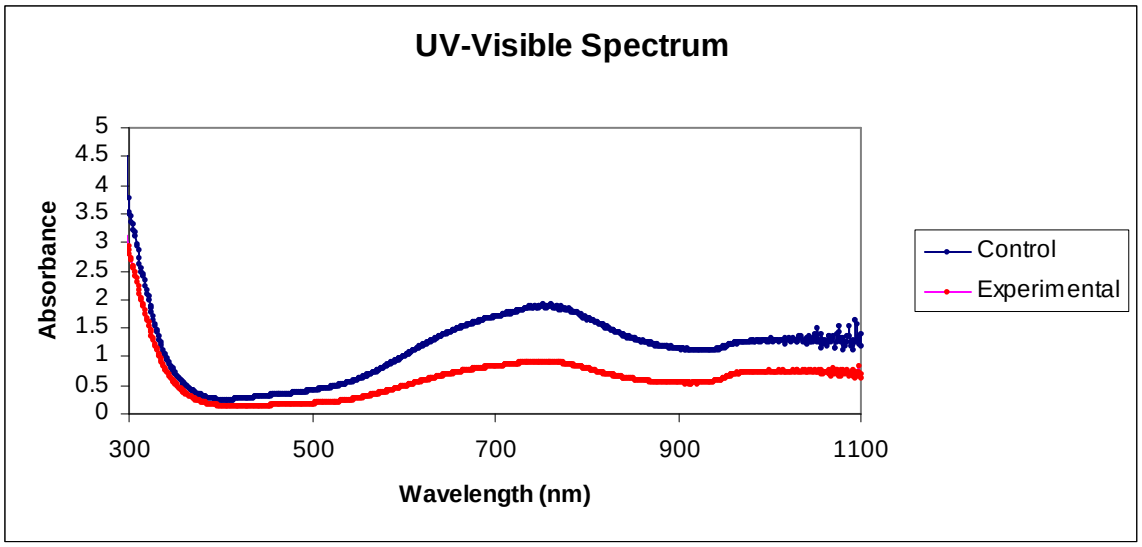

Figure 3-5: "Comparison of the UV-Visible Spectra of the Sodium Bronze - Chlorine Control and Experimental Solution"

Detection of Peroxide Using Sodium Bronze Test Strip

When a sodium bronze impregnated test strip was immersed into 1 % hydrogen peroxide solution a color change from blue to white occurred indicating that the bronze was being oxidized by the hydrogen peroxide. Figure 3-6 illustrates a set of time elapsed photographs of the test strip reacting in the hydrogen peroxide solution at reaction times of 0, 2, 4, 6, 8, 10, 15, and 20 minutes. After two minutes the strip changed color sufficiently to unequivocally indicate the presence of the hydrogen peroxide. Considering that at least 10 wt % hydrogen peroxide is required for the preparation of peroxide explosives, the sodium bronze reagent is an excellent reagent for the detection of hydrogen peroxide as an explosive precursor.

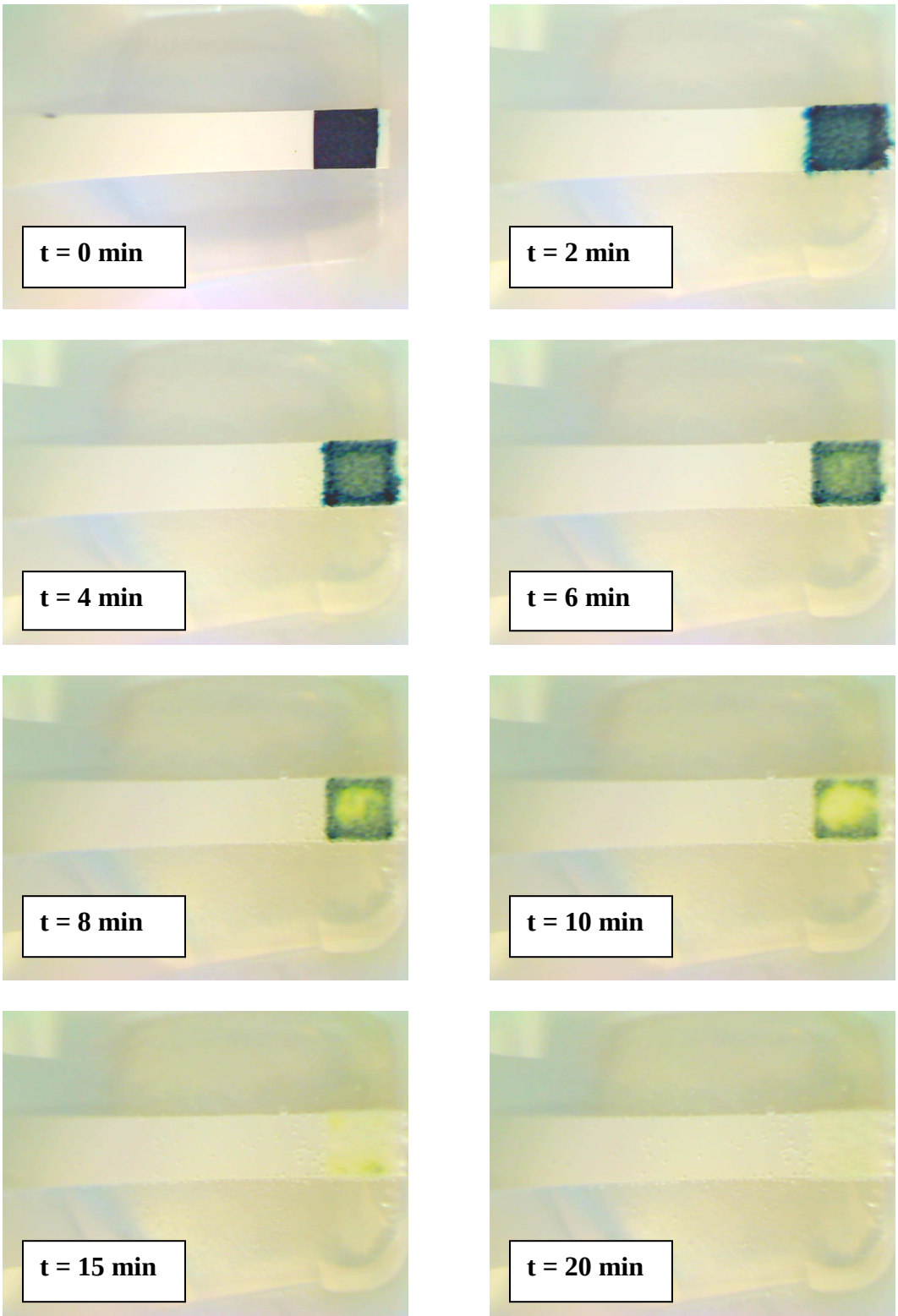

Figure 3-6: "Time Elapsed Photographs of Sodium Bronze Test Strip in Hydrogen Peroxide Solution"

Detection of Chlorates Using Sodium Bronze Solution

The sodium bronze solution was not reactive with the solid chlorate. This is likely because both the chlorate and the sodium bronze are anionic and the possible requirement for protonation of chlorate to accelerate the redox reaction. However, the sodium bronze solution could be used with a hydrogen bronze based detection ink to in a test to differentiate a chlorate compound from a solid peroxide compound since both the sodium bronze based ink will react with a peroxide but only the hydrogen bronze ink will react with a chlorate compound.

Electronic Detection of Peroxide Vapor Using Sodium Bronze-Vycar Material

Within the first five minutes of exposure to the peroxide vapor stream the detector resistance changed linearly with respect to time. This detector resistance response is plotted in Figure 3-7. Over the five minute range the resistance changed from 44 kohms to 56 kohms, which is a large enough change to be easily read by a device. The change in resistance of the detector is a consequence of the oxidation of the conductive bronze to its non-conductive oxidation product.

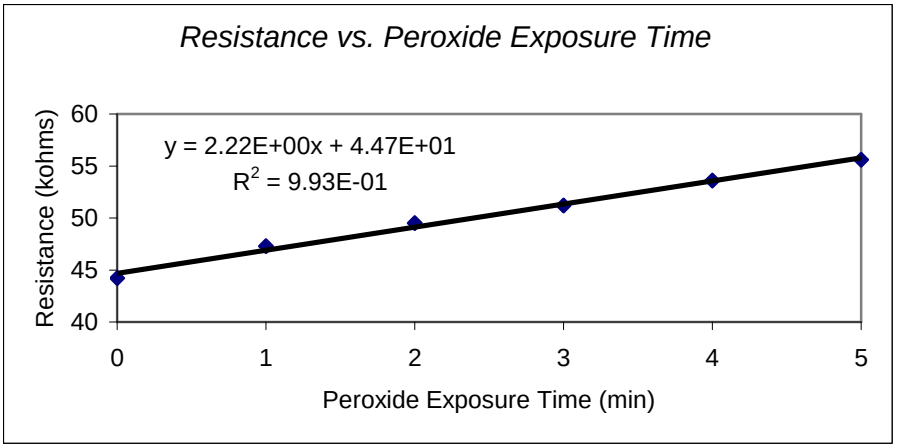

Figure 3-7: "Plot of Resistance Response of Sodium Bronze Based Peroxide Detector vs. Peroxide Exposure Time"

CONCLUSION

It was determined that disproportionation of the sodium hydrogen bronze synthesized in aqueous ethanol occurred when it was contacted with water. As a result, the sodium bronze solution had a different composition than that of the bulk material and was richer in sodium and poorer in hydrogen. Whereas the bulk material had a sodium to molybdenum ratio of 0.26 the solution phase material had a sodium to molybdenum ratio ~0.39, similarly the bulk phase material had a hydrogen to molybdenum ratio of ~0.24 while the solution phase material had a hydrogen to molybdenum ratio ~0.09. As a consequence of the lower hydrogen composition the molar reducing equivalents were also lower in comparison to the bulk material.

The sodium bronze solution was an excellent quantitative colorimetric reagent for the detection of chlorine and would be expected to work for other oxidizing species as

well. As a result of the solution being brightly colored in the reduced state and colorless in the oxidized state, it can also be used in qualitative applications in the form of test strips or in a solution form which could be added to a sample containing the species to be tested for.

The sodium bronze test strips are very responsive to hydrogen peroxide and would be successful in the detection of peroxide based explosives and their synthetic precursors and could find applications in transportation safety and law enforcement industries. Also, the fact that the sodium bronze reacts with peroxides but not chlorates makes it a good test reagent to determine if an unknown explosive is a chlorate or a peroxide, such that if the unknown reacts with both the hydrogen bronze based detection ink and the sodium bronze solution it is likely that the unknown explosive is a peroxide, however if it reacts with the hydrogen bronze ink but not the sodium bronze solution it is likely to be a chlorate. The resistance response of the bulk sodium bronze-Vycar paste was linear and of sufficient magnitude that it could be used as a vapor phase peroxide detector that could be used in shipping containers and cargo holds in airplanes to detect the vapors associated with any improvised peroxide explosive device.

CHAPTER IV

REMOVAL OF HEAVY METAL CATIONS FROM WATER USING MOLYBDENUM OXIDE BRONZES

INTRODUCTION

The problem of chromate pollution is fairly common since widespread contamination of surface and ground waters with chromium has resulted from its industrial use in corrosion inhibition, leather tanning, electroplating, wood preserving, and metallurgy [70]. Chromium (VI) pollution is of particular concern due to chromate's carcinogenicity in humans [71, 72]. Technologies that have been developed for the removal and recovery of hexavalent chromium from wastewaters include adsorption[73, 74], ion exchange technology [75, 76], and membrane processes, [77] including microfiltration [78], ultrafiltration, [79], and nanofiltration; [80] and solvent extraction processes, such as emulsion liquid membranes [81], supported liquid membranes [82], nondispersive solvent extraction [83], and emulsion pertraction [84]). An attractive alternative to such methods involves reduction of chromium (VI) to chromium (III) since the latter ion is significantly less toxic and much less soluble and mobile in natural waters. For this reason, on-site chromium remediation procedures mostly rely on the

reduction of Cr(VI) via either natural processes[85] or addition of reducing agents.[86-88]. Many inorganic and organic constituents are capable of reducing Cr(VI). Examples include zerovalent iron ([87], hydrogen (using a bioreactor), [89], ferrous ions [81, 90-93], hydrogen sulfide [94, 95], Fe(II)/Fe(III) carbonate green rust [96, 97], and ascorbic acid[98].

Nanotechnology has also been employed for the removal or reduction of chromium(VI) from contaminated waters, For example magnetite nanoparticles and surface-modified jacobsite ($MnFe_2O_4$) nanoparticles were found to swiftly adsorb chromate [99, 100]. Nanoscale zero valent iron particles have been found to rapidly reduce and immobilize hexavalent chromium on the nanoparticle surface [106-109].

In this investigation we explored the efficacy of hydrogen molybdenum bronze for reduction of chromate and the possible immobilization of the chromium(III) product. This reagent is a dark blue metallic oxide prepared by reduction of molybdenum oxide with nascent hydrogen generated by the reaction of zinc metal and hydrochloric acid. The potential for reduction of molybdenum trioxide to the hydrogen bronze is 0.47 V [101], suggesting that the bronze is thermodynamically capable of reducing chromium(VI) to chromium(III) under standard conditions as shown in Equation 4-1. One noteworthy difference between the molybdenum hydrogen bronze and most other solid reducing agents employed in reducing chromate is the presence of protons that are released in the redox process that can prevent the precipitation of chromium(III) hydroxide on the surface. Fouling of reagent surfaces with these by-products occurs

readily under neutral and basic pH conditions and can seriously hamper achievement of stoichiometric reduction reactions. Finally, both the molybdenum bronze and molybdenum trioxide are known to react with polyvalent metal cations to generate insoluble molybdate salts, so it is possible that the chromium(III) produced by the redox reaction could subsequently be immobilized by such reactions.

EXPERIMENTAL

Materials

Potassium chromate (Mallinckrodt), potassium dichromate (Mallinckrodt), hydrochloric acid (Pharmco), potassium permanganate (Aldrich), zinc (Aldrich) and molybdenum trioxide (Alfa-Aesar) were obtained commercially and used as received without further purification. Nanometric iron was purchased from Aldrich. Water was purified by reverse osmosis and then deionized using a Barnsted E-Pure deionization unit.

Analyses

Water quality measurements were performed on the ground water samples using a variety of techniques. Determination of pH was performed using an IQ 400 meter equipped with a stainless steel ISFET probe using a three-point calibration (pH= 4.0. 7.0, and 10.0) and automatic temperature correction. Oxidation research potential was

measured using a Milwaukee SM 500 ORP meter calibrated with an Orion 967901 ORP standard solution (+ 420 mV). Conductivity was measured using a Milwaukee SM 301 EC meter calibrated with a Fisher brand 1000 µS NIST-traceable conductivity standard. Alkalinity and hardness were assessed with Hach Aquacheck test strips. A Hach DR/890 colorimeter was used to determine hexavalent chromium concentrations via a colorimetric method that relies on the formation of a purple chromium(VI) diphenylcarbohydrazide complex (complexing agent is 1,5-diphenylcarbohydrazide). The detection limit of the colorimeter is 10 ppb. If necessary, samples were diluted prior to analysis.

Synthesis of Bulk Molybdenum Hydrogen Bronze

MoO_3 (30.00 g, 208.4 mmol) and zinc metal (56.8 g, 868.8 mmol) were placed in a round bottom flask with 2 ground glass fittings and one stopcock valve. A magnetic stir rod and 5 to 10 ml of deionized water were then added to the reaction vessel. A dropping funnel containing 200 ml concentrated hydrochloric acid (~2478 mmol) was installed in the center neck while the other ground glass fitting was sealed with a stopper. The stopcock valve neck was opened and vented to a paraffin bubbler. The reaction vessel was then placed in a room temperature water bath and magnetically stirred to form a slurry. (It was occasionally necessary to start the spinning of the stir bar along with a glass stir rod due to the initially high solid loading). The valve of the dropping funnel was then opened to allow introduction of the hydrochloric acid to the reaction vessel at an approximate rate of 1 to 2 drops per second. The reaction took place almost immediately

to give a dark blue solid but was allowed to proceed overnight in order to ensure that all of the zinc metal had completely dissolved. After the reaction period, the product was isolated by filtration through a medium porosity sintered-glass frit filter funnel. The product was initially greenish-gold metallic solid indicating it was one of the more highly-reduced hydrogen bronzes. It quickly changed to reddish-purple and, more slowly, to blue upon reaction with air. It was found that it was best to allow these reactions to go to completion before washing the solid to prevent clogging of the glass frit. Therefore, approximately 12 hours were allowed to pass between the initial filtration and the successive washing with 3 times 350 ml of water. The washed product was then vacuum dried to yield 28.77 g (95.59%)of dark blue solid.

Determination of Reaction Kinetics

Chromate reduction kinetics were determined using a sufficient excess of the hydrogen bronze so that the reaction followed kinetics that were only dependent on the chromium concentration. In a typical reaction with bulk hydrogen molybdenum bronze, 400 ml of a potassium dichromate solution with a chromium concentration of 0.63 ppm was reacted with 29.0 mg of the reducing agent in a magnetically stirred sealed flask. Aliquots of the reaction mixture were removed periodically (5-10 minutes), filtered through a 0.45 µm PTFE syringe filter and analyzed for chromate. The reactions were found to follow pseudo first order kinetics with respect to chromium(VI) with an observed rate constant k_{obs}= k[Hydrogen Bronze] The observed rate constant was calculated by plotting the natural logarithm of the Cr^{6+} concentration vs. time. A linear

fit of the data returned the k_{obs} as the negative slope of the data. The kinetic experiment was repeated with higher loadings of the hydrogen molybdenum bronze (33.7 mg and 39.2 mg). A true rate constant was then determined from the slope of a linear fit of the k_{obs} vs. hydrogen molybdenum bronze loading.

RESULTS AND DISCUSSION

Chromate Reduction in Water Samples

Well water was obtained from a monitoring well in Oklahoma where a plume of chromate was spreading from a landfill. Analysis of the water yielded the water quality parameters shown in Table 4-1. Most values fall within normal ranges for groundwater with the exception of pH. It is exceptionally high and outside the limits of natural water and too high to be accounted for by dissolved calcium carbonate since saturated calcium carbonate has a pH of 8.3. The high pH makes the chromate ions less prone to natural attenuation by reaction with reducing agents such as humic acids or sulfides in the ground water. This is a result of the fact that the potential for reduction of Cr(VI) to Cr(III) is reduced to 0.83 mV from 1.38 mV under the conditions found in the ground water. The redox potentials of the well waters were positive and fell in the normal range for well-oxygenated water. The water does possess considerable alkalinity and hardness that along with the high pH can be expected to make the water harder to treat.

Table 4-1: "Water Quality Measurements for Chromate Contaminated Groundwater"

pH	ORP (mV)	$[Cr^{6+}]$ (ppm)	Conductivity µS/cm	Alkalinity (ppm)	Hardness (ppm)
8.8	240	9.3	750	800	800

The hydrogen molybdenum bronze used in this investigation was prepared by deliberately producing a highly-reduced bronze via the dissolving metal reduction using zinc and hydrochloric acid and then allowing it to oxidize in air to yield an air-stable bronze with the maximum hydrogen loading, as described in Chapter II. The number of reducing equivalents per gram of the bronze was determined using two independent methods, oxidation with dichromate and iodometry. These gave 3.157 mEq/g and 4.022 mEq of reducing equivalents respectively for the bronze leading to respective theoretical capacities of 54.7 mg/g and 69.7 mg/g for reduction of chromium(VI).

Before using the molybdenum hydrogen bronze to treat the contaminated groundwater, experiments were first performed with aqueous dichromate. Two different experiments were performed at each of three different pH points. In one experiment an excess of reducing agent was used in order to confirm that chromate was reduced below the detection limit of 10 ppb. In the second, an excess of chromate was used so that the reduction capacity of the reagent could be calculated. For example, the treatment of 20 milliliters of a 11.1 ppm (as Cr^{6+}) solution of dichromate at near-neutral pH conditions with 9.9 milligrams of hydrogen molybdenum bronze reduced the Cr^{6+} concentration below the 10 ppb detection limit of the calorimeter. In a second experiment, using 2.3 mg of the bronze, the final concentration of the Cr^{6+} was 2.2 ppm. This indicated that the bronze had a reduction capacity of 77 mg of Cr^{6+} at near neutral pH conditions (pH of

7.1). Similar experiments at other pH conditions gave the results shown in Table 4-2. The pH dependence of the reduction capacity is illustrated in Figure 4-1.

Table 4-2: "Hexavalent Chromium Reduction Data"

Mass Of Bronze (mg)	Initial pH	Mass of chromate sample (g)	Initial Cr^{6+} concentration (ppm)	Final Cr^{6+} concentration (ppm)	Reduction capacity (mg/g)
10.6	2.0	19.999	10.21	BDL	-
2.1	2.0	20.001	10.21	1.698	79.99
10.2	5.2	20.009	10.90	BDL	-
2.3	5.2	20.011	10.90	1.853	79.85
9.9	7.0	20.007	10.30	BDL	-
2.4	7.0	20.005	10.30	2.052	67.21
10	7.25	20.012	10.56	BDL	-
2.1	7.25	20.011	10.56	2.951	70.58
10.2	8.68	20.026	9.814	BDL	-
2.2	8.68	20.024	9.814	2.160	72.02
10.1	9.72	20.008	9.397	BDL	-
2.1	9.72	20.007	9.397	1.950	71.79

BDL: Below detection limit of 10 ppb

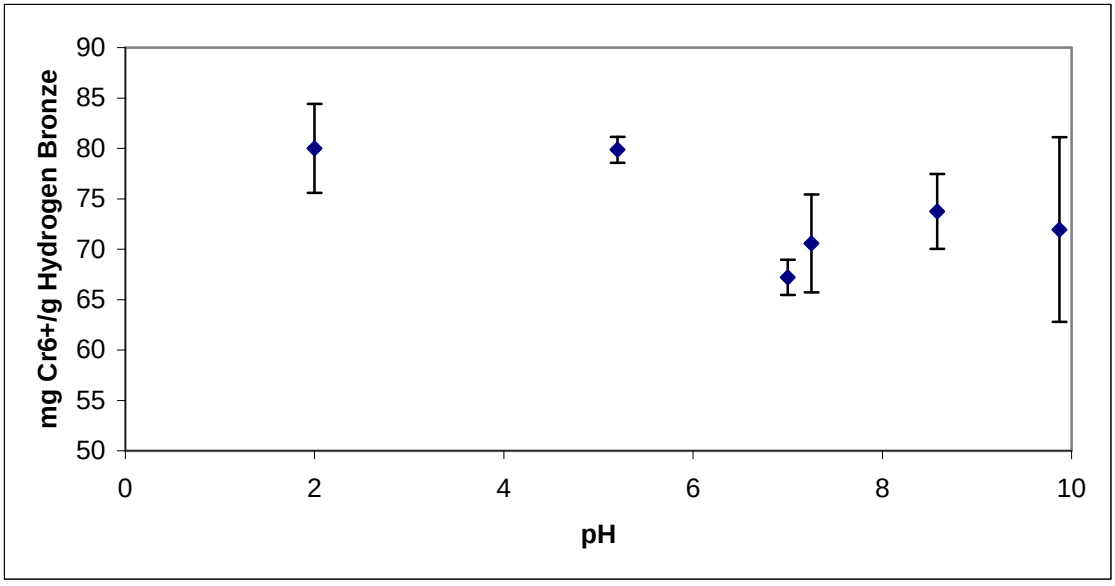

Figure 4-1: "Plot of Reduction Capacity (in Units of mg Cr^{6+}/g Bronze) vs. pH." Error bars represent one standard deviation from the mean.

The hydrogen molybdenum bronze was next used to treat the groundwater from the chromate-contaminated plume. Similar experiments were also performed with nanometric zero-valent iron to compare the efficacy of the two reagents. The results are provided in Table 4-3. The performance of nanometric iron was extremely disappointing but not surprising considering the high pH of the water that leads to rapid fouling of the iron surface with chromium hydroxide. Notably, the hydrogen molybdenum bronze performed very well, but its reduction capacity was somewhat lower than that found for pure aqueous chromate solutions. Whether this change is due to other oxidizing substances present in the groundwater or the influence of other cations and anions cannot be ascertained at this time.

Table 4-3: "Hexavalent Chromium Reduction Data for Chromate-Contaminated Groundwater"

Reagent	Mass of Reagent (mg)	Mass of chromate sample (g)	Initial Cr^{6+} concentration (ppm)	Final Cr^{6+} concentration (ppm)	Reduction capacity (mg/g)
Nano-Iron	10.2	20.0	9.3	9.1	0.39
Bulk HMo_2O_6	10.2	20.0	9.0	BDL	-
Bulk HMo_2O_6	2.3	20.0	9.0	2.13	60

BDL: Below detection limit of 10 ppb

In order to address whether the chromium was immobilized during the reduction process, the total chromium content of treated solutions was measured in an experiment was performed using an 103 performed with sufficient hydrogen molybdenum bronze to reduce all chromium(VI) to chromium(III). After the reduction was completed, the solution was filtered through a 0.45 µm PTFE syringe filter and analyzed by XRF

spectroscopy. It was found that the chromium concentration had been reduced below the detection limit of 0.64 ppm. Thus, the treatment did result in the immobilization of chromium.

Kinetic Measurements

Figures 4-2 illustrates a typical result the reduction of chromium(VI) to chromium(III) with molybdenum hydrogen bronze. The natural log of Cr^{6+} concentration vs. time data is plotted for each loading reflecting the pseudo first-order kinetics of the experiments. The data shows that there is a large initial decrease in the Cr^{6+} concentration in the first 5 minutes followed by decay in concentration that follows first order kinetics. It was hypothesized that this behavior was due to a rapid adsorption of chromate onto the surface followed by a slower reaction as shown in Scheme 1. Assuming that the adsorption equilibrium is established within the first 5 minutes, the nominal concentration of the chromate after the adsorption takes place can be estimated by the linear fit of the data with the zero time point removed. This data is presented in Figure 2 for each of the three hydrogen molybdenum bronze loadings. The amount of adsorbed chromate can be estimated by extrapolating these linear plots back to the start of the reaction. Using the 29.0 mg hydrogen molybdenum bronze data as an example, the calculated solution concentration of hexavalent chromium at t = 0 is 0.31 ppm indicating that 0.32 ppm (over half) of the original dichromate ions was adsorbed onto the hydrogen bronze. This leads to approximately 4.4 mg of Cr^{6+} adsorbed per gram of molybdenum hydrogen bronze. In order to test the hypothesis of molybdate adsorption by chromate, a reaction was

performed with 27.5 mg of molybdenum trioxide and 400 ml of 0.62 M Cr^{6+} solution. The molybdenum trioxide was used as an analogue of the bronze that does not reduce chromate. The final chromate concentration was found to be 0.52 ppm indicating an uptake of 1.5 mg/g of Cr^{6+}. Since the surface area of the molybdenum trioxide (0.71 m^2/g) is approximately half that of the hydrogen molybdenum bronze (1.4 m^2/g), the uptake on a surface-area corrected basis would be 3.0 mg/g, Thus, the adsorption of chromate by the hydrogen molybdenum bronze extrapolated from the kinetic data is not unreasonable.

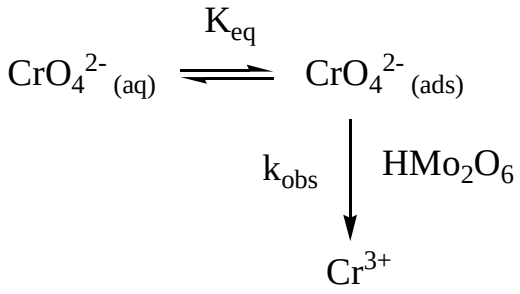

Scheme 1: Reaction scheme for Chromate Reduction by Hydrogen Molybdenum Bronze

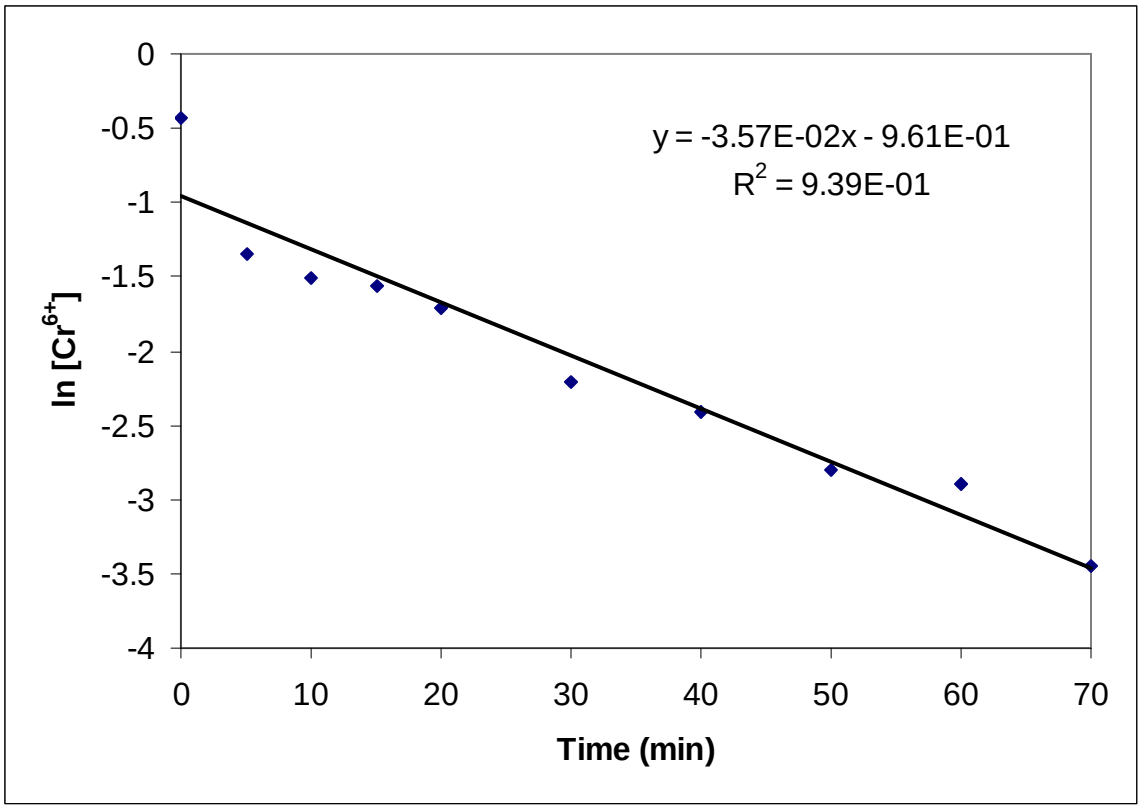

Figure 4-2: Plot of ln[Cr^{6+}] vs. Time for 29.0 mg Hydrogen Molybdenum Bronze Loading

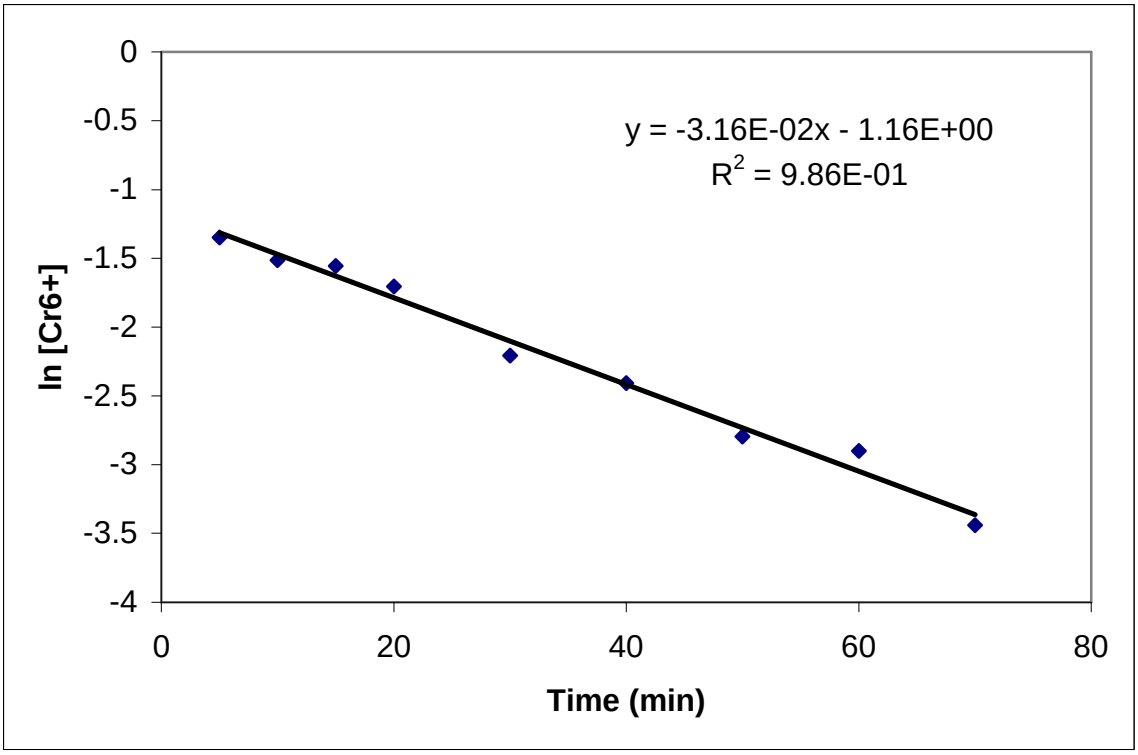

Figure 4-3: "Plot of ln[Cr^{6+}] vs. Time for 29.0 mg Molybdenum Bronze Loading with the Zero Point Removed"

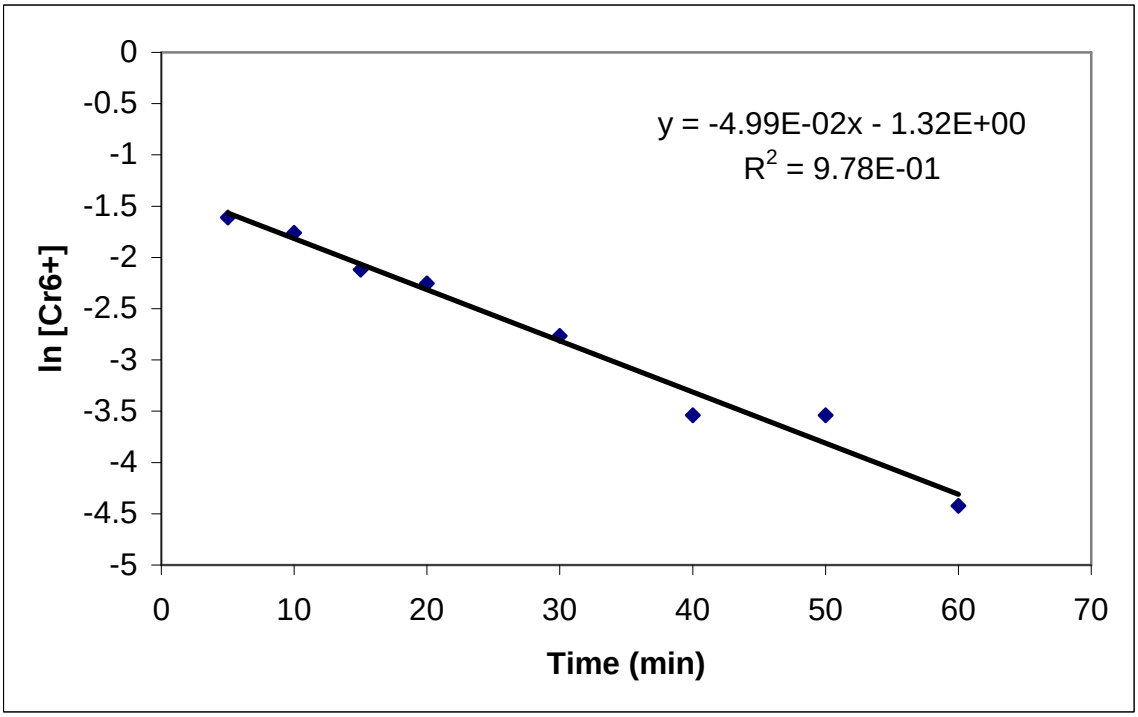

Figure 4-4: "Plot of ln[Cr^{6+}] vs. Time for 33.7 mg Molybdenum Bronze Loading with the Zero Point Removed"

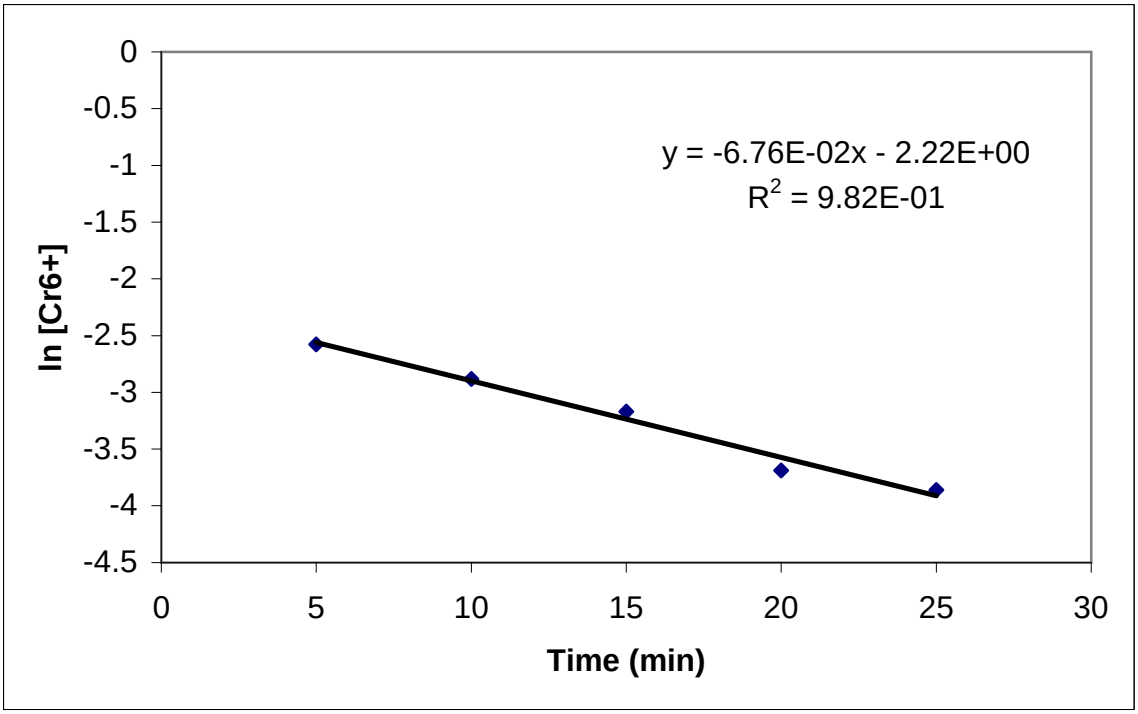

Figure 4-5: "Plot of ln[Cr^{6+}] vs. Time for 39.2 mg Molybdenum Bronze Loading with the Zero Point Removed"

Eliminating the zero time point gave data that gave a linear fit for first order kinetics for the disappearance of Cr. The calculated observed rate constants, are summarized in Table 3. Figure 3 represents a linear plot of k_{obs} vs. Hydrogen Molybdenum Bronze loading, which was used to determine the value of the true rate constant. The value of k was determined to be 1.40 $Lg^{-1}min^{-1}$.

Table 4-4: "Observed Rate Constant at Various Hydrogen Molybdenum Bronze Loadings"

Hydrogen Molybdenum Bronze Concentration (g/L)	Observed Rate Constant, k_{obs} (min^{-1})	R^2 for Linear Fit
0.0725	0.0316	0.9864
0.0843	0.0499	0.9782
0.0980	0.0676	0.9824

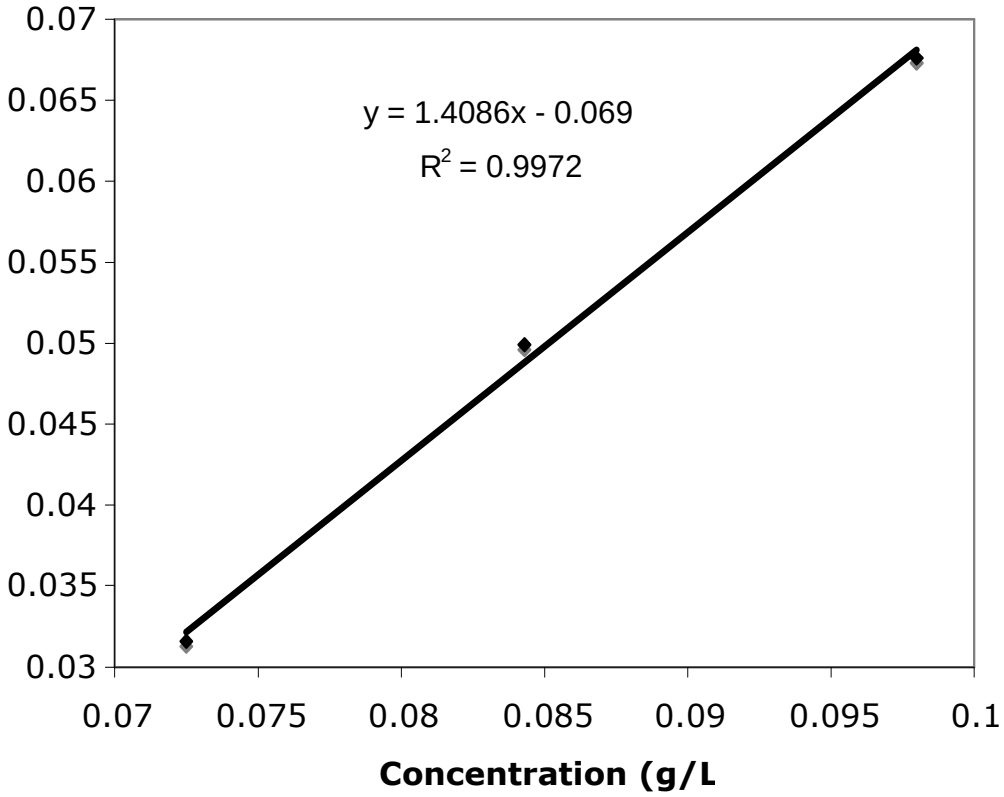

Figure 4-6: "Plot of k_{obs} vs. Hydrogen Molybdenum Bronze Loading"

Adsorption of Chromium(III)

Adsorption of chromium(III) was examined for both hydrogen molybdenum bronze and molybdenum trioxide. The adsorption of chromium(III) was determined to be around 1.1 mg Cr^{3+}/g of molybdenum trioxide after a reaction time of 24 hours and remained stable with time. Chromium(III) adsorption on hydrogen molybdenum bronze was determined to be 6.7 mg Cr^{3+}/g hydrogen bronze after 24 hours and was observed to increase to 7.7 mg Cr^{3+}/g of bronze after 72 hours. This suggests that the hydrogen molybdenum bronze product does chemically adsorb the chromium(III) species, and does so to a significantly greater extent than does molybdenum trioxide.

CONCLUSIONS

Hydrogen molybdenum bronze has been shown to reduce aqueous hexavalent chromium to trivalent chromium over a wide range of conditions in the laboratory and groundwater samples. Furthermore it has been shown to outperform a zero valent iron reagent especially under conditions of higher pH the iron surface fouls with chromium hydroxide. This does not happen with the hydrogen molybdenum bronze because the acidic bronze is resistant to hydroxide fouling. The data also indicates that the bronze immobilized the chromium(III) product form the chromium(IV) reduction reaction.

The hydrogen bronze reagent can be used for a wide variety of chromium treatment applications including use in treatment of wastewater from chromium plating baths and corrosion inhibition industries. In the event that the hexavalent chromium contaminant is already in the groundwater, this reagent may be used to reduce the hexavalent chromium using pump-and-treat methodologies or *in situ* using permeable reactive barriers, of similar technology.

CHAPTER V

MOLYBDATE PROCESS FOR COPPER ORE PROCESSING

INTRODUCTION

The direct conversion of metal sulfides to metals via carbothermal reduction or other processes is problematic. Therefore, conventional pyrometallurgical approaches to refining of sulfide ores usually include a roasting step to convert them to oxides that are more readily reduced [102]. Unfortunately, roasting produces sulfur dioxide as a by-product and thus contributes to acid rain, see Equation 5-1. While modern smelters capture this gas and turn it into sulfuric acid (at an additional cost) that can be used in the extraction process, there is a significant interest in alternative greener processes that have lower energy needs and reduced environmental impact [103].

$$2\ MS + 3\ O_2 \rightarrow 2\ MO + 2\ SO_2 \qquad \text{(Equation 5-1)}$$

The focus of this investigation is copper ore refining but the processes are applicable to other transition metal sulfide ores. The most common copper ore, accounting for 50% of copper production, is chalcopyrite, $CuFeS_2$. There are also a number of other sulfide ores (such as covellite, CuS, and chalcocite, Cu_2S) as well as

some oxide ores such as malachite ($Cu_2(CO_3)(OH)_2$ and cuprite, Cu_2O [104]. The oxide ores are the most economic to refine since they are readily leached by sulfuric acid, usually using a heap or dump leach process with subsequent isolation of copper by the SX-EW process, a combination of solvent extraction and electrowinning [105]. Notably, the process described below could be used to isolate copper hydroxide from the initially formed sulfuric acid leachate. In the case of sulfide ores, hydrometallurgical processes have also been developed as alternatives to pyrometallurgy [106]. An excellent example is using a bacterial oxidation process to oxidize the sulfides to sulfuric acid, which also leads to simultaneous leaching with sulfuric acid [107]. As with the oxide ores, the SX-EW process can be used to recover the copper from the pregnant leach solution. The same result can be realized abiotically using sulfuric acid accompanied by aerial oxidation.

This study examines the development of a "green" method of copper processing. The starting copper material for this process is copper(II) sulfate. Copper(II) sulfate can be easily produced from copper(II) sulfide, or other copper ores, by a number of methods including leaching in sulfuric acid, oxidation with trivalent iron, biological oxidation, et cetera.

The first step of this process is to use an alkali metal molybdate to precipitate copper from a copper(II) sulfate stream as an insoluble copper-molybdate-hydroxide species.

$$CuSO_{4(aq)} + x\ A_2MoO_{3(aq)} \rightarrow Cu(MoO_4)_x(OH)_{y(s)} + A_2SO_{4(aq)} \qquad \text{(Equation 5-2)}$$

The choice of the alkali metal should not impact the chemistry of the system, however, using potassium molybdate results in the formation of a potassium sulfate solution as the byproduct which can be used as a component in fertilizer, thus resulting in a the production saleable commodity stream from the process. Separation of the copper-containing solid and recovery of the sulfate salt byproduct should be industrially straightforward for a system with the properly adjusted stoichiometric ratios.

This product is then reacted with the alkali metal hydroxide in order to form the copper(II) hydroxide product and the alkali metal molybdate.

$$Cu(MoO_4)_x(OH)_{y(s)} + AOH_{(aq)} \rightarrow Cu(OH)_{2(s)} + A_2MoO_{4(aq)} \qquad \text{(Equation 5-3)}$$

At this stage the alkali metal molybdate solution can be separated from the copper hydroxide and processed for reuse. The copper(II) hydroxide can then be dehydrated in air to form copper(II) oxide if desired or left in the hydroxide form.

$$Cu(OH)_2 + \text{Heat} \rightarrow CuO + H_2O \qquad \text{(Equation 5-4)}$$

The copper(II) oxide or copper(II) hydroxide can then be easily reduced to the metal using standard industrial copper smelting methods.

The fundamental advantages of this proposed process is threefold. With the elimination of the roasting step, the need to produce SO_2 gas as a byproduct is alleviated thus saving the costs associated with scrubbing and processing of the waste stream. The sulfur is retained as sodium (or potassium) sulfate, which can be sold as a commodity, potassium sulfate being a component of fertilizer. The heat energy requirement for the roasting of the sulfide ore is also eliminated resulting in savings in fuel expense and a decrease in associated carbon emissions. Finally, since the molybdate from the process is recoverable it can be recycled, and can ultimately be considered a one-time capital cost instead of a recurring supply cost.

This study examined the reaction between copper(II) sulfide and sodium molybdate in detail. The composition of the copper-molybdate-hydroxide product was determined to be somewhat similar to lindgrenite with some important differences. A hydrothermal synthesis of lindgrenite was also attempted.

EXPERIMENTAL

Chemicals and Characterization Methods

All reagents were commercial products (ACS Reagent grade or higher) and were used without further purification. Sodium molybdate dihydrate ($Na_2MoO_4 \bullet 2H_2O$;; CAS # 10102-40-6; ACS Grade +99.5%) was purchased from Alfa Aesar. Copper(II) sulfate pentahydrate ($CuSO_4 \bullet 5H_2O$; CAS # 7758-99-8) was purchased from EM Science. The

0.1 N HCl was purchased from Fisher Scientific. The 0.997 M NaOH was purchased from Sigma Aldrich. Water was purified by reverse osmosis followed by deionization. Bulk pyrolyses at various temperatures were performed in ambient air in a digitally-controlled muffle furnace using approximately 1 g samples, a ramp of 10 °C/min and a hold time of 4 hr, unless otherwise noted. X-ray powder diffraction (XRD) patterns were recorded on a Bruker AXS D-8 Advance X-ray powder diffractometer using copper K_α radiation (λ=1.5418 Å). Crystalline phases were identified using a search/match program and the PDF-2 database of the International Centre for Diffraction Data [i]. X-ray fluorescence spectroscopy (XRF) was performed on a Thermo Electron QuanX XRF spectrometer. Thermogravimetric analysis was performed using a Seiko SII Thermogravimetric Analyzer.

Reaction of Sodium Molybdate with Copper Sulfate

Copper sulfate and sodium molybdate were reacted in the following respective molar ratios: 1:5, 1:4, 1:3, 1:2, 1:1, 1:0.67, and 0:0.5. The 1:0.67 ratio was chosen as it corresponds stoichiometrically to the Cu:Mo ratio present in the mineral lindgrenite. The 1:5 Cu:Mo ratio reaction will be described as an example of how the reactions were performed.

Two solutions were prepared; the first comprising 25 mmoles of $CuSO_4$ dissolved in 50 ml water. The second solution contained 125 mmol Na_2MoO_4 dissolved in 50 ml water. These two solutions were poured together into the reaction vessel; a magnetically

stirred 250 ml media bottle. Care was taken to first pour the Na_2MoO_4 solution into the reaction vessel followed by the $CuSO_4$ solution in the event that the order of addition was significant. The beakers initially containing the two solutions were rinsed with water into the reaction vessel. The total volume of rinse water was maintained at 44 ml, such that the total volume of the reaction vessels were maintained at 144 ml. The reactions were allowed to proceed for 48 hours in order to ensure that the reactions had reached equilibrium and then removed and vacuum filtered using a 350 ml medium pore glass frit filter. The initial filtrate was saved and the filter cake rinsed with 1000 ml water. The remaining solid product was dried at 60°C to constant mass (1 to 2 days).

Hydrothermal Reaction of Copper Sulfate and Sodium Molybdate

A Teflon-lined hydrothermal bomb reactor was charged 5 ml of 0.6 M copper(II) sulfate solution and 0.4 M sodium molybdate solution. A green precipitate was immediately formed. The bomb was sealed and heated to 160 ºC at a rate of 10 ºC/min. The temperature was held at 160 ºC for 8 hours and slowly cooled back to room temperature at a rate of 0.5 ºC/min. After cooling, the reactor was allowed to sit another 24 hours, undisturbed. The bomb reactor was then opened and the product was washed with water by decanting. The product was a green crystalline solid.

Copper Assay of Products as CuO

Assay of the copper product was carried out by reacting it with an excess of sodium hydroxide resulting in the formation of copper(II) hydroxide. Since the

copper(II) hydroxide is unstable toward dehydration it was necessary to heat the hydroxide to 480 °C to produce an air stable oxide, CuO, that could be used for gravimetric assay of copper. The proper dehydration temperature was determined by synthesizing a sample of copper hydroxide and performing thermogravimetric analysis on it to determine the optimal temperature. The copper hydroxide product was prepared according to the reaction:

$$[Cu(NH_3)_6]SO4 + 2\ NaOH \rightarrow Cu(OH)_2 + Na_2SO_4 + 6\ NH_3 \quad \text{(Equation 5-5)}$$

A solution of copper sulfate was prepared by dissolving 4.999 g $CuSO_4 \cdot 5H_2O$ (~20 mmol) in 100.42 g H_2O. The copper sulfate solution was then treated ammonium hydroxide sufficient to form a dark blue solution of hexamine copper(II) sulfate. This was then reacted with 40.06 g of 0.997 N sodium hydroxide to precipitate the copper(II) hydroxide product. The product was then separated using vacuum filtration and vacuum dried to a constant weight of 1.95 g. The copper hydroxide product was then analyzed by TGA and formula weight was determined to be 97.867 g/mol, corresponding to $Cu(OH)_2$. The minimum temperature for pyrolysis of the copper hydroxide was determined from the TGA to be around 380 °C. The pyrolysis was performed at 480 °C to ensure completion.

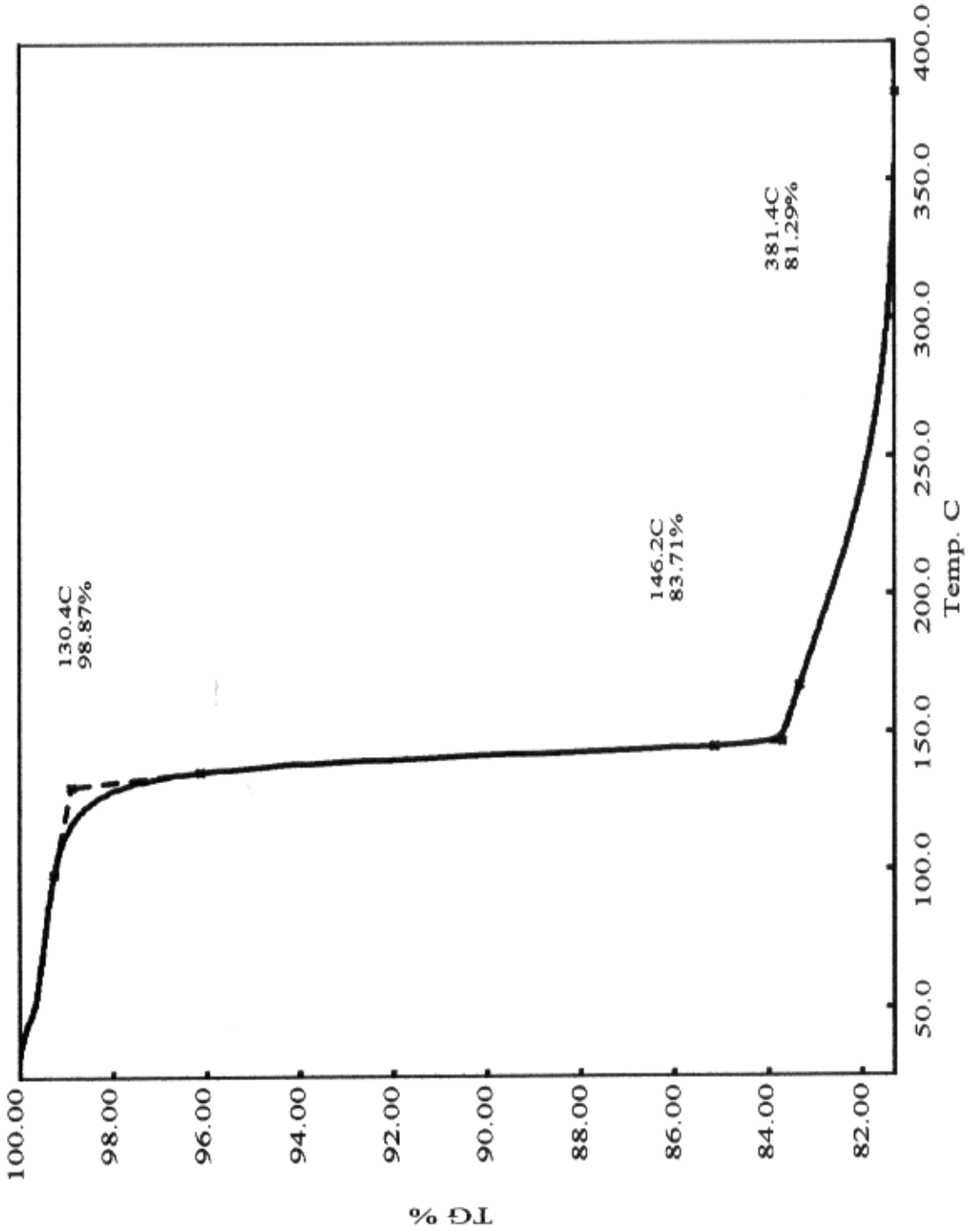

Figure 5-1: "TGA Trace of Copper Hydroxide"

Copper assay of the copper molybdate products as CuO was carried out in 30 ml glass centrifuge tubes that could be heated to the required 480 °C, the rationale being that product would remain in the centrifuge tubes for the duration of the analysis in order to avoid loss of product during transfer from one vessel to the next. Approximately one gram of the product was placed in a preweighed 30 ml glass centrifuge tube. Approximately 5 g of 0.997 M NaOH was added to the tube. The tube was then capped and manually shaken vigorously for ten minutes. The reaction of the product was immediate and was evidenced by a color change from the initial mint green to the turquoise blue of copper hydroxide. The tube was then centrifuged until the solid was stable at the bottom (typically 20 minutes @ 3000 rpm was sufficient) and the supernatant was poured off. The reaction with the 0.997 M NaOH was repeated two more times in order to ensure that all of the copper molybdate product reacted with the NaOH. The additional reactions did in some cases result in the ultimate formation of a black product. This black product is copper oxide and resulted from the dehydration of the quite unstable copper hydroxide that is catalyzed by excess base. The resulting copper hydroxide product was washed three times with 15 ml water. For each wash 15 ml water was added to the centrifuge tube which was capped, shaken vigorously for 10 minutes and centrifuged. This product was then dried at 80°C to remove any remaining water and heated in a muffle furnace at 480 °C overnight.

Determination of Copper by UV-Visible Spectroscopy

A solution of copper (II) chloride of known concentration (0.1583 M) was used to determine an extinction coefficient (10.03 $M^{-1}cm^{-1}$ at 725 nm). The copper samples were dissolved in 0.1 N hydrochloric acid with a target copper concentration near that of the copper chloride solution. The absorption was determined for each sample at 725 nanometers and their concentrations determined by Beer's Law.

RESULTS AND DISCUSSION

It was determined that the product yield increased with increasing copper to molybdate ratio and this was accompanied by a concomitant increase in the pH of the filtrate. The yield and pH data obtained at various copper to molybdenum starting material ratios are summarized in Table 5-1. The mass of the recovered product increased as the copper to molybdenum ratio decreased as shown in Table 5-1 and Figure 5-2. It was also observed that the lower yield filtrates became a darker blue suggesting that unreacted copper remained in the solution phase. In the lower ratio (1:1, 1:0.67, 1:0.5) reactions a small amount of product was formed after the filtration at the 48 hour limit, however the filtrate was still very dark blue. These observations suggest two things, first since the higher copper to molybdenum sample filtrates contained more unreacted copper as evidenced by the blue remaining in the solution, it is implied that increasing the molybdenum concentration in the starting material increases the yield of the reaction. Secondly, considering that a small amount of amount of product was

formed in the filtrate after the 48 hour reaction time, an increasing concentration of molybdenum in the system also increases the reaction rate.

Table 5-1: "Mass Recovery and pH Data for Products Obtained from Reactions of Various Copper to Molybdenum Ratios"

Cu:Mo Molar Ratio (Starting Materials)	Product Yield (g)	pH of Filtrate
1:5	4.56	6.7
1:4	4.55	6.6
1:3	4.54	6.5
1:2	4.51	6.0
1:1	3.82	4.0
1:0.67	2.60	3.6
1:0.5	1.92	3.2

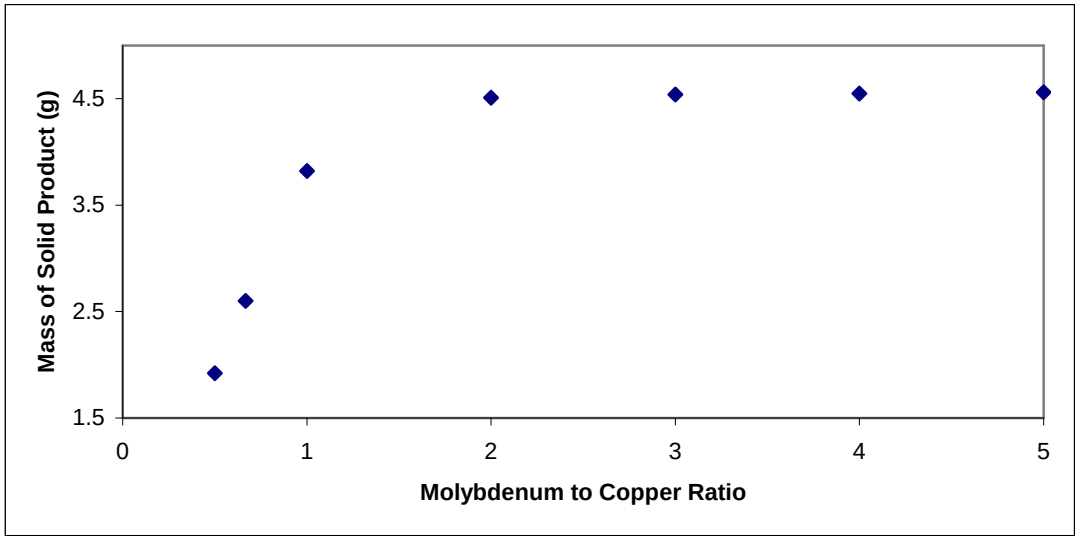

Figure 5-2: "Mass of Solid Product Recovered vs. Molybdenum to Copper Ratio"

The yield of product at the 1:0.67 Cu:Mo ratio was quite low . Notably, the solution pH was fairly low as well indicating that the root cause of the low yield is solubilization of the copper molybdate product that has been demonstrated to occur at low pH. As more molybdate is used in the reaction, the molybdate ions serve as bases to

neutralize the acidity of the hexaaqua copper(II) ions and result in higher yields. Notably, the copper:molybdenum ratios are strongly correlated to each other as shown in Figures 5-3 and 5-4.

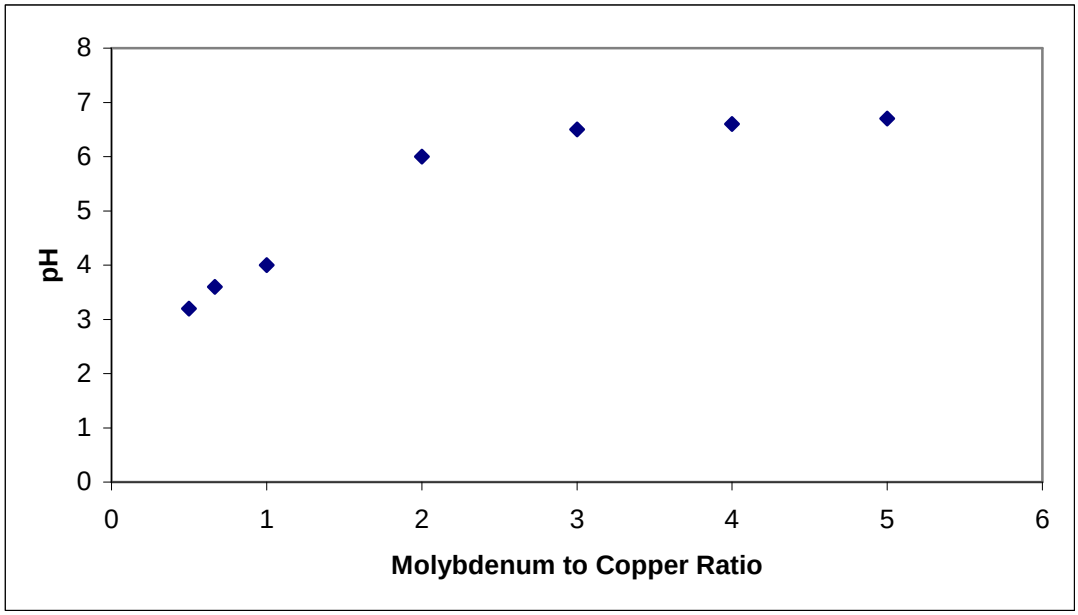

Figure 5-3: "Filtrate pH vs. Molybdenum to Copper Ratio"

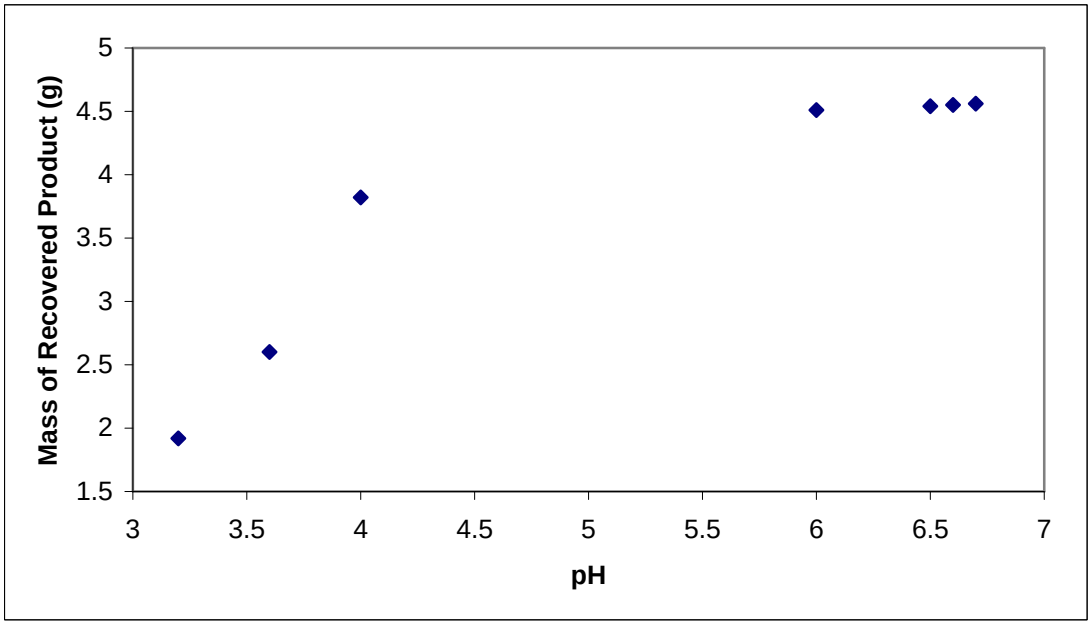

Figure 5-4: "Mass of Recovered Product vs. pH"

A qualitative X-ray fluorescence analysis of an as prepared prototypical solid product sample, shown in Figure 5-5, indicated that the only metals present in the product was copper and molybdenum.

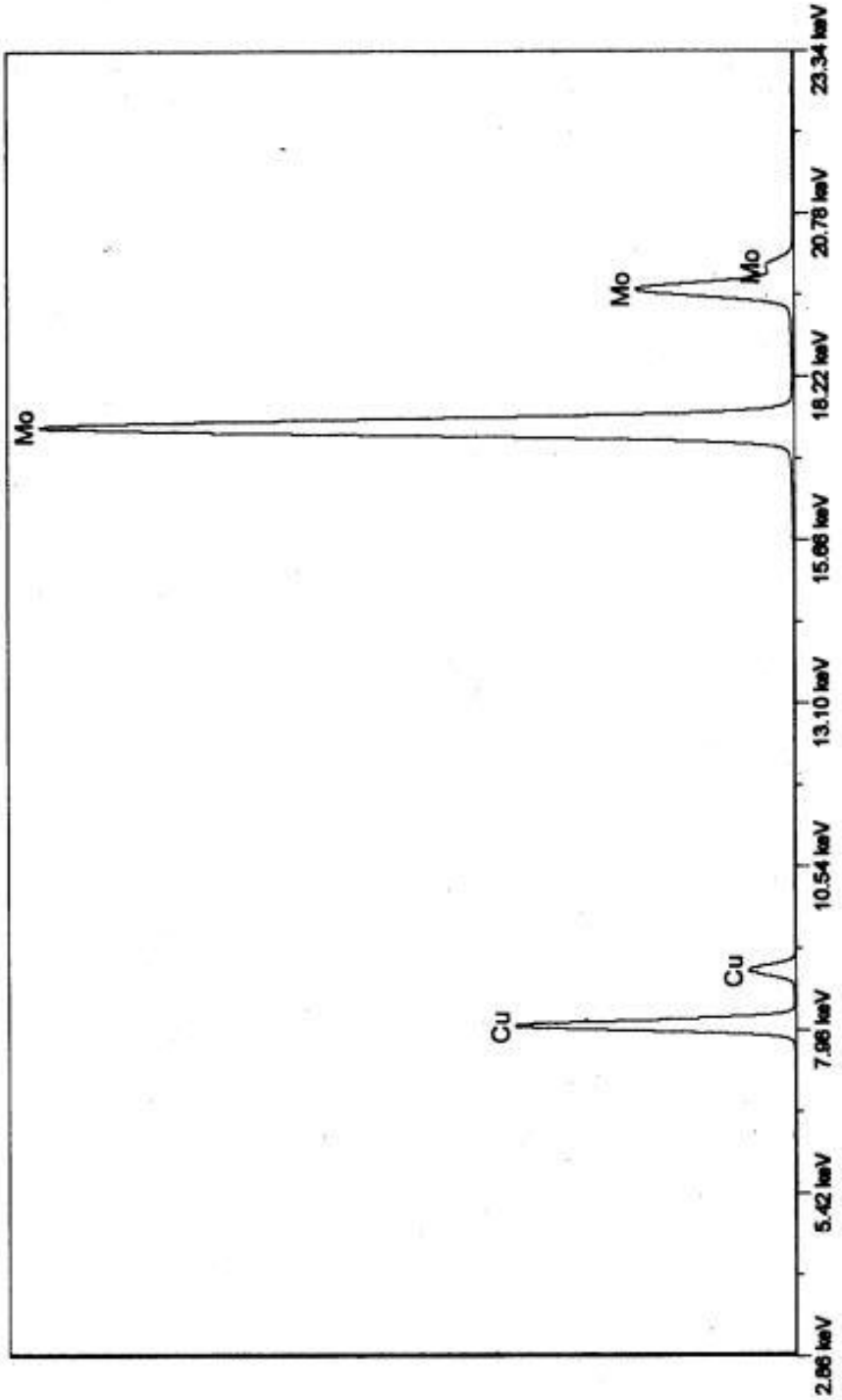

Figure 5-5: "Plot of Relative Peak Intensities of Copper and Sulfur from Qualitative Assay Using X-Ray Fluorescence"

Powder X-ray diffraction analysis of the copper(II)-molybdenum product suggests a moderately amorphous product with definite lindgrenite, $Cu_3(MoO4)(OH)_2$, peaks. The lindgrenite peaks were present in all of the samples regardless of the molybdate to copper ratio. Powder X-ray diffraction analysis determined that the pyrolysis product of the copper-molybdenum product was essentially pure copper molybdate. As no sodium-containing phases were present in the pyrolysis product it was determined that there was no sodium present in the initial product.

More quantitative methods were used to determine the amount of copper, molybdenum and water in the product. Copper was determined using two different methods the first method was by a gravimetric method in which the copper molybdate species was reacted to copper(II) oxide. The second method employed UV-visible spectroscopy. Molybdenum was calculated using the determined copper content and the ceramic yield after complete conversion to oxides. Water content was determined by thermogravimetric analysis.

The yield of the copper(II) oxide was determined gravimetrically and from this data the percent copper content of the product was determined and is summarized in Table 5-2. Additionally, it was possible by this method to determine the overall conversion of copper in the starting materials to copper oxide, which is a measure of the overall efficiency of the molybdate process for the conversion of copper sulfate to copper oxide, as shown in Table 5-2.

Table 5-2: "Determination of the Copper Composition of the Product by Gravimetric Determination of Copper Oxide"

Copper to Molybdenum Ratio (Starting Materials)	% CuO (by mass)	% Cu (by Mass)
1:5	42.52	33.97
1:2	42.41	33.88
1:1	42.05	33.59
3:2	42.34	33.81

Table 5-3: "Percent Copper Recovery from the Starting Solution"

Copper to Molybdenum Ratio (Starting Materials)	% Cu Recovery from Starting Materials
1:5	97.42
1:2	96.01
1:1	80.78
3:2	53.74

The UV-visible spectroscopic analysis examined a larger range of copper to molybdenum ratios than did the gravimetric method. The results of the UV-Visible analysis are summarized in Table 5-4.

Table 5-4: "Percent Copper by Mass, UV-Visible Data"

Copper to Molybdenum Ratio (Product)	% Cu (by Mass)
1 to 5	33.73
1 to 4	33.90
1 to 3	33.53
1 to 2	34.27
1 to 1	33.41
1 to 0.667	33.41
1 to 0.5	33.25
Hydrothermal	34.08

The UV-visible data is likely more accurate than the gravimetric data, because the gravimetric procedure involved multiple washing and decanting steps in which some of

the product may have been lost which would underestimate the amount of copper in the sample. Additionally, if the sodium molybdate was not completely washed out prior to pyrolysis of the hydroxide to the oxide, there would be some sodium oxide and molybdenum trioxide impurities which would overestimate the amount of copper present. These difficulties are not present in the UV-visible analysis.

Samples of the products were examined by thermogravimetric analysis in order to determine the water content of the products by examining the weight loss of the product as the temperature increased. Figures 5-6 through 5-8 illustrate the weight loss of the sample with respect to time.

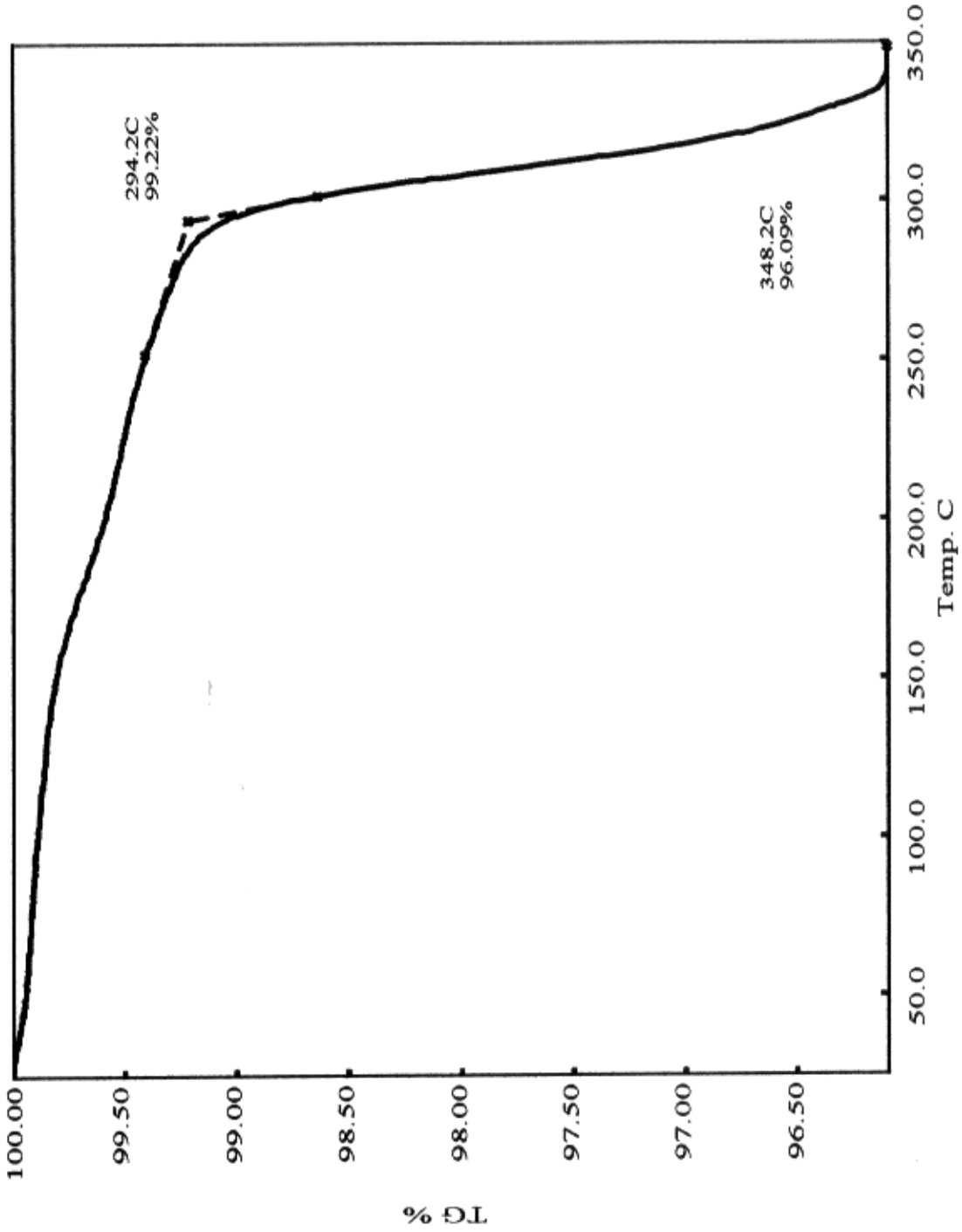

Figure 5-6: "Thermogravimetric Trace of Product from Reaction with 1:5 Copper to Molybdenum Starting Material Ratio"

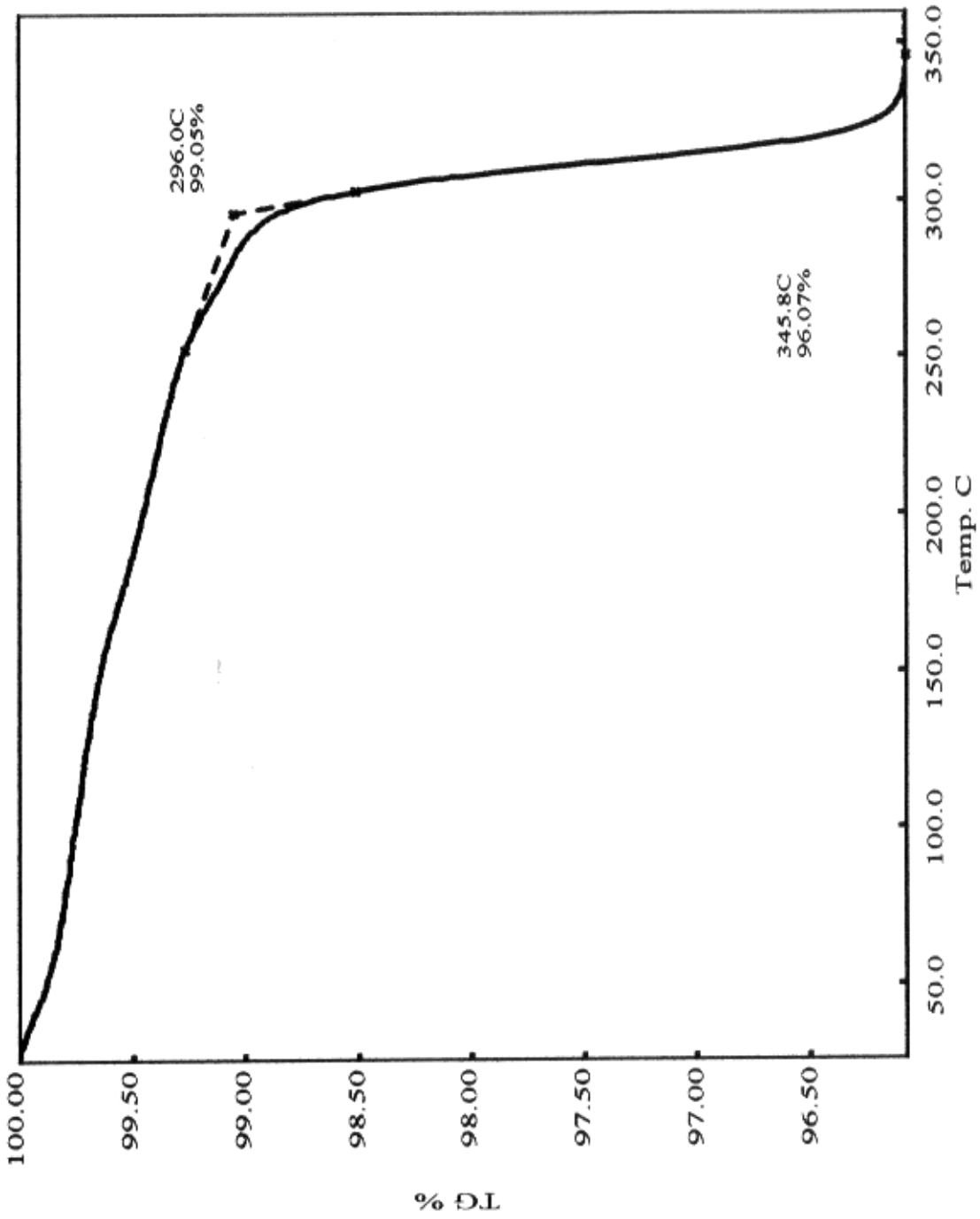

Figure 5-7: "Thermogravimetric Trace of Product from Reaction with 1:4 Copper to Molybdenum Starting Material Ratio"

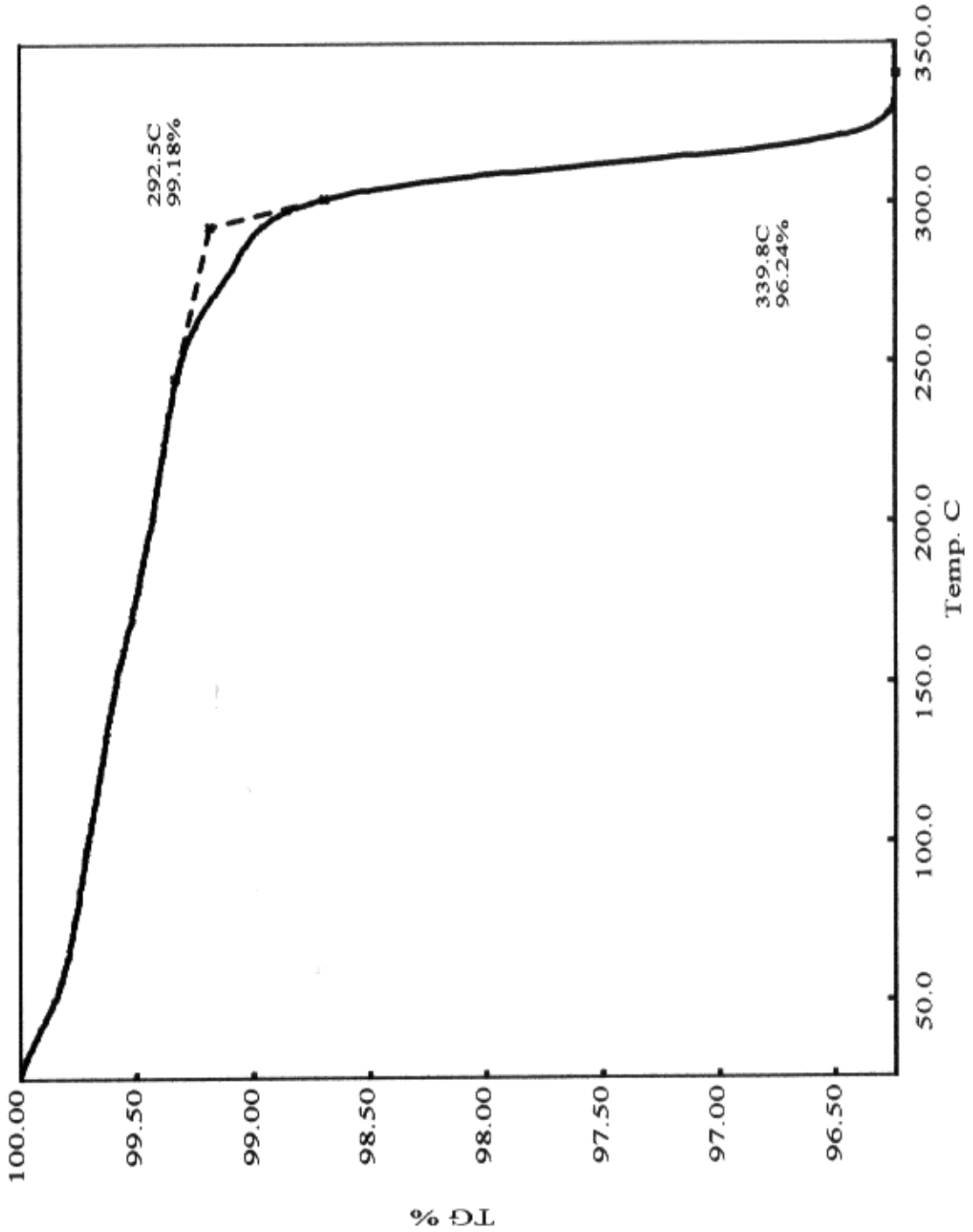

Figure 5-8: "Thermogravimetric Trace of Product from Reaction with 1:3 Copper to Molybdenum Starting Material Ratio"

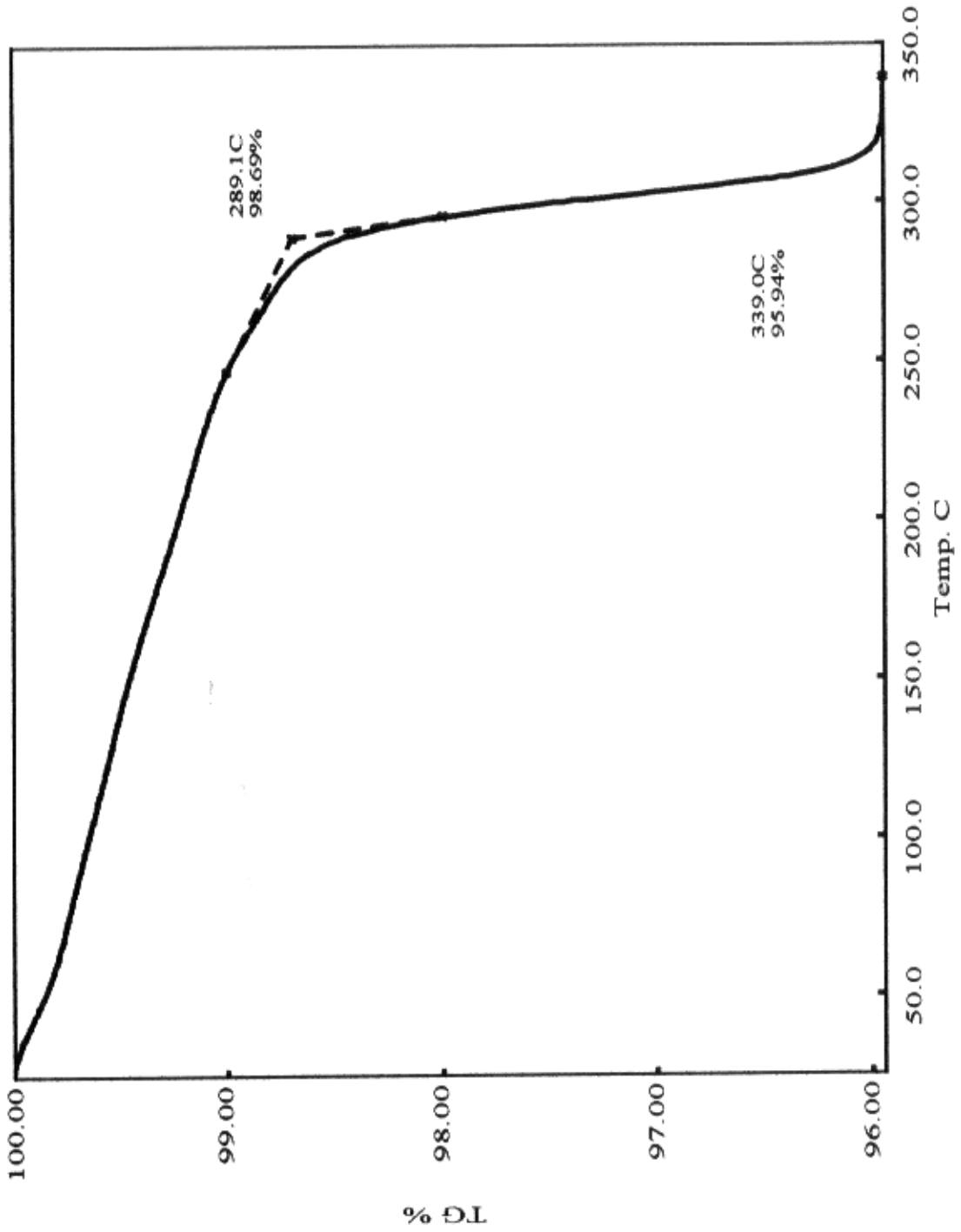

Figure 5-9: "Thermogravimetric Trace of Product from Reaction with 1:2 Copper to Molybdenum Starting Material Ratio"

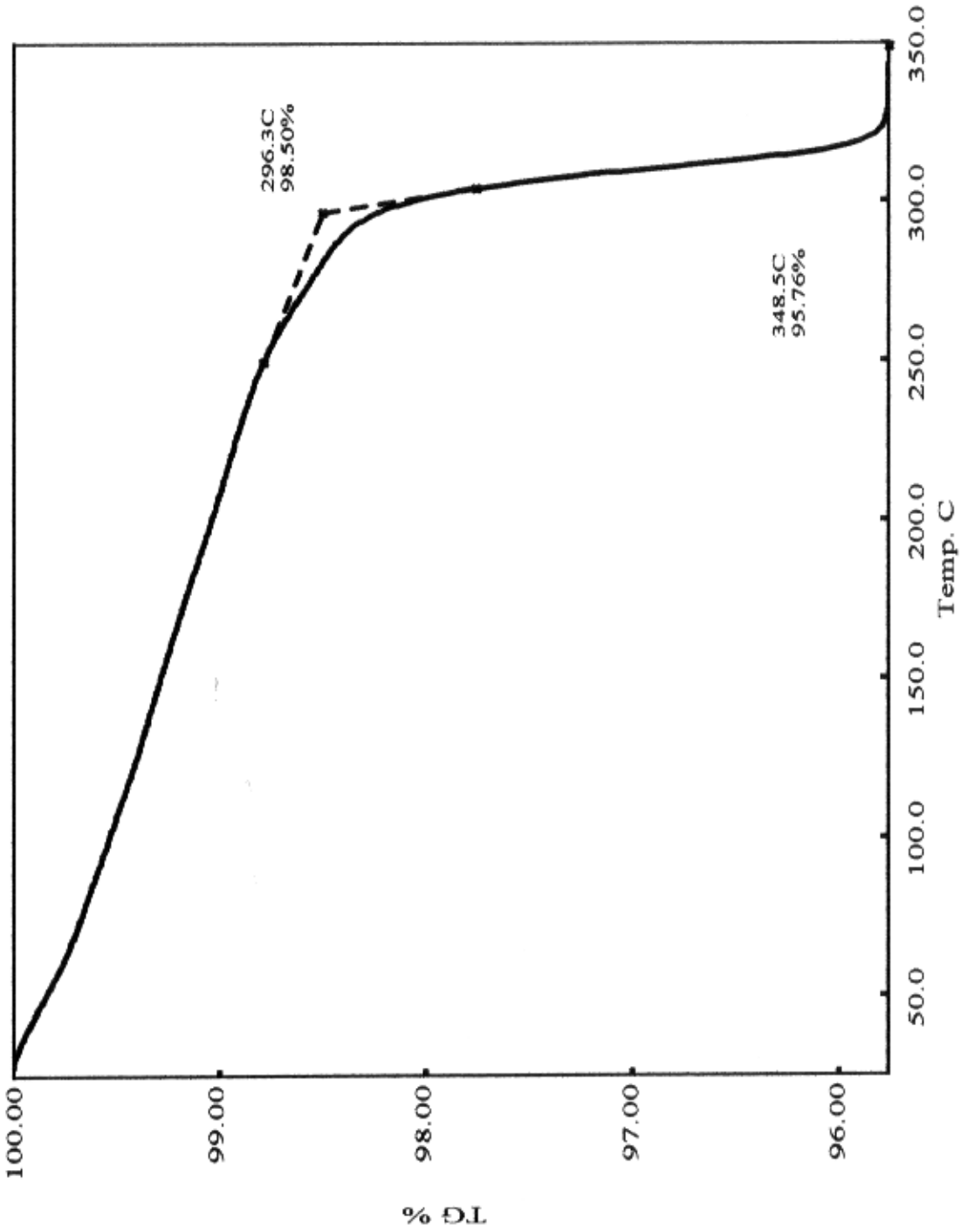

Figure 5-10: "Thermogravimetric Trace of Product from Reaction with 1:1 Copper to Molybdenum Starting Material Ratio"

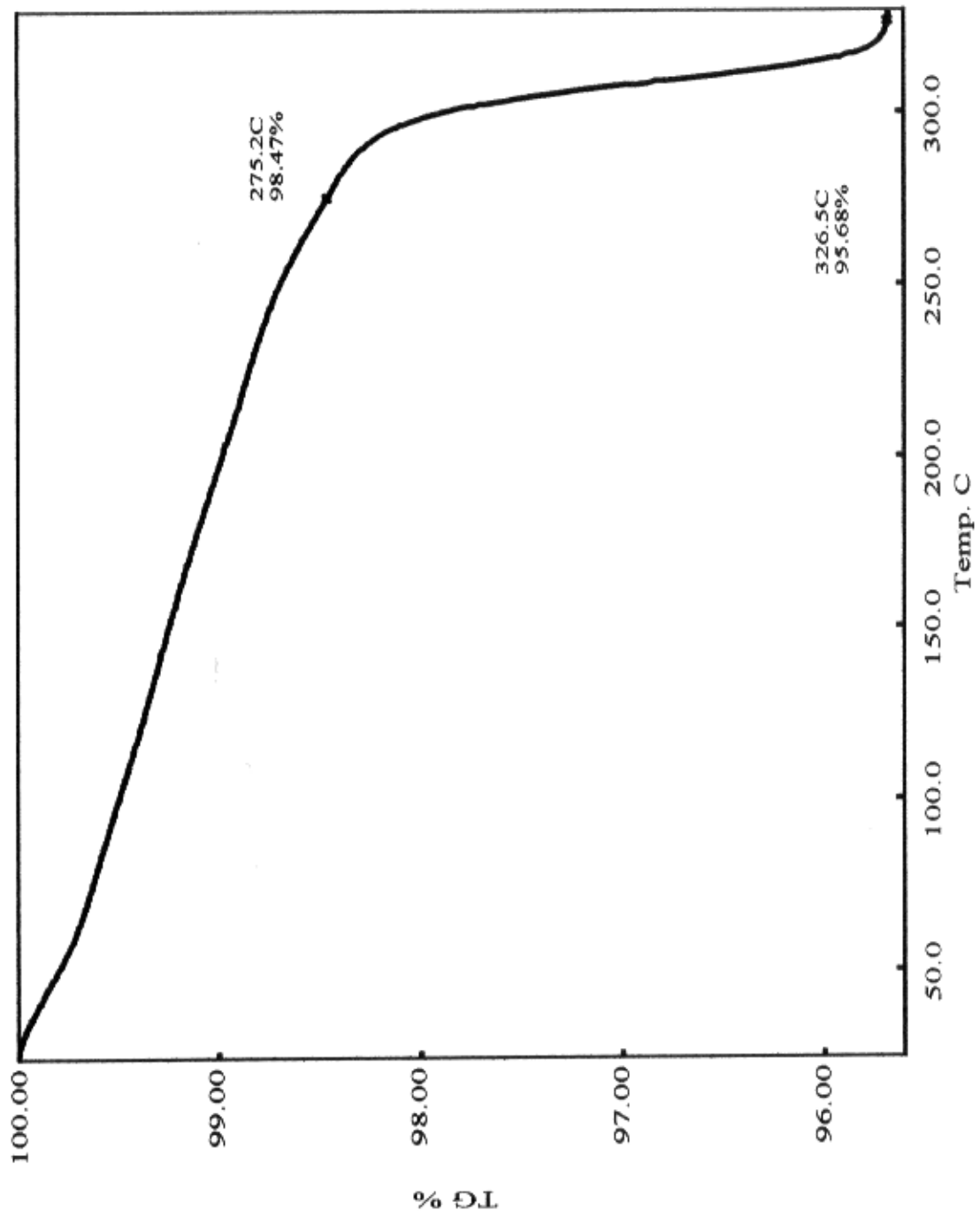

Figure 5-11: "Thermogravimetric Trace of Product from Reaction with 1:0.67 Copper to Molybdenum Starting Material Ratio"

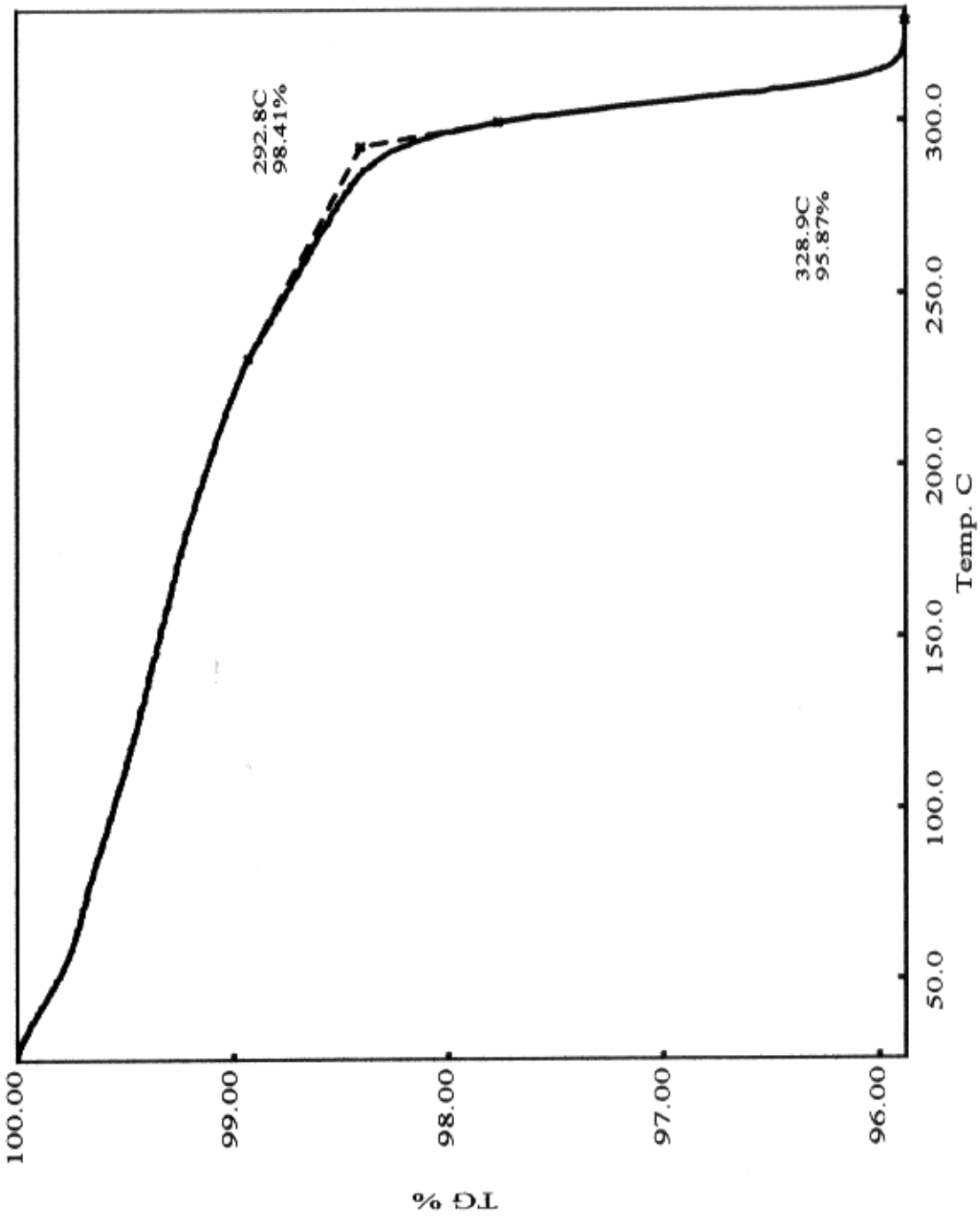

Figure 5-12: "Thermogravimetric Trace of Product from Reaction with 1:0.5 Copper to Molybdenum Starting Material Ratio"

The dehydration of the product occurs slowly at room temperature up to approximately 300 °C where it accelerated significantly. A similar pattern is observed for pure $Cu(OH)_2$. The shape of the TGA curve likely reflects the pairwise combination of the adjacent hydroxides in the low temperature range followed by rapid dehydration at higher temperature that allows migration of the hydroxyl groups. Notably, there is an inverse correlation between the size of the initial dehydration step and the copper to molybdenum ratio used in the synthesis. The hydrothermal product that most closely approaches the lindgrenite has no initial dehydration step. The results suggest the presence of additional hydroxyl groups and/or waters of hydration in the copper molybdate products as compared to lindgrenite. The mass loss data for each of the product samples examined are summarized in Table 5-5.

Table 5-5: "Thermogravimetric Weight Loss Data"

Copper:Molybdenum (Starting Materials)	1st Mass Loss (weight %)	2nd Mass Loss (weight %)	Total Mass Loss (weight %)
1:5	0.83	3.03	3.93
1:4	0.81	3.12	3.93
1:3	0.78	2.98	3.76
1:2	1.19	2.87	4.06
1:1	1.46	2.78	4.24
3:2	1.58	2.75	4.33
2:1	1.30	2.82	4.12
Hydrothermal	0	3.23	3.23

Lindgrenite would decompose to copper molybdate and water by dehydration as shown in Equation 5-8.

$$Cu_3(MoO_4)_2(OH)_2 + \text{heat} \rightarrow Cu_3Mo_2O_9 + H_2O \qquad \text{(Equation 5-8)}$$

If the lindgrenite was anhydrous, the percentage of mass lost by dehydration of the hydroxides would be 3.31 %. Thermogravimetric data from a synthetic lindgrenite synthesized from a hydrothermal method [108] also appeared to be almost identical to that found in this study, and is presented in the Figure 5-13.

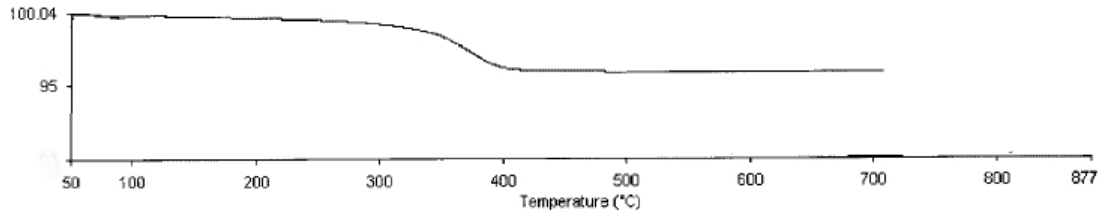

Figure 5-13: "Thermogravimetric Trace for Synthetic Lindgrenite" (Adapted from Ref. [108])

Isothermal TGA analysis of the product was performed at various temperatures in order to determine the fraction of the water that was due to hydration. The 1:2 Cu:Mo sample was examined at a temperature of 121.3 °C for a duration of 1199 minutes. The sample experienced a weight loss of 0.441%.

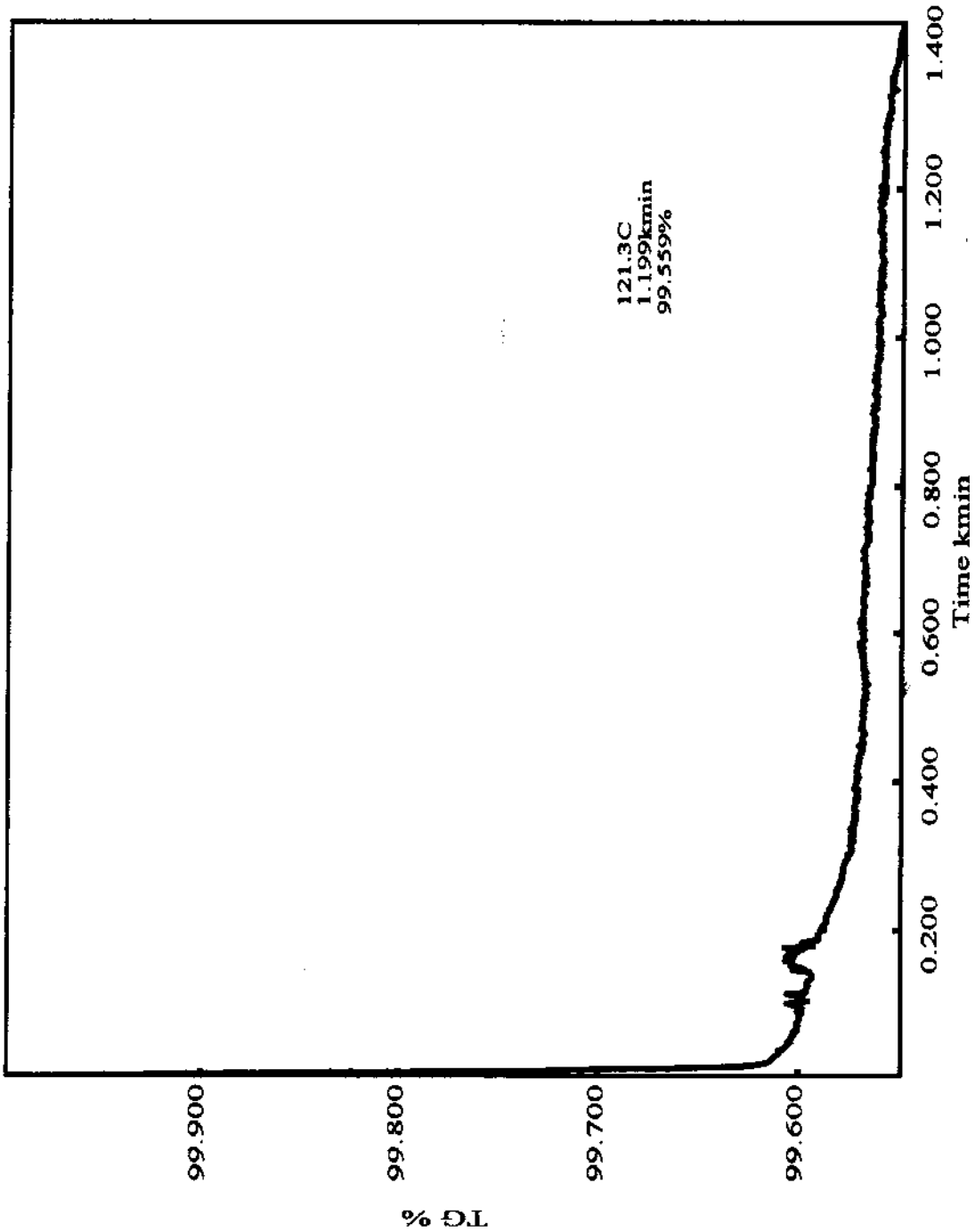

Figure 5-14: "Isothermal TGA Trace of the 1:2 Cu:Mo Product at T = 121.3 °C, t = 1199 minutes."

The differential scanning calorimetry data from the representative 2:1 Mo:Cu solid product indicates two endothermic reactions illustrated by the two valleys in the DSC spectrum. The first valley begins at 273.29 C, is centered at 293.69 C, and corresponds to a heat flow of 1.813 J/g. The second valley begins at 325.16 C, is centered at 339.93 C, and corresponds to a heat flow of 112.2 J/g. The second valley appears to correspond to the sharper weight loss, ca. 3%.

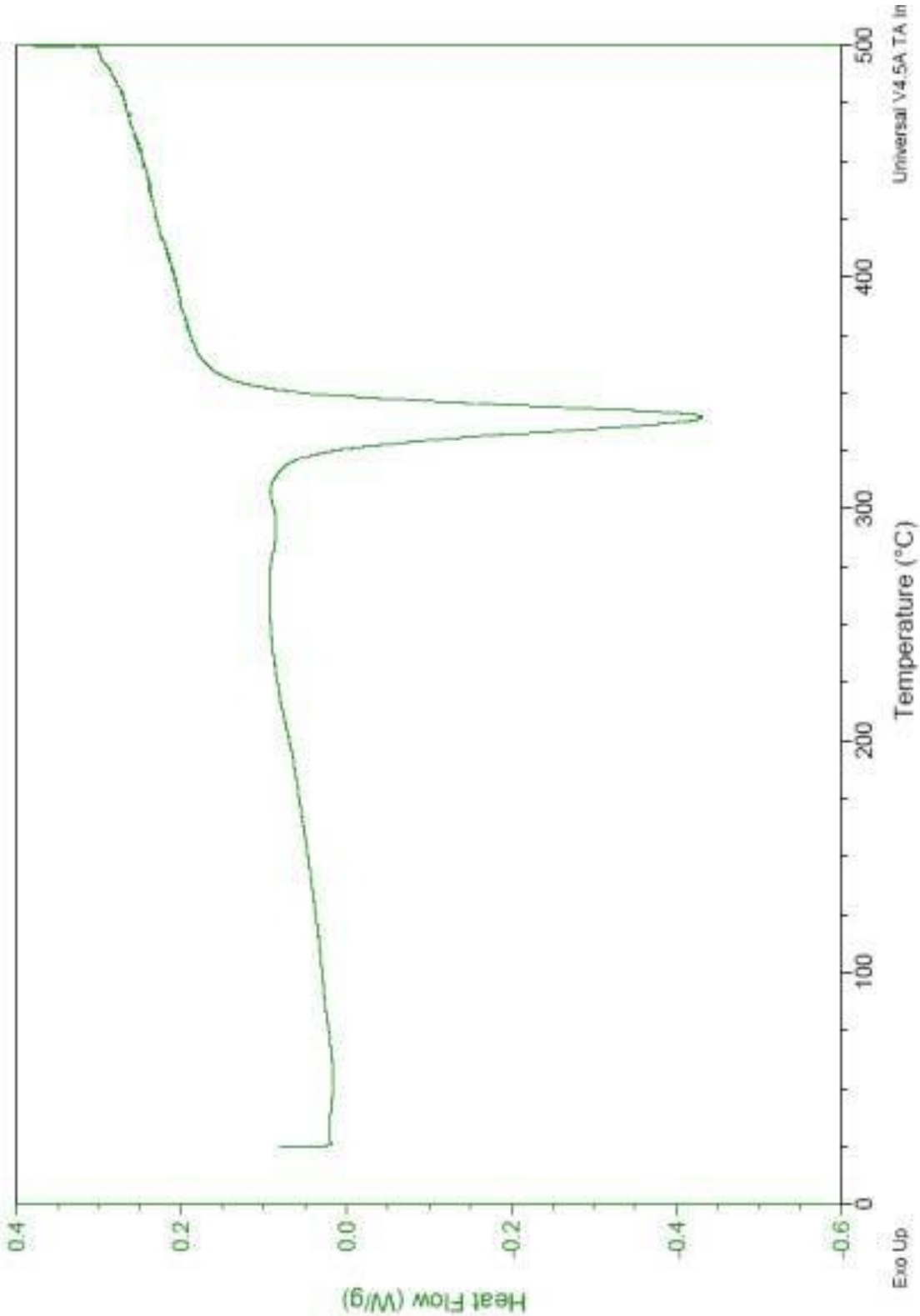

Figure 5-15: "DSC Trace for 1:2 Copper to Molybdate Sample"

The molybdenum content was determined by subtracting the percent copper content as copper oxide from the products ceramic yield. The molybdenum was assumed to be present as molybdenum trioxide in the final product. Given this data it was possible to determine the ratio of copper, molybdenum and hydroxide ions in each product. Notably, it was found that the copper deficiency of the products was compensated by the protonation of the oxo groups to produce additional hydroxyl groups with respect to lindgrenite, $Cu_{3-2x}O_{8-2x}(OH)_{2+2x}$, or $Cu_{2.84}Mo_2O_{7.68}(OH)_{2.32}$ for the 1:5 Cu:Mo product.

Some of the products isolated at lower pH had additional protonation to yield coordinated water molecules. The hydrothermal product was also copper deficient but in this case the charge was balanced by the presence of fewer oxo groups so that the product was also slightly water deficient.

Table 5-6: "Calculated Copper to Molybdenum Product Ratios"

Cu:Mo Starting Materials	Cu:Mo
1 to 5	1.419
1 to 4	1.432
1 to 3	1.399
1 to 2	1.464
1 to 1	1.403
3 to 2	1.406
2 to 1	1.388
Hydrothermal	1.426
Theoretical Lindgrenite (anhyd.)	1.500

Table 5-7: "Calculated Formulas for the Various Products"

Copper to Molybdenum (Starting Material)	Formula
5 to 1	$Cu_{2.84}Mo_2O_{7.68}(OH)_{2.32}\cdot 0.07\ H_2O$
4 to 1	$Cu_{2.86}Mo_2O_{7.72}(OH)_{2.28}\cdot 0.07\ H_2O$
2 to 1	$Cu_{2.82}Mo_2O_{7.64}(OH)_{2.36}\cdot 0.07\ H_2O$
1 to 1	$Cu_{2.81}Mo_2O_{7.62}(OH)_{2.38}\cdot 0.02\ H_2O$
3 to 2	$Cu_{2.81}Mo_2O_{7.62}(OH)_{2.38}\cdot 0.07\ H_2O$
2 to 1	$Cu_{2.78}Mo_2O_{7.56}(OH)_{2.44}\cdot 0.10\ H_2O$
Hydrothermal	$Cu_{2.85}Mo_2O_{8.1}(OH)_{1.9}\cdot 0.07\ H_2O$
Theoretical Lindgrenite	$Cu_{3.00}(OH)_{2.00}(MoO_{3.00})_2$

CONCLUSIONS

A green process was developed for the processing of copper sulfide ore, ultimately to the oxide. The purpose was to obtain an alternative process to the sulfide roasting presently employed which results in the formation of sulfur dioxide gas as a by-product. Application of this process requires an initial conversion of the copper sulfide to copper sulfate by a number of possible methods. The resulting copper sulfate solution is next reacted with an alkali metal molybdate to precipitate a copper molybdate. Treatment of the latter with an alkali metal hydroxide allows the isolation of solid copper hydroxide and regenerates the alkali metal molybdate. The hydroxide product can be reduced in the hydroxide form or dehydrated to the oxide form and subsequently reduced by existing processes. The advantages of this process over the existing ore roasting operation are manifold. There is not sulfur dioxide produced in this process making it much more environmentally friendly. Additionally, cost saving benefits of this process include the recyclability of the molybdate reagent, and as this process is carried out in the aqueous phase at a temperature of around 100 °C, decreased energy requirement and capital cost.

This study examined the nature of the copper molybdate intermediate and determined that it was a copper molybdate hydroxide material similar to the mineral lindgrenite, however the material was copper deficient and rich in hydroxide. Additionally, the yield of the copper molybdate intermediate was dependant upon the pH of the system, such that the yield, and thus the copper recovery, increased with increasing pH. Additionally it was determined that the molybdate in the starting materials served to increase the pH by acting as a buffer, and in the process is reacted to a water soluble polymolybdate species which is not usefully recyclable. Since the molybdate is the most expensive reagent in the process, it will be necessary to perform future work to adjust the pH using an alkali metal hydroxide base, likely in the same proportions as present in the lindgrenite mineral. The successful negotiation of this challenge should make the molybdate process a viable industrial process for copper ore processing.

CHAPTER VI

CATALYTIC DISPROPORTIONATION OF AQUEOUS SULFITE

INTRODUCTION

Sulfur dioxide gas is a by-product in a large number of industrial processes including coal-fired power production, ore refining, petroleum refining, etc. Sulfur dioxide when released into the atmosphere is converted into sulfuric acid by a number of mechanisms ultimately returning to earth as "acid-rain" which is responsible for a number of problems such as acid erosion of infrastructure and damage to plants and wildlife.

Sulfur dioxide is produced in the ore refining industry during the roasting of metal sulfide ores such as nickel or copper sulfides. A generalized reaction of this type is illustrated in Equation 6-1, in which a metal(II) sulfide, denoted as MS, is roasted with excess oxygen to produce the metal oxide and sulfur dioxide.

$$2\ MS_{(s)} + 3\ O_{2(g)} \rightarrow 2\ MO_{(s)} + 2\ SO_2 \qquad \text{(Equation 6-1)}$$

Sulfur dioxide is produced in petrochemical and coal-fired power production from the oxidation of organosulfur compounds as illustrated generally in Equation 6-2.

$$C_xH_yS_z + \text{excess } O_2 \rightarrow x\ CO_{2(g)} + 0.5y\ H_2O_{(g)} + z\ SO_{2(g)} \qquad \text{(Equation 6-2)}$$

In the environment, sulfur dioxide reacts by either a gas phase reaction to sulfuric acid, or by an aqueous phase reaction to sulfurous acid. In the gas phase reaction, sulfur dioxide reacts with hydroxyl radical, HO·, already present in the atmosphere to form an intermediate $HSO_3\cdot$ radical, see Equation 6-3, which subsequently reacts with molecular oxygen to form sulfur trioxide and the peroxy radical, HOO·, see Equation 6-4. The sulfur trioxide reacts with water to form gaseous hydrogen sulfate as the hydration product, as shown in Equation 6-5. Ultimately the gas phase hydrogen sulfate aggregates with water molecules to form an aerosol of sulfuric acid droplets, see Equation 6-6, which, when they grow sufficiently large, fall to earth as acid rain[109].

$$SO_2 + HO\cdot \rightarrow HSO_3\cdot \qquad \text{(Equation 6-3)}$$

$$HSO_3\cdot + O_2 \rightarrow SO_3 + HOO\cdot \qquad \text{(Equation 6-4)}$$

$$SO_3 + H_2O \rightarrow H_2SO_{4(g)} \qquad \text{(Equation 6-5)}$$

$$H_2SO_{4(g)} + n\ H_2O \rightarrow H_2SO_{4(aq)} \qquad \text{(Equation 6-6)}$$

A second reaction for the environmental production of sulfuric acid occurs in the aqueous phase when sulfur dioxide gas is dissolved in water droplets, such as clouds, mist, etc. The dissolved sulfur dioxide then reacts with water to form sulfurous acid,

$H_2SO_{3(aq)}$. The sulfurous acid is then oxidized by environmental ozone or hydrogen peroxide to produce aqueous sulfuric acid [109].

$$SO_{2(g)} \rightarrow SO_{2(aq)} \qquad \text{(Equation 6-7)}$$

$$SO_{2(aq)} + H_2O_{(l)} \rightarrow H_2SO_{3(aq)} \qquad \text{(Equation 6-8)}$$

$$H_2SO_{3(aq)} + O_{3(aq)} \rightarrow H_2SO_{4(aq)} + O_{2(aq)} \qquad \text{(Equation 6-9)}$$

$$H_2SO_{3(aq)} + H_2O_{2(aq)} \rightarrow H_2SO_{4(aq)} + H_2O_{(l)} \qquad \text{(Equation 6-10)}$$

In order to avoid the release of sulfur dioxide gas the industries have implemented several methods to remove it from the stack. The processes used to accomplish this include:

1) Reacting the sulfur dioxide with hydrogen sulfide gas to form elemental sulfur and sulfuric acid, in a reaction known as the Claus Process.

$$H_2S + SO_2 \rightarrow 3\ S + 2\ H_2O \qquad \text{(Equation 6-11)}$$

2) Reacting the sulfur dioxide with calcium carbonate to initially form calcium sulfite. The calcium sulfite is then oxidized with oxygen (or air) to form calcium sulfate, which is a synthetic form of the mineral gypsum.

$$SO_{2(g)} \rightarrow H_2SO_{3(aq)} \qquad \text{(Equation 6-12)}$$

$$H_2SO_{3(aq)} + CaCO_3 \rightarrow CaSO_{3(s)} + H_2O_{(l)} + CO_{2(g)} \qquad \text{(Equation 6-13)}$$

$$2\ CaSO_{3(s)} + O_{2(g)} \rightarrow CaSO_{4(s)} \qquad \text{(Equation 6-14)}$$

3) Reacting the sulfur dioxide with aqueous hydroxide to form an aqueous sulfite salt, see Equations 6-15 and 6-16. A slight variation on this reaction uses a water/liquid amine mixture to generate alkylammonium sulfites.

$$SO_{2(g)} \rightarrow H_2SO_{3(aq)} \qquad \text{(Equation 6-15)}$$

$$H_2SO_{3(aq)} + 2\ KOH_{(aq)} \rightarrow K_2SO_{3(aq)} + 2\ H_2O_{(l)} \qquad \text{(Equation 6-16)}$$

A catalytic reaction that can easily be used for the conversion of a sulfite stream to elemental sulfur and sulfate was discovered serendipitously in the course of this research while attempting to synthesize potassium molybdenum bronze by reduction of MoO_3 with potassium metabisulfite. Upon observing the presence of a blue solution as well as a brownish solid containing what appeared to be yellow sulfur crystals, a crude extraction was performed that resulted in the isolation of sulfur.

Metabisulfite ion, $S_2O_5^{2-}$, is the anhydride of bisulfite, HSO_3^-. For this reason, when the metabisulfite is dissolved in an aqueous solution it partially reacts with water to form bisulfite ion. The bisulfite ion is, in turn, in equilibrium with sulfite.

$$S_2O_5^{2-} + H_2O \leftrightarrow 2\ HSO_3^- \qquad \text{(Equation 6-17)}$$

$$HSO_3^- \leftrightarrow SO_3^{2-} + H^+ \qquad \text{(Equation 6-18)}$$

The purpose of this study was to examine the catalytic reaction of sulfite to form sulfur and sulfate.

EXPERIMENTAL

The hydrogen molybdenum bronze used in these experiments was produced using the zinc/hydrochloric acid method previously discussed. The source of iron(III) used in these experiments came from a ferric sulfate reagent of initially unknown hydration. The percent iron by mass was determined from the ceramic yield of the reagent to contain 20.67 wt% Iron. All other reagents were used as received without further purification unless otherwise specified.

Determination of the Iron Content of the Ferrous Sulfate Reagent

A preweighed crucible was charged with 2.0090 g of the ferric sulfate reagent and placed in a muffle furnace in which it was heated to a final temperature of 700 ºC at a rate of 1 ºC/min. After cooling the mass of the product, which was assumed to be Fe_2O_3, was determined to by 0.5937 g by subtraction, which corresponds to 0.0037179 moles of Fe_2O_3, or 0.0074358 moles (0.41525 g) of iron. Comparison of the mass of iron present with the mass of the initial reagent before heating gave an iron(III) composition of 20.67 wt%.

Preparation of the Iron Molybdate Catalyst

The iron molybdate catalyst was prepared by reacting a solution of potassium molybdate with a solution of ferric sulfate. The potassium molybdate solution was prepared by dissolving 6.780 g (0.12 moles) of potassium hydroxide in 200 ml of water. After the potassium hydroxide solution, 8.635 g (0.06 moles) of molybdenum trioxide was slowly added to the solution while stirring, resulting in a solution of potassium molybdate with no solid remaining. The ferric sulfate solution was prepared by dissolving 10.85 g (0.04016 moles) of ferric sulfate in 100 ml of water and stirred until all of the reagent dissolved. The two solutions were poured together, immediately producing a yellow precipitate. The product was stirred for 48 hours and filtered through a glass frit funnel and dried at 80 ºC to constant mass.

Reaction of MoO_3 with Potassium Metabisulfite

A hybridization tube was charged with 2.020 g (14.03 mmoles) of molybdenum trioxide, 22.236 g (100 mmoles) potassium metabisulfite, and 100 g of water. The reaction mixture was allowed to react in a hybridization oven for 145 hours at 100 ˚C. The reaction product was then removed and vacuum filtered to recover the solid. The solid was dried at 80 ˚C to constant mass and extracted with toluene in a Soxhlet extractor to recover the sulfur. There was 0.91 g (28.4 mmoles) of sulfur recovered, corresponding to a yield of 42.6 % (based on the disproportionation of metabisulfite to sulfur and sulfate).

Reaction of Hydrogen Molybdenum Bronze with Potassium Metabisulfite

A hybridization tube was charged with 2.022 g (14.00 mmoles) of hydrogen molybdenum bronze, 22.233 g (100 mmoles) potassium metabisulfite, and 100 g of water. The reaction mixture was allowed to react in a hybridization oven for 145 hours at 100 ˚C. The reaction product was then removed and vacuum filtered to recover the solid. The solid was dried at 80 ˚C to constant mass and extracted with toluene in a Soxhlet extractor to recover the sulfur. There was 0.99 g (30.9 mmoles) of sulfur recovered, corresponding to a yield of 46.3 % (based on the disproportionation of metabisulfite to sulfur and sulfate).

Reaction of Potassium Metabisulfite with Hydrogen Molybdenum Bronze and Iron-Promoted Hydrogen Molybdenum Bronze Catalyst

Reaction mixtures were prepared by charging hybridization tubes with 100 mmol of potassium metabisulfite, 100 g of water, and varying amounts of hydrogen bronze and ferrous sulfate. These mixtures were then placed in a hybridization oven at 100 ºC for 72 hours. Each resulting product mixture was filtered through a glass frit filter. The solid portion was dried under vacuum and subsequently extracted with toluene in a Soxhlet extractor for ~ 8 hours. The resulting toluene phase, which was bright yellow when it contained significant amounts of sulfur, was placed in a preweighed beaker and allowed to evaporate. The mass of sulfur obtained was determined by subtraction.

Kinetic Analysis of Iron-Promoted Hydrogen Molybdenum Bronze Catalytic Reaction

Reaction mixtures were prepared containing 25 mmoles of hydrogen bronze, 4.8 mmoles of iron(III) as $Fe_2(SO_4)_3$, 100 moles of $K_2S_2O_5$ and 100 mmoles of water in a hybridization tubes and placed in a hybridization oven at 100 ˚C for the required reaction time. The reaction times examined were 2, 4, 6, 8, and 53 hours. At the end of the reaction time the reaction products were vacuum filtered through a glass frit filter. The solid material was dried without washing at 80 ˚C to a constant mass. Upon completion of the drying step, any sulfur present was extracted from the solid in a Soxhlet extractor with toluene.

Examination of the Cation Effect on the Iron-Promoted Hydrogen Molybdenum Bronze Catalytic Reaction

Three separate reactions were performed using 25 mmoles of hydrogen bronze, 4.8 moles of iron (III) (as $Fe_2(SO_4)_3$), and 100 mmoles of sodium metabisulfite. To each of the reactions was added 200 mmoles of a different alkali metal salt: sodium chloride, potassium chloride, and cesium chloride. Each reaction was ran at 100 ˚C in a hybridization oven for 24 hours. These products were then vacuum filtered to recover the solids. The solids were then dried to constant mass and extracted with toluene in a Soxhlet extractor to recover the sulfur.

Reaction of the Iron Molybdate Catalyst with Potassium Metabisulfite

Two grams of the iron molybdate catalyst was reacted at 100˚C for 24 hours with 100, 150, and 200 mmoles of potassium metabisulfite in 100 ml H_2O. After the reaction was stopped, the solid was removed by vacuum filtration, dried at 80 ºC to constant mass and extracted with toluene to recover the sulfur.

Kinetic Analysis of Iron Molybdate Reaction

A series of experiments were prepared using hybridization tubes charged with 2.00 g of the iron molybdate catalyst, 200 mmoles of potassium metabisulfite, and 100 g of water. The reactions were carried out at 100˚C for 6, 12, 18, and 24. The products were worked up as in similar experiments and the sulfur extracted.

RESULTS AND DISCUSSION

The reaction of 25 mmoles of hydrogen bronze with 100 mmoles of potassium metabisulfite resulted in the formation of 0.59 g (35.57 mmoles) of sulfur in 72 hours. This suggests that the reaction of the sulfite to sulfur cannot be due to direct reduction of the S(IV) to S(0) by the hydrogen molybdenum bronze because there are not enough reducing equivalents present. Based on this, it was determined that this must be a catalytic reaction. However, the spent catalyst was an orange-brown solid and did not

resemble the blue hydrogen molybdenum bronze, which was suggestive of the formation of a catalytic material that is different from the hydrogen bronze material.

Based on the knowledge that sulfur does undergo disproportionation reactions and the fact that both elemental sulfur and sulfate was observed it was hypothesized that the reaction might take place as shown in Equation 6-19.

$$3\ S^{IV}{}_2O_5^{2-} + H_2O \rightarrow 4\ S^{VI}O_4^{2-} + 2\ S^0 + 2\ H^+ \text{ (Equation 6-19)}$$

A disproportionation reaction is one in which a compound with an element one oxidation state reacts to produce a product in which the element is in a higher oxidation state and a second product where it is in a lower oxidation state. In this case, four of the six S(IV) atoms from the three metabisulfite ions are oxidized to S(VI) (forming sulfate) and two of the same are reduced to S(0) forming elemental sulfur.

Iron(III) has been used as a catalytic promoter in many desulfurization reactions such as the previously mentioned Claus process. Therefore the effect of ferric ions on the catalytic disproportionation reaction was investigated. When 4.8 mmoles of iron(III) was added to the reaction mixture in the form of ferric sulfate, in an experiment run under otherwise identical conditions as the one described above, the sulfur recovery increased to 1.10 g (57.55 moles). This suggested that the iron(III) did play the part of a catalytic promoter for this reaction.

In order to determine the effect of the catalyst and promoter loading on the sulfur yield, a series of experiments were performed under the same conditions but with decreasing hydrogen molybdenum bronze and iron(III) promoter loadings. The results of this series as well as those of the hydrogen molybdenum bronze only experiments are summarized in Table 6-1 and presented graphically in Figure 6-1.

Table 6-1: "Effects of Hydrogen Molybdenum Bronze and Iron(III) Promoter on Yield of Sulfur"

mmoles Potassium Metabisulfite	mmoles Hydrogen Bronze	mmoles Iron(III) Promoter	mmoles Sulfur	% Yield Sulfur based on proposed mechanism
100	25	0	19.70	29.54
100	25	4.8	34.57	51.84
100	5	1.0	57.55	86.31
100	1	0.20	61.14	91.70

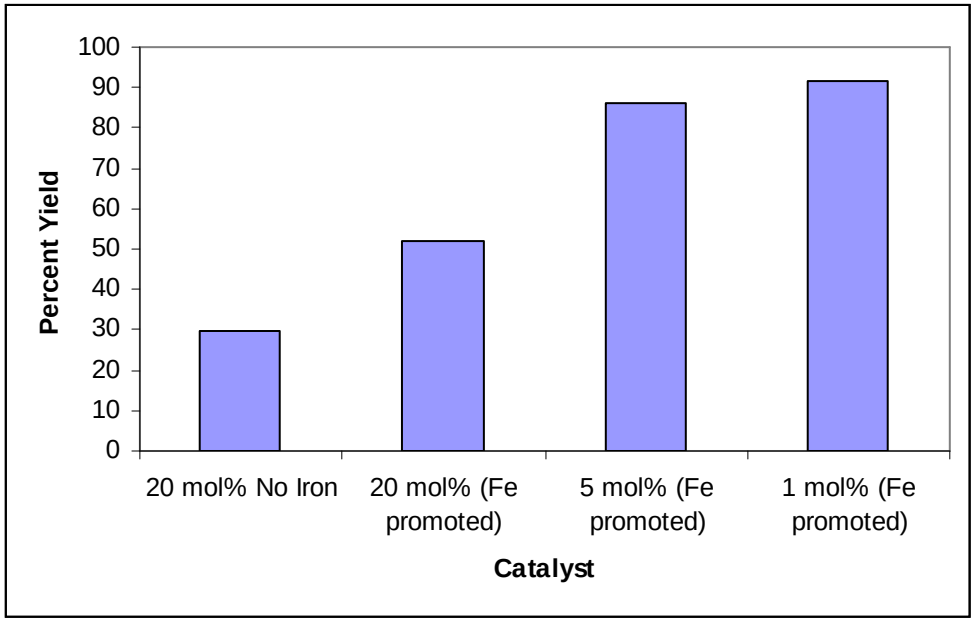

Figure 6-1: "Bar Graph Illustrating the Effects of Decreasing the Hydrogen Bronze and Iron(III) Loading"

It was observed from the data that as the amount of catalyst and promoter in the system was increased the yield of sulfur product decreased. The most likely explanation for this is that the initial catalyst material becomes sulfided. In this case, if more of catalyst is present, less sulfur product is produced. The question arises whether sulfidation produces a more active catalyst or acts as a catalyst poison.

In order to determine whether or not the catalyst was poisoned or activated by the uptake of sulfur, kinetic studies were performed for the iron-promoted reaction. In this study, 25 mmoles of hydrogen bronze, 4.8 mmoles of iron(III), and 100 mmoles of potassium metabisulfite were reacted in 100 g of water at 100 ºC for 2, 4, 6, 8, and 53 hours. Table 6-2 summarizes the resulting kinetic data and Figures 6-2 and 6-3 illustrate respectively the mmoles of sulfur produced as a function of reaction time and the pH of the reaction mixture as a function of reaction time.

Table 6-2: "Kinetic Data for Iron(III)-Promoted Hydrogen Bronze Catalyzed Disproportionation of Potassium Metabisulfite"

Reaction Time (hours)	Mass of Sulfur Product (g)	mmoles of Sulfur	% Yield of Sulfur
0	0.0000	0.0000	0.0000
2	0.0000	0.0000	0.0000
4	0.0024	0.0755	0.1132
6	0.0038	0.1209	0.1815
8	1.01	32.80	49.19
53	1.10	34.57	51.85

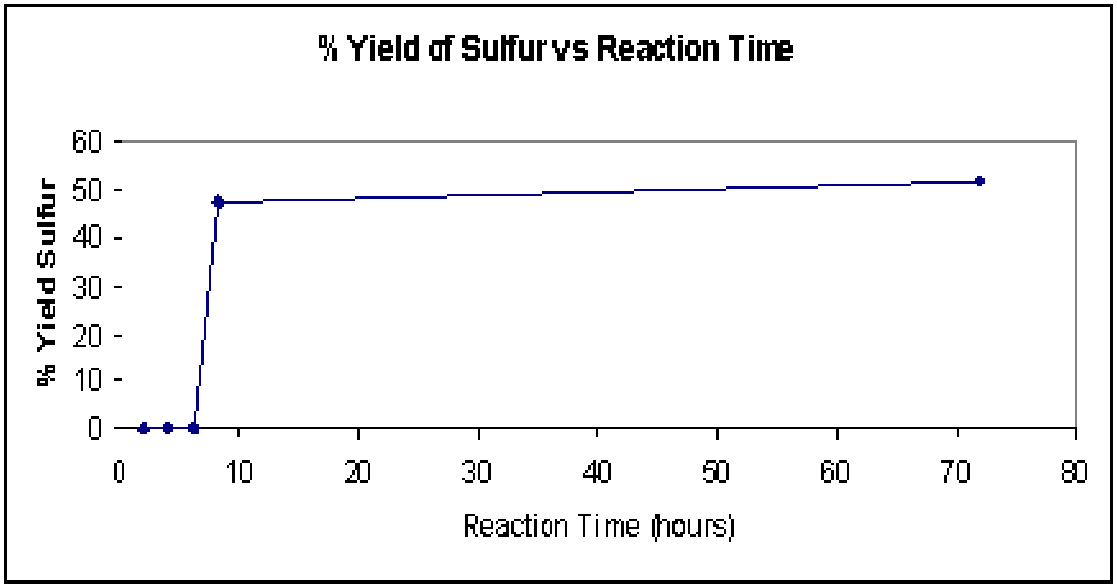

Figure 6-2: "Plot of Sulfur Yield vs. reaction time, Iron(III)-Promoted Reaction"

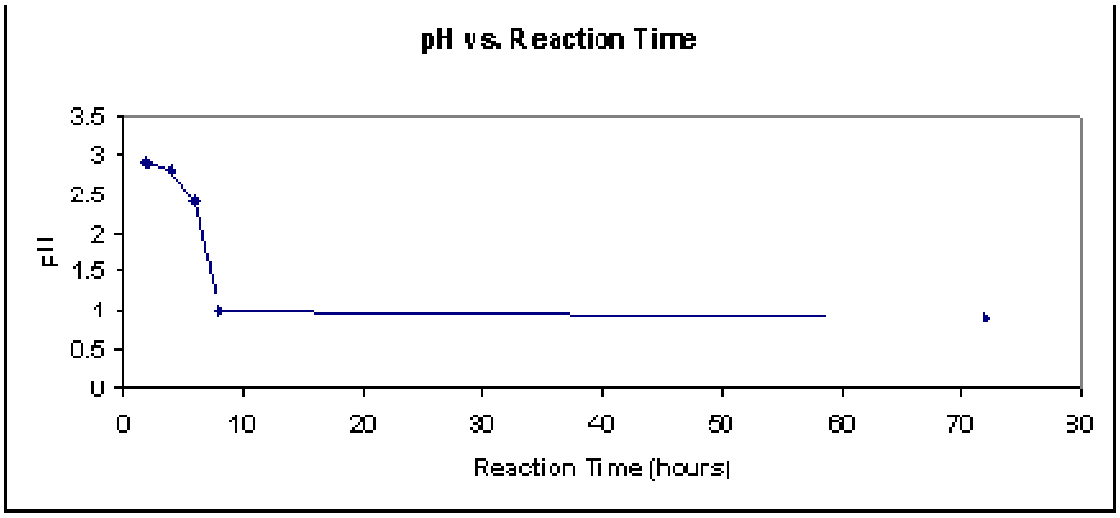

Figure 6-3: "Plot of pH of the Reaction Mixture as a Function of Reaction Time"

From the kinetic data it was observed that there is an induction time in which very little product is produced followed by very fast reaction rate greater than 16 mmol/hr. That is, the catalyst is initially producing very little sulfur(0) product. After a time, the catalyst becomes active and the reaction very quickly proceeds to completion.

This suggests that in the initial stages of the reaction, meaningful chemistry takes place producing intermediate species and protons, but no sulfur. As the pH decreases to a threshold value around pH = 1, these reactive species react to form the sulfur. Thiosulfate is known to disproportionate under acidic conditions [110, 111] and can be produced from metabisulfite by first reducing the metabisulfate to dithionite [112] and then reducing the dithionite to thiosulfate. Thiosulfate is an especially likely intermediate because in addition to disproportionation to sulfur it can sulfide the molybdenum(IV) centers by oxidation.

X-ray photoelectron spectroscopy analysis shown in Figure 6-4 of the surface of the spent catalyst indicated the presence of sulfur on its surface, which suggests the likelihood of sulfided active sites on the catalyst. Interestingly, no iron was observed on the surface of the catalyst. Considering that both molybdenum trioxide and hydrogen bronze were catalytic for this reaction without the iron, but much slower, it suggests that the iron plays a role in the increasing the rate of sulfidation of the catalyst, which is ultimately the rate limiting step in the process, rather than in the disproportionation of the sulfite.

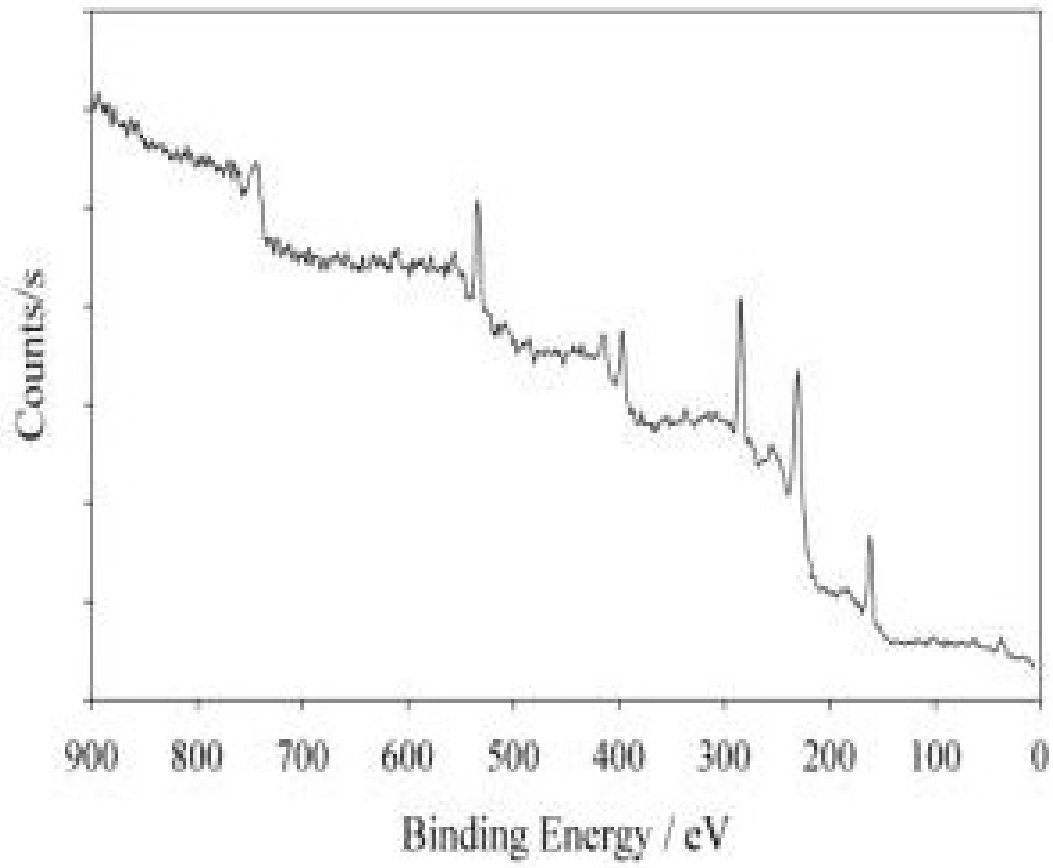

Figure 6-4: "X-ray Photoelectron Spectrum of Spent Catalyst Surface"

Other experiments were carried out in which 100 mmoles of sodium metabisulfite was reacted with 25 mmoles of hydrogen bronze and 4.8 mmoles of iron(III) in which the resulting sulfur yield of 15.4 % (0.33 g) was much lower than that for the potassium metabisulfite. This suggested the possibility of a cation effect in which the potassium cation promoted the reaction kinetics to a greater degree than the sodium cation. Such effects are common in heterogeneous catalysis, such as the use of potassium to promote iron oxide catalysts for ammonia synthesis.

In order to determine this effect an experiment was performed in which excess sodium, potassium, and cesium cations were added to the iron (III)-hydrogen bronze catalyzed reaction with sodium metabisulfate. These cations were added to produce solutions with identical ionic strengths. Additionally, one experiment was performed with iron (III)-hydrogen bronze and sodium metabisulfite with no added salt in order to determine the effect of increasing the ionic strength. Table 6-3 and Figure 6-5 and 6-6 summarize the experiments and their results.

Table 6-3: "Cation Effect on Kinetic Yield of Sulfur in the Iron(III)-Promoted Hydrogen Bronze Catalyzed Reaction."

Bronze (mmol)	Fe(III) (mmol)	$Na_2S_2O_5$ (mmol)	NaCl (mmol)	KCl (mmol)	CsCl (mmol)	Sulfur (g)	% Sulfur Yield
25	4.8	100	200	0	0	0.84	39.3
25	4.8	100	0	200	0	0.91	42.6
25	4.8	100	0	0	200	1.49	71.1
25	4.8	100	0	0	0	0.72	33.7

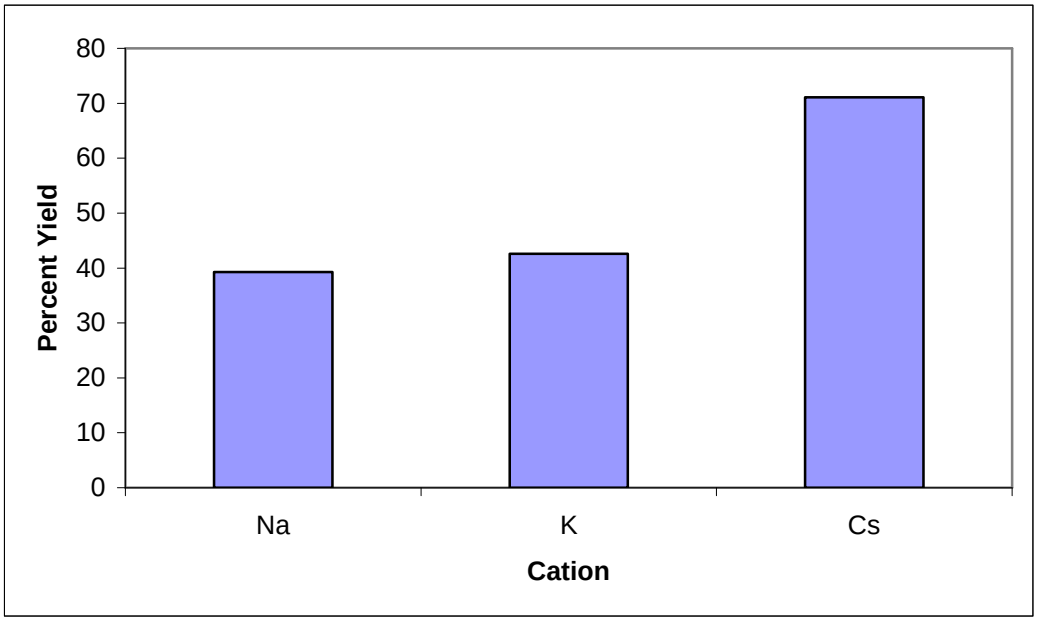

Figure 6-5: "Graph of Cation Effect on the Percent Kinetic Yield of the Iron Promoted Hydrogen Bronze Catalyzed Reaction, Reaction Time = 24 hours"

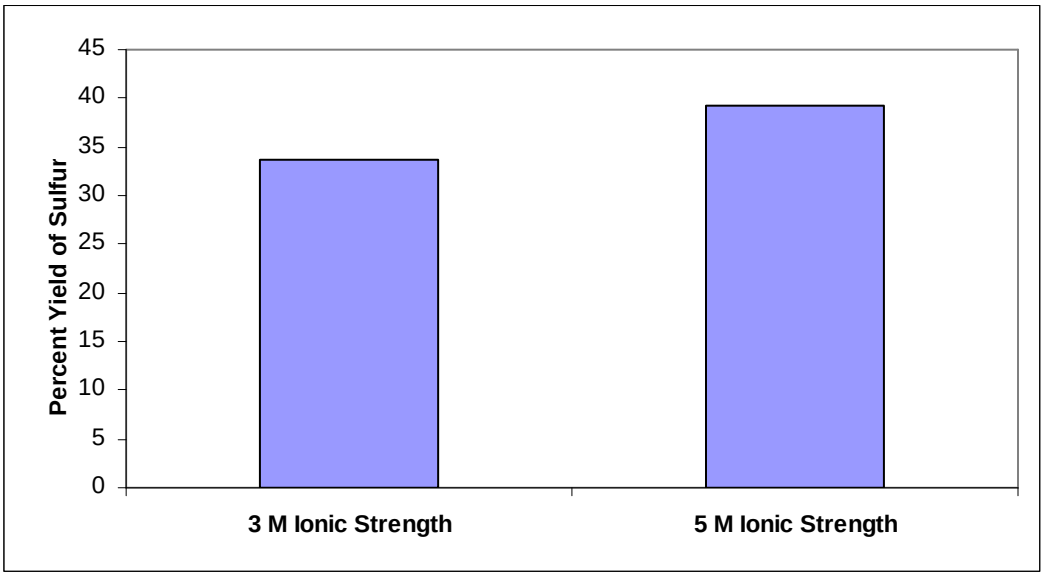

Figure 6-6: "Effect of Ionic Strength on Percent Sulfur Yield"

From these experiments, it is clear that the yield of sulfur increased as the molecular weight of the alkali metal cation increased. This suggests that the large polarizable cesium cation likely serves to stabilize some of the reactive sulfur intermediates. Additionally, comparison of the reaction containing 200 mmoles of added sodium chloride (net ionic strength of 5M) with the reaction containing no additional salt (net ionic strength of 3 M) further suggested that there is was a small but significant yield increase observed with increasing ionic strength. Based on what is known about the layered structure of the hydrogen bronze, it is possible that increasing the ionic strength of cations in the reaction mixture serves to delaminate the hydrogen bronze layers resulting in increased surface area.

In an attempt to create a single component catalyst containing the molybdenum catalyst and iron promoter an iron molybdate catalyst was prepared as previously

described. Two gram portions of the iron molybdate catalyst were reacted with varying amounts of potassium metabisulfite in 100 ml of water at 100 ºC for 24 hours (the results are summarized in Table 6-4). The reaction containing the 100 mmoles (1 M) of metabisulfite did not react within the time allotted. The higher concentration reactions did produce sulfur in the time allotted. At first, it was thought that the inactivity of the catalyst might be due to the sulfidization reaction required for the activation of the catalyst. However if this was true, then the recovered sulfur from the 150 mmol (1.5 M) reaction, would have produced no more than ~ 33 mmoles (1.06g) of sulfur, the amount corresponding to the 0.50 M difference between the 1.00 M reaction and the 1.50 M reaction. However the 1.50 M concentration produced 2.64 g of sulfur corresponding to a yield of 82.3%. This implied that it was not an issue of saturating the catalyst prior to activation. However the pH of 2.8 for the unreactive sample, as previously suggested, implied that the pH is too high for production of sulfur.

Table 6-4: "Percent Yield and Final pH Data for the Reaction of the Iron Molybdate Catalyst with Increasing Concentrations of Potassium Metabisulfite"

Catalyst (g)	$K_2S_2O_5$ (M)	Sulfur Obtained (g)	Percent Yield	Final pH
2.00	1.00	0.00	0.00	2.8
2.00	1.50	2.64	82.3	0.5
2.00	2.00	3.43	80.2	0.6

A kinetic analysis was performed for the iron molybdate catalyst, in which 2.00 g of the catalyst was allowed to react with 100 ml of 2 M potassium metabisulfite. The reaction times examined were 6, 12, 18, and 24 hours. The percent yield of sulfur obtained for each reaction time is summarized in Table 6-5.

Table 6-5: "Kinetic Data for Iron Molybdate-Catalyzed Disproportionation of Potassium Metabisulfite"

Reaction Time (hours)	Mass of Sulfur Product (g)	% Yield of Sulfur	pH
6	0.00	0.00	3.6
12	0.00	0.00	3.0
18	3.42	80.0	0.9
24	3.39	79.3	1.0

There was an induction time observed for the iron molybdate catalyst as well as decrease in the pH similar to that observed for the iron promoted hydrogen bronze catalyzed reaction, suggesting that the two reactions are similar. One very interesting observation from the 6 hour and 12 hour reactions is that there was very little solid obtained after the reaction previous to extraction. In fact the recovered solids decrease from 6 hours to 12 hours and then increase from 12 hours to 18 hours and then levels off.

Table 6-6: "Total Solid Recovery as a Function of Reaction Time, Iron Molybdate Catalyst"

Reaction Time (hours)	Total Solids Recovered after Reaction (g)	Solids Adjusted for Sulfur Removal (g)
6	1.159	1.159
12	0.191	0.191
18	4.792	1.37
24	4.807	1.42

The molecular weight of the spent catalyst per molybdenum was estimated by determining the weight of the recovered solids and making the assumption that all of the recovered solid was the spent catalyst and sulfur. Then the mass of the sulfur was subtracted out and the mass of the spent catalyst per unit mole of molybdenum starting material was determined. These estimates were determined for the molybdenum trioxide

after 6 days, hydrogen bronze only after 6 days, iron(III)-promoted hydrogen bronze after 72 hours, and iron molybdate catalyst after 24 hours, and are summarized in Table 6-7.

Table 6-7: "Estimated Molecular Weights (per Molybdenum Basis) for the Various Spent Catalysts"

Catalyst	Estimated molecular weight of the spent catalyst per molybdenum (g/mol per Mo)
molybdenum trioxide	178
hydrogen bronze	169
iron(III)-promoted hydrogen bronze	202
iron molybdate	163

A possible mechanism for the disproportionation reaction is given in Figure 6-7. The first proposed step is oxo transfer to sulfite to produce a Mo^{IV} center and sulfate. This reaction has a precedent in the sulfite oxidase enzyme that performs the same transformation using a MoO_3S_2 catalytic center. The next steps involve sequential reduction of metabisulfite to dithionite and thiosulfate by Mo^{VI} centers. These are known products from the reaction of sulfites with mild reducing agents such as formates. Under acidic conditions, the thiosulfate undergoes rapid disproportionation to sulfur and sulfite (or other oxidized species – the reaction is complex and produces a variety of products under varying conditions). Part of the thiosulfate is also likely responsible for sulfiding the molybdenum oxide catalyst. We have shown that this reaction occurs when thiosulfate solutions are contacted with molybdenum trioxide at 100 ºC. Notably, a partially sulfided catalyst would mimic the active site of the sulfite oxidase catalyst, which has a molybdenum active site with a coordination of three sulfurs and three oxygens [113].

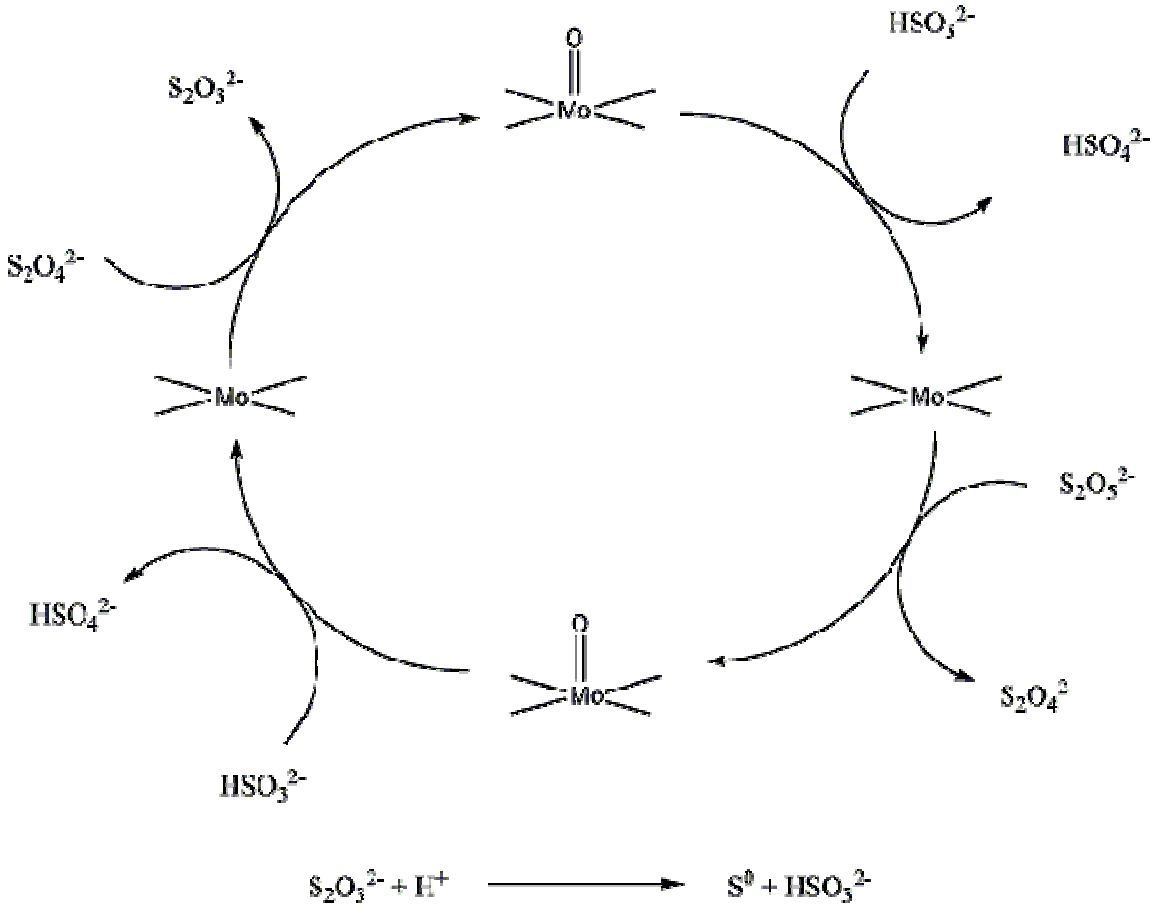

Figure 6-7: "Proposed Mechanism for the Catalytic Disproportionation of Sulfite"

CONCLUSION

A new catalytic method was developed for the disproportionation of aqueous sulfite to elemental sulfur and hydrogen sulfate ion using several catalysts based on molybdenum oxides. These reactions were conclusively determined to be catalytic and were found to be promoted by the presence of iron(III) and/or cesium in the solution. Furthermore, the surface of the catalyst was determined to be partially sulfided giving the molybdenum center similar coordination to the active molybdenum center of the sulfite oxidase enzyme used by humans, which is coordinated by three sulfurs and two oxygens.

This process has potential to be of great industrial importance because many large industrial processes produce large quantities of sulfur dioxide as a by-product which must be “scrubbed” using liquid-gas extraction methods resulting in a aqueous sulfite stream which must be further processed and disposed of. Utilization of this process would allow that sulfite stream to be used not as a waste but as a feedstock for the production of sulfur and sulfuric acid, both of which are valuable commodities. The only similar industrial process to this method is the Claus Process, a high temperature process, which is energy intensive and requires a hydrogen sulfide feedstock, while this process requires only the sulfite feedstock, from the sulfur dioxide waste stream, and is viable at much lower temperatures in the neighborhood of 100 °C.

ACKNOWLEDGEMENTS

Special thanks are in order for Dr. Nick Materer for performing the XPS measurements on the catalysts.

CHAPTER VII

CONCLUSION

This study has examined the applications of molybdenum oxides in a variety of environmentally green applications as well as detection of explosives and oxidants. Additionally it has served to develop some soft synthetic methods for these materials and, ultimately, to elucidate some previously misunderstood aspects of the structure and chemistry of the sodium molybdenum bronzes, or more correctly, sodium hydrogen molybdenum bronzes.

Specifically, numerous low-temperature synthetic methods were developed for the hydrogen and sodium hydrogen bronzes. The hydrogen bronzes were synthesized by low-pH aqueous dithionite reduction and dissolving metal reduction utilizing zinc and hydrochloric acid. The low-pH dithionite method resulted in a mixture of hydrogen and sodium hydrogen bronzes which were separable by washing out the more soluble sodium hydrogen bronze. The dissolving metal synthesis resulted in pure hydrogen bronze at a yield of (95.6%) in its most reduced air-stable form, with a formula of $H_{0.58}MoO_3$. Sodium hydrogen bronze was synthesized by a high-pH dithionite reduction method that resulted in a low yield of the product (56.5%). However, by changing the solvent from pure water to a 35:65 v:v water:ethanol mixture the yield increased to (78.0%).

The formula of the sodium hydrogen bronze was determined to be $(Na \cdot H_2O)_{0.26}H_{0.24}MoO_3$. Furthermore, it was determined that the protons were associated with a Mo^{V} center and thus chemically reducing, while the sodium cations were associated with a Mo^{VI} center that was not reducing in nature. This suggests a structure made up of sodium molybdenum oxide, hydrogen molybdenum bronze, and molybdenum trioxide building blocks in roughly a 0.25:0.25:0.50 ratio.

The sodium hydrogen bronze bulk material was found to disproportionate to a soluble species in aqueous media. This observed species was determined to be approximately $Na_{0.039}H_{0.09}MoO_3$. A possible reason for this enhanced solubility upon disproportionation of the bulk material is the increase in the ionic sodium oxygen bonds formed at the expense of the acidic hydroxide groups. Additionally, the formation of the sodium molybdenum oxide centers require the molybdenum-oxygen bonds to be broken, serving to decrease the particle size by both delamination and particle erosion.

A number of very successful applications were developed for the sodium hydrogen molybdenum bronze material including an aqueous colorimetric reagent for chlorine, and, likely, many other aqueous oxidants. A test strip was developed with this material which successfully detected peroxide solutions. The sodium hydrogen bronze was found to be unreactive with chlorates, unlike the hydrogen bronze analog, makes it a good co-reagent for the discrimination of peroxide explosives form chlorate explosives, especially as a field test as both reagents are solutions, rely on a color change and require

no bulky equipment. Lastly, a sodium hydrogen bronze based electronic vapor-phase peroxide detector device was developed and successfully tested resulting in an immediate linear decrease in conductivity while in contact with the vapor.

One of many environmental applications for the hydrogen molybdenum bronze product was as a reducing agent for hexavalent chromium in groundwater and wastewater. When tested in a high pH groundwater sample against nanometric iron (a reagent touted for this purpose) the hydrogen bronze greatly outperformad the nanometric iron with a reducing capacity of 60 mg hexavalent chromium/g compared to 0.39 mg hexavalent chromium/g observed for the nanometric iron. This is because the surface of the nanometric iron reagent fouls with chromium hydroxide at high pH. The hydrogen bronze reagent is immune to this fouling problem because the surface is acidic. In other studies the hydrogen bronze removed chromium consistently over a wide range of pH values with a very slight enhancement at lower pH values. Additionally, the hydrogen bronze was shown to remove much of the trivalent chromium product as well by absorption.

A second environmental application of the molybdenum oxide based materials that was developed is an environmentally friendly SO_2-free copper processing technique by which copper can be processed from copper sulfide ore, or more importantly a mix of copper and iron sulfides, without the need for the a roasting step normally needed to convert the sulfide to the oxide. This is especially important as the roasting step not only requires a large heat expenditure, but that it also produces sulfur dioxide gas which a

major contributor to acid rain. This method employed copper(II) sulfate as a starting material, easily obtained from copper sulfide by a number of methods. The copper sulfate is then reacted with alkali metal molybdate to form a copper molybdate hydroxide material which is similar to the mineral lindgrenite but deficient in copper and rich in hydroxide. This copper species is then reacted with an alkali metal hydroxide solution to recover the molybdate and convert the copper to copper hydroxide which is easily dehydrated to the oxide by heating under air. The remaining copper oxide, or the copper hydroxide for that matter, can then be reduced to copper metal by existing industrial methods.

The last application discussed in this study was a catalytic method for the disproportionation of sulfite to elemental sulfur and hydrogen sulfate ion. The sulfite starting material can be obtained from industrial sulfur dioxide sources by presently existing and commonly used scrubbing methods. The sulfur dioxide is typically extracted from the gas phase waste stream by vapor-liquid extraction with a solution of alkali of alkaline earth metal hydroxides, or by basic amines. The resulting solution can by reacted with the catalyst developed in this study in a solid/liquid heterogeneous system. Several catalysts were developed including molybdenum trioxide, hydrogen molybdenum bronze, iron(III)-promoted hydrogen bronze and an iron molybdate catalyst, all of which proved to be successful to varying degrees. The active catalyst was determined to be in the form of a molybdenum oxide sulfide species, and a reasonable mechanism was proposed. Furthermore this catalyst may be considered a synthetic

analog to the sulfite oxygenase enzyme which contains a molybdenum center coordinated by three sulfur and two oxygen species.

REFERENCES

1. Moini, A.; Subramanian, A.; Clearfield, A.; DiSalvo, F. J.; McCarroll, W. H., Structure and properties of $La_2Mo_2O_7$: a quasi-two-dimensional metallic oxide with strong Mo-Mo bonds. *Journal of Solid State Chemistry* **1987,** 66, 136-143.

2. Ostertag, W., Rare Earth Tungsten Bronzes. *Inorganic Chemistry* **1966,** 5, (5), 758-760.

3. Wohler, F., *Annales des Chimie et des Physique* **1823,** 42, (2).

4. Banks, E.; Wold, A., *Oxide Bronzes*. John Wiley and Sons: New York, 1968; Vol. 4.

5. Hagg, G., *Zeitschrift für Physikalische Chemie* **1935,** B29.

6. Andersson, G.; Magneli, A., On the crystal structure of molybdenum trioxide. *Acta Chemica Scandinavica* **1950**, 793-797.

7. Chehbouni, M. Environmental, synthetic, and materials applications of molybdenum trioxide. Oklahoma State University, Stillwater, Oklahoma, 2006.

8. Itoh, M.; Hayakawa, K.; Oishi, S., Optical Properties and Electronic Structures of Layered MoO_3 Single Crystals. *Journal of Physics: Condensed Matter* **2001,** 13, 6853-6864.

9. Kihlborg, L., *Arkiv foer Kemi* **1963,** 21, 357-364.

10. Papakondylis, A.; Sautet, P., Ab Initio Study of the Structure of the alpha-MoO_3 Solid and Study of the Adsorption of H_2O and CO Molecules on its (100) Surface. *Journal of Physical Chemistry* **1996,** 100, 10681-10688.

11. Ressler, T.; Timpe, O.; Neisius, T.; Find, J.; Mestl, G.; Dieterle, M.; Schlogl, R., Time-Resolved XAS Investigation of the Reduction/Oxidation of MoO_{3-x}. *Journal of Catalysis* **2000,** 191, 75-85.

12. Chippindale, A. M.; Dickens, P. G.; Powell, A. V., Insertion Compounds of Transition-Metal and Uranium Oxides. *Progress in Solid State Chemistry* **1991,** 21, 133-198.

13. McCarron, E. M. I., β-Molybdenum trioxide: a metastable analog of tungsten trioxide. *Journal of the Chemical Society, Chemical Communications* **1986**, (4), 336-338.

14. Glemser, O., "Genotypical" hydroxides of molybdenum, tungsten, and vanadium. *Nachr. Akad. Wiss. Gottingen, Math. Physik.-Kl. Abt.* **1955,** IIa, 121-126.

15. Glemser, O.; Hauschild, U.; Lutz, G., Preparation of hydroxides by the action of atomic hydrogen on oxides. *Zeitschrift fur Anorganische und Allgemeine Chemie* **1952,** 269, (269), 93-98.

16. Glemser, O.; Lutz, G., Molybdenum oxides and molybdenum blue. *Naturwissenschaften* **1947,** 34, 215.

17. Glemser, O.; Lutz, G., Hydroxide-hydride of molybdenum. *Naturwissenschaften* **1950,** 37, 539-540.

18. Glemser, O.; Lutz, G., Molybdenum blue II. *Zeitschrift fur Anorganische und Allgemeine Chemie* **1951,** 264, 17-33.

19. Glemser, O.; Lutz, G.; Meyer, G., Lower molybdenum hydroxides. *Zeitschrift fur Anorganische und Allgemeine Chemie* **1956,** 40, 552-553.

20. Dickens, P. G.; Birtill, J. J., Hydrogen molybdenum bronzes. *Journal of Electronic Materials* **1978,** 7, (5), 679-686.

21. Dickens, P. G.; Birtill, J. J.; Wright, C. J., Elastic and Inelastic Neutron Studies of Hydrogen Molybdenum Bronzes. *Journal of Solid State Chemistry* **1979,** 28, 185-193.

22. Slade, R. C. T.; Halstead, T. K.; Dickens, P. G., NMR Study of Hydrogen Molybdenum Bronzes:$H_{1.71}MoO_3$ and $H_{0.36}MoO_3$. *Journal of Solid State Chemistry* **1980,** 34, 183-192.

23. Dickens, P. G.; Crouch-Baker, S.; Weller, M. T., Hydrogen Insertion in Oxides. *Solid State Ionics* **1986,** 18 &19, 89-97.

24. Greenblatt, M., Molybdenum Oxide Bronzes with Quasi-Low-Dimensional Properties. *Chemical Reviews* **1988,** 88, (1), 31-53.

25. Marcus, J.; Escribe-Filippini, C.; Chevalier, R.; Buder, R., Magnetic properties and ^{151}Eu Mossbauer spectroscopy of a new molybdenum bronze: $Eu_{0.08}MoO_3$. *Solid State Communications* **1987,** 62, (4), 221-223.

26. Escribe-Filippini, C.; Marcus, J., Magnetic ordering in new rare earth molybdenum bronzes. *Journal of Magnetism and Magnetic Materials* **1995,** 140-144, 1183-1184.

27. Ganne, M.; Boumaza, A.; Dion, M., The blue bronze $Tl_{0.30}MoO_3$ structure and physical properties. *Materials Research Bulletin* **1985,** 20, (11), 1297-1308.

28. Schollhorn, R.; Kuhlmann, R.; Besenhard, J. O., Topotactic redox reactions and ion exchange of layered MoO_3 Bronzes. *Materials Research Bulletin* **1976,** 11, 83-90.

29. Dickens, P. G.; Pye, M. F., Oxide Insertion Compounds. In *Intercalation Chemistry*, Whittingham, M. S.; Jacobson, A. J., Eds. Academic Press, Inc.: New York, 1982.

30. Birtill, J. J.; Dickens, P. G., Phase Relationships in the System H_xMoO_3 ($0<x\leq2.0$). *Materials Research Bulletin* **1978,** 13, (4), 311-316.

31. Schollhorn, R.; Schulte-Nolle, T.; Steinhoff, G., Layered intercalation complexes of the hydrogen bronze $H_{0.5}MoO_3$ with organic Lewis bases. *Journal of the Less-Common Metals* **1980,** 71, 71-78.

32. Iwamoto, T.; Itoh, Y.; Ohwaka, K.; Takashi, M., Intercalates of anoinic molybdenum(V, VI) oxide host $MoO_3^{0.5-}$. *Nippon Kagaku Kaishi* **1983,** 2, 273-276.

33. Thomas, D. M.; McCarron, E. M. I., The composition and proposed structure of the alkali metal layered molybdenum bronzes *Materials Research Bulletin* **1986,** 21, 945-960.

34. Dickens, P. G.; Neild, D. J., Some electronic properties of the molybdenum bronzes. *Transactions of the Faraday Society* **1968,** 64, 13-18.

35. Hibble, S. J.; Dickens, P. G., Hydrogen insertion compounds of the mixed molybdenum tungsten oxides $Mo_yW_{1-y}O_3$ ($0.1 < y < 0.9$) *Materials Research Bulletin* **1985,** 20, 343-349.

36. Parise, J. B.; McCarron, E. M., III; Sleight, A. W., A new modification of ReO_3-type MoO_3 and the deuterated intercalation compound from which it is derived: $D_{0.99}MoO_3$. *Materials Research Bulletin* **1987,** 22, 803-811.

37. Sermon, P. A.; Bond, G. C., Studies of hydrogen spillover, part I: the rate, extent and products of hydrogen spillover from platinum to the trioxides on tungsten and

molybdenum. *Journal of the Chemical Society, Faraday Transactions 1: Physical Chemistry in Condensed Phases* **1976,** 72, (3), 730-744.

38. Sotani, N.; Eda, K.; Sadamatu, M.; Takagi, S., Preparation and characterization of hydrogen molybdenum bronzes, H_xMoO_3. *Bulletin of the Chemistry Society of Japan* **1989,** 62, 903-907.

39. Eda, K.; Hatayama, F.; Kunitomo, M.; Kohmoto, T.; Sotani, N., Preparation and characterization of a sodium insertion compound of hydrogen molybdenum bronze, $Na_{0.25}(H_2O)_y[H_{0.21}MoO_3]$. *Journal of Materials Chemistry* **1994,** 4, (2), 205-207.

40. Sotani, N.; Miyazaki, T.; Eda, K.; Hatayama, F., Preparation of hydrated rubidium molybdenum bronze from hydrated sodium molybdenum bronze by ion exchange and its characterization and thermal decomposition. *Journal of Materials Chemistry* **1997,** 7, (11), 2253-2258.

41. Ayyappan, S.; Rao, C. N. R., A simple method of hydrogen insertion in transition metal oxides to obtain bronzes. *Materials Research Bulletin* **1995,** 30, (8), 947-951.

42. Bollapragada, P. K. S. Chemical transformations using tungsten and molybdenum hydrogen bronzes. Thesis (Ph D), Oklahoma State University, Stillwater, Oklahoma, 2003.

43. Birtill, J. J. Oxford University, 1977.

44. Gopalakrishnan, J.; Bhat, V., Oxidative extraction and ion-exchangeof lithium in Li_2MoO_3: synthesis of $Li_{2-x}MoO_3$ ($0 < x \leq 2.0$) and $H_2MoO_3^+$. *Materials Research Bulletin* **1987,** 22, 769-774.

45. James, A. C. W. P.; Goodenough, J. B., Structure and bonding in Li_2MoO_3 and $Li_{2-x}MoO_3$ ($0 \leq x \leq 1.7$). *Journal of Solid State Chemistry* **1988,** 76, (87-96).

46. Schollhorn, R., Solvated Intercalation Compounds of Layered Chalcogenide and Oxide Bronzes. In *Intercalation Chemistry*, Whittingham, M. S.; Jacobson, A. J., Eds. Academic Press, Inc.: New York, 1982.

47. Chin, K.; Eda, K.; Sotani, N.; Whittingham, M. S., Hydrothermal synthesis of the blue potassium molybdenum bronze, $K_{0.28}MoO_3$. *Journal of Solid State Chemistry* **2002,** 164, 81-87.

48. Eda, K.; Chin, K.; Sotani, N.; Whittingham, M. S., Hydrothermal synthesis of potassium molybdenum oxide bronzes: structure-inheriting solid-state route to blue bronze and dissolution/deposition route to red bronze. *Journal of Solid State Chemistry* **2005,** 178, 158-165.

49. Chin, K.; Eda, K.; Suzuki, T.; Sotani, N., Hydrothermal synthesis and calorimetric study of blue molybdenum bronze, $K_{0.28}MoO_3$. *Bulletin of the Chemistry Society of Japan* **2003,** 76, 557-560.

50. Wold, A.; Kunnmann, W.; Arnott, R. J.; Ferretti, A., Preparation and Properties of Sodium and Potassium Molybdenum Bronze Crystals. *Inorganic Chemistry* **1964,** 3, (4), 545-547.

51. Bouchard, G. H., Jr.; Perlstein, J. H.; Sienko, M. J., Solid-state studies of potassium molybdenum bronzes. *Inorganic Chemistry* **1967,** 6, (9), 1682-1685.

52. Mumme, W. G.; Watts, J. A., The Crystal Structure of the Molybdenum Bronze Cs_xMoO_3 (x ~ 0.25). *Journal of Solid State Chemistry* **1970,** 2, 16-23.

53. Perloff, D. S.; Vlasse, M.; Wold, A., Anisotropic electrical behavior of the blue potassium bronze. $K_{0.30}MoO_3$. *Journal of Physical Chemistry of Solids* **1969,** 30, 1071-1076.

54. Reid, A. F.; Watts, J. A., Single crystal synthesis by the electrolysis of molten titanates, molybdates and vanadates. *Journal of Solid State Chemistry* **1970,** 1, 310-318.

55. Schneemeyer, L. F.; DiSalvo, F. J.; Fleming, R. M.; Waszczak, J. V., Sliding charge-density wave conductivity in potassium molybdenum bronze. *Journal of Solid State Chemistry* **1984,** 54, 358-364.

56. Schneemeyer, L. F.; DiSalvo, F. J.; Spengler, S. E.; Waszczak, J. V., Dramatic impurity effects on the charge-density wave in potassium molybdenum bronze. *Physical Review B: Condensed Matter* **1984,** 30, (8), 4297-4301.

57. Schneemeyer, L. F.; Spengler, S. E.; DiSalvo, F. J.; Waszczak, J. V.; Rice, C. E., Electrochemical crystal growth in the cesium molybdate-molybdenum trioxide system. *Journal of Solid State Chemistry* **1984,** 55, 158-164.

58. Strobel, P.; Greenblatt, M., Crystal growth and electrical properties of lithium, rubidium, and cesium molybdenum oxide bronzes. *Journal of Solid State Chemistry* **1981,** 36, 331-338.

59. Lisnyak, V. V.; Stus, N. V.; Stratiychuk, D. A.; Tkach, V. M.; Popovich, P., New high-temperature-high pressure synthetic route: from crystalline hydrates to molybdenum bronzes Na_xMoO_3. *Journal of Alloys and Compounds* **2003,** 359, 307-309.

60. Deb, S. K., Opportunities and challenges of electrochromic phenomena in transition metal oxides. *Solar Energy Materials and Solar Cells* **1992,** 25, 327-338.

61. Hussain, Z., Optical and electrochromic properties of annealed lithium-molybdenum-bronze thin films. *Journal of Electronic Materials* **2002,** 31, (6), 615-630.

62. Abdellaoui, A.; Martin, L.; Donnadieu, A., Structure and optical properties of MoO_3 thin films prepared by chemical vapor deposition. *Physica Status Solidi (a)* **2006,** 109, (2), 455-462.

63. Wu, Y. M.; Li, W. S.; Lu, J.; Du, J. H.; Lu, D. S.; Fu, J. M., Electrocatalytic oxidation of small organic molecules on polyaniline-Pt-H_xMoO_3. *Journal of Power Sources* **2005,** 145, 286-291.

64. Lu, J.; Du, J. H.; Li, W. S.; Fu, J. M., Formation and Oxidation of Hydrogen Molybdenum Bronze on Platinum Electrode in Sulfuric Acid Solution. *Chinese Chemical Letters* **2004,** 15, (6), 703-706.

65. Eda, K.; Sukejima, A.; Matsuura, N.; Sotani, N., New family member of hydrogen molybdenum bronze, H_xMoO_3. *Chemistry Letters* **1998,** 27, (8), 819-820.

66. 2006 Edition of the Drinking Water Standards and Health Advisories, EPA 822-R-06-013. In Washington, D. C., 2006.

67. LaMotte Company www.lamotte.com.

68. HACH Company www.hach.com.

69. Xu, X.; van de Craas, A. M.; Kok, E. M.; de Bruyn, A. M., "Trace analysis of peroxide explosives by high performance liquid chromatography-atmospheric pressure chemical ionization-tandem mass spectrometry (HPLC-APCI-MS/MS) for forensic applications" *Journal of Forensic Sciences* **2002,** 49, 1230-1236.

70. Bencko, V., Chromium: a review of environmental and occupational toxicology. *Journal of Hygiene, Epidemiology, Microbiology, and Immunology* **1985,** 29, (1), 37-46.

71. Kimbrough, D. E., A review of the carcinogenicity of chromate in drinking water. *Proceedings - Annual Conference, American Water Works Association* **2002**, 497-517.

72. Paustenbach, D.; Finley, B.; Mowat, F.; Kerger, B., Human Health Risk and Exposure Assessment of Chromium(VI) in Tap Water. *Journal of Toxicology and Environmental Health, Part A* **2003,** 66, (14), 1295-1339.

73. Lalvani, S. B.; Wiltowski, T.; Hu¨bner, A.; Weston, A.; Mandich, N., Removal of hexavalent chromium and metal cations by a selective and novel carbon adsorbent. *Carbon* **1998,** 36, 1219.

74. Dakiky, M.; Khamis, M.; Manassra, A.; Mer'eb, M., Selective adsorption of chromium (VI) in industrial wastewater using low-cost abundantly available adsorbents. *Advances in Environmental Research* **2002,** 6, 533.

75. Rengeraj, S.; Yeon, K. H.; Moon, S. H., Removal of chromium from water and wastewater by ion-exchange resins. *Journal of Hazardous Materials* **2001,** B87, B87.

76. Rivero, M. J.; Primo, O.; Ortiz, M. I., Modelling of Cr(VI) removal from polluted groundwaters by ion exchange. *Journal of Chemical Technology and Biotechnology* **2004,** 79, 822.

77. Sirkar, K. K., Membrane separation technologies: current developments. *Chemical Engineering Communications* **1997,** 157, 145.

78. Keskinler, B.; Danis, U.; Cakici, A.; Akay, G., Chromate removal from water using surfactant-enhanced crossflow filtration. *Separations Science and Technology* **1997,** 32, 1899.

79. Bohdziewicz, J., Removal of chromium ions (VI) from underground water in the hybrid complexation-ultrafiltration process. *Desalination* **2000,** 129, 227.

80. Hafiane, A.; Lemordant, D.; Dhahbi, M., Removal of hexavalent chromium by nanofiltration. *Desalination* **2000,** 130, 305.

81. Salazar, E.; Ortiz, M. I.; Urtiaga, A. M., Kinetics of the separation and concentration of chromium (VI) with emulsion liquid membranes. *Industrial and Engineering Chemistry Research* **1992,** 31, 1523.

82. Chaudry, M. A.; Ahmad, S.; Malik, M. T., Supported liquid membrane technique applicable forremoval of chromium from tannery wastes *Waste Management* **1997,** 17, (4), 211-218.

83. Alonso, A. I.; Gala´n, B.; Gonza´lez, M.; Ortiz, I., Experimental and theoretical analysis of a nondispersive solvent extraction pilot plant for the removal of Cr(VI) from a galvanic process wastewaters. *Industrial and Engineering Chemistry Research* **1999,** 38, 1666.

84. Bringas, E.; Román, M. F. S.; Ortiz, I., Separation and Recovery of Anionic Pollutants by the Emulsion Pertraction Technology. Remediation of Polluted Groundwaters with Cr(VI). *Industrial and Engineering Chemistry Research* **2006,** 45, 4295-4303.

85. Puls, R. W.; Clark, D. A.; Paul, C. J.; Vardy, J., Transport and transformation of hexavalent chromium through soils and into ground water. *Journal of Soil Contamination* **1994,** 3, 203-224.

86. Amonette, J. E.; Szecsody, J. E.; Schaef, H. T.; Templeton, J. C.; Gorby, Y. A.; Fruchter, J. S., Abiotic Reduction of Aquifer Materials by Dithionite: a Promising In-Situ Remediation Technology. In *In-situ Remediation: Scientific Basis for Current and Future Technologies, Proceedings of the 33rd Hanford Symposium on Health and the Environment*, Gee, G. W.; Wing, R. W., Eds. Battelle Press: Columbus, Ohio, 1994; pp 851–881.

87. Blowes, D. W.; Ptacek, C. J.; Jambor, J. L., In-situ remediation of Cr(VI)-contaminated groundwater using permeable reactive walls: laboratory studies. *Environmental Science and Technology* **1997,** 31, 3348–3357.

88. Thornton, E. C.; Amonette, J. E., Hydrogen sulfide gas treatment of Cr(VI)-contaminated sediment samples from a plating-waste disposal site: implications for in situ remediation. *Environmental Science and Technology* **1999,** 33, 4096–4101.

89. Battaglia-Brunet, F.; Touze, S.; Michel, C.; Ignatiadis, I., Treatment of chromate-polluted groundwater in a 200 dm^3 pilot bioreactor fed with hydrogen. *Journal of Chemical Technology and Biotechnology* **2006,** 81, (9), 1506-1513.

90. Espenson, J. H., Rate studies on the primary step of the reduction of chromium(VI) by iron(II). *Journal of the American Chemical Society* **1970,** 92, 1180.

91. Fendorf, S. E.; Li, G., Kinetics of chromate reduction by ferrous iron. *Environmental Science and Technology* **1995,** 30, 1614–1617.

92. Seaman, J. C.; Bertsch, P. M.; Schwallie, L., In situ Cr(VI) reduction within coarse textured, oxide-coated soil and aquifer systems using Fe(II) solution. *Environmental Science and Technology* **1999,** 33, 938–944.

93. Eary, L. E.; Rai, D., Chromate removal from aqueous wastes by reduction with ferrous ion. *Environmental Science and Technology* **1988,** 22, 972–977.

94. Kim, C.; Zhou, Q.; Deng, B.; Thornton, E. C.; Xu, H., Chromium (VI) reduction by hydrogen sulfide in aqueous media: stoichiometry and kinetics. *Environmental Science and Technology* **2001,** 35, (11), 2219-2225.

95. Pettine, M.; Millero, F. J.; Passino, R., Reduction of chromium(VI) with hydrogen sulfide in NaCl media. *Marine Chemistry* **1994,** 46, 335–344.

96. Legrand, L.; El Figuigui, A.; Mercier, F.; Chausse, A., Reduction of Aqueous Chromate by Fe(II)/Fe(III) Carbonate Green Rust: Kinetic and Mechanistic Studies. *Environmental Science and Technology* **2004,** 38, (17), 4587-4595.

97. Bond, D. L.; Fendorf, S., Kinetics and Structural Constraints of Chromate Reduction by Green Rusts. *Environmental Science and Technology* **2003,** 37, (12), 2750-2757.

98. Dixon, D. A.; Sadler, N. P.; Dasgupta, T. P., Oxidation of biological substrates by chromium(VI). Part 1. Mechanism of the oxidation of L-ascorbic acid in aqueous solution. *Journal of the Chemical Society, Dalton Transactions* **1993**, 3489–3495.

99. Hu, J.; Lo, I. M. C.; Chen, G., Fast removal and recovery of Cr(VI) using surface-modified jacobsite ($MnFe_2O_4$) nanoparticles. *Langmuir* **2005,** 21, (24), 11173-11179.

100. Hu, J.; Lo, I. M. C.; Chen, G., Removal of Cr(VI) by magnetite nanoparticles. *Water Science and Technology* **2004,** 50, (12, Nano and Micro Particles in Water and Wastewater Treatment), 139-146.

101. Whittingham, M. S.; Jacobson, A. J., *Intercalation Chemistry*. Academic Press: New York, 1982.

102. Moskalyk, R. R.; Alfantazi, A. M., Review of Copper Pyrometallurgical Practice: Today and Tomorrow. *Minerals Engineering* **2003,** 16, 893-919.

103. Dicinoski, W., A revolution in copper recovery. *Mining Magazine* **2000,** 182, 258, 260, 262.

104. Samans, C. H., *Engineering Metals and their Alloys*. MacMillan: 1949.

105. Prasad, M. S.; Kenyen, V. P.; Assar, D. N., Development of SX-EW Process for Copper Recovery-An Overview. *Mineral Processing and Extractive Metallurgy Review* **1992,** 8, 95-118.

106. Peacey, J.; Guo, X.-J.; Robles, E., Copper Hydrometallurgy-Current Status, Preliminary Economics, Future Direction and Positioning Versus Smelting. *Transactions of Nonferrous Metals Society of China* **2004,** 14, 560-568.

107. Rossi, G., Biohydrometallurgy of Copper Ores: State of the Art and Prospects. *Mines & Carrieres: Les Techniques* **1992**, 10-21.

108. Pavani, K.; Ramanan, A., Influence of 2-aminopyridine on the formation of molybdated under hydrothermal conditions. *European Journal of Inorganic Chemistry* **2005**, 3080-3087.

109. Baird, C.; Cann, M., *Environmental Chemistry*. 3rd ed.; W. H. Freeman and Company: New York, 2004.

110. Mizoguchi, T.; Takei, Y.; Okabe, T., The chemical behavior of low valence sulfur compounds. X. Disproportionation of thiosulfate, trithionite, tetrathionate and sulfite under acidic conditions. *Bulletin of the Chemical Society of Japan* **1976,** 49, (1), 70-75.

111. Dhawale, S. W., Thiosulfate. *Journal of Chemical Education* **1993,** 70, (1), 12-14.

112. Greenwood, N. N.; Earnshaw, A., *Chemistry of the Elements*. Pergamon Press: 1989.

113. Hille, R., The mononuclear molybdenum enzymes. *Chemical Reviews* **1996,** 96, 2757-2816.

VITA

Kevin Nakia Barber

Candidate for the Degree of

Doctor of Philosophy

Dissertation: NOVEL ENVIRONMENTAL AND EXPLOSIVES DETECTION APPLICATIONS FOR MOLYBDENUM OXIDES

Major Field: Chemistry

Biographical:

Education:
Completed the requirements for the Doctor of Philosophy in Chemistry at Oklahoma State University, Stillwater, Oklahoma in July, 2009.

MS Chemical Engineering, Oklahoma State University, Stillwater, Oklahoma, July, 2005.

BS Chemical Engineering, University of Oklahoma, Norman, Oklahoma, December 1999.

Experience:
Research Engineer, NewMan Technologies, Inc., Norman, Oklahoma, (2000-2002)
Engineering Co-Op, Arkansas Nuclear One, Russellville, Arkansas (1995, 1996)

Professional Memberships:
American Chemical Society, (2006 – Present)
American Society for Testing and Materials, International, (2008 – Present)
American Association for the Advancement of Science (2003 – 2008)
Phi Lambda Upsilon, Chemistry Honor Society (2006 – Present)

Name: Kevin Nakia Barber Date of Degree: July, 2009

Institution: Oklahoma State University Location: Stillwater, Oklahoma

Title of Study: NOVEL ENVIRONMENTAL AND EXPLOSIVES DETECTION APPLICATIONS FOR MOLYBDENUM OXIDES

Pages in Study: 184 Candidate for the Degree of Doctor of Philosophy

Major Field: Chemistry

Scope and Method of Study:

This study developed synthetic methods and novel applications for molybdenum oxides and oxide bronzes.

Findings and Conclusions:

Novel low temperature solution phase methods were developed for the synthesis of the hydrogen molybdenum bronzes and sodium hydrogen molybdenum bronzes resulting in yields of 95.6 % and 78.0%, respectively. It was discovered, based on analysis of reducing equivalents, that the sodium bronze was in fact a hydrogen bronze with sodium molybdenum oxide centers and has the general formula of $Na_xH_{0.5-x}MoO_3 \cdot 2xH_2O$, where $x \cong 0.25$. This sodium hydrogen bronze disproportionates in aqueous media to a more sodium-rich, proton-poor species, with $x \cong 0.40$ and a correspondingly reduced reduction capacity of 0.10 mEq/mole. The aqueous sodium species was used as a colorimetric reagent for the detection of aqueous chlorine, a test strip for detection of peroxide explosives, and a discriminating reagent for differentiation of peroxide and chlorate explosives. The bulk sodium species was used in an electronic device for detection of peroxide vapor. The bulk hydrogen bronze was used as a reagent for the reduction of chromate in groundwater and wastewater. It was immune to chromium hydroxide fouling experienced by nanometric iron at high pH. A sulfur dioxide-free solution phase method was developed for processing copper sulfide ore using alkali metal molybdates, resulting in a copper recovery of 97.4 %. Additionally, a new catalytic method was discovered and developed for the disproportionation of sulfite to elemental sulfur and sulfate using catalysts derived from the hydrogen bronzes and from iron molybdates.

Name: Kevin Nakia Barber Date of Degree: July, 2009

Institution: Oklahoma State University Location: Stillwater, Oklahoma

ADVISER'S APPROVAL: Allen W. Apblett

ADVISER'S APPROVAL: Allen W. Apblett